TECHNICAL OPERATING REPORT [redacted]

REFERENCE NO. 64 321

COPIES

CLASSIFICATION CHANGE

To UNCLASSIFIED

By authority of Date

Changed by

Classified Document Master Control Station, NASA

Scientific and Technical Information Facility

BELLCOMM, INC.
1100 17th ST., N. W.
WASHINGTON 6, D. C.

C72 72555

(UNCLASSIFIED TITLE)

APOLLO HEAT SHIELD
PHASE I

BI-WEEKLY PROGRESS REPORT

Prepared by

RESEARCH AND ADVANCED DEVELOPMENT DIVISION
AVCO CORPORATION
Wilmington, Massachusetts

RAD-SR-62-130

Letter Contract M2H43X-406012

THIS REPORT WAS PREPARED IN ACCORDANCE WITH NAA/S&ID LETTER CONTRACT M2H43X-406012. IT IS SUBMITTED IN PARTIAL FULFILLMENT OF THE CONTRACT AND IN ACCORDANCE WITH NAA/S&ID PROCUREMENT SPECIFICATION MC304-0001 AND SID62-420 (PARAGRAPH 4.0).

(NASA-CR-127990) APOLLO HEAT SHIELD, PHASE 1 Biweekly Progress Report (Avco Corp., Wilmington, Mass.) 116 p

N79-76592

Unclas
00/34 11692

30 June 1962

This document contains [redacted] affecting [redacted] United States, within the mea[redacted] Espionage Laws, Title 18, U.S.[redacted] Section 793 [redacted] the transmission or [redacted]ation of which in any [redacted] to an unauthorized person is prohibited by [redacted]

Prepared for

NORTH AMERICAN AVIATION, INC.
SPACE AND INFORMATION SYSTEMS DIVISION
Downey, California

[redacted]

TECHNICAL OPERATING REPORT

[redacted]

This document consists of 116 pages, 89 copies, Series A

(UNCLASSIFIED TITLE)

APOLLO HEAT SHIELD

PHASE I

BI-WEEKLY PROGRESS REPORT

Prepared by

RESEARCH AND ADVANCED DEVELOPMENT DIVISION
AVCO CORPORATION
Wilmington, Massachusetts

RAD-SR-62-130
Letter Contract M2H43X-406012

THIS REPORT WAS PREPARED IN ACCORDANCE WITH NAA/S&ID LETTER CONTRACT M2H43X-406012. IT IS SUBMITTED IN PARTIAL FULFILLMENT OF THE CONTRACT AND IN ACCORDANCE WITH NAA/S&ID PROCUREMENT SPECIFICATION MC304-0001 AND SID62-420 (PARAGRAPH 4.0).

30 June 1962

APPROVED

E. Offenhartz	C. F. Berninger
Project Manager	Project Director
Apollo R & D	Apollo Project Office

Prepared for

NORTH AMERICAN AVIATION, INC.
SPACE AND INFORMATION SYSTEMS DIVISION
Downey, California

[redacted]

(NOT USED)

CONTENTS

(NOT USED)

ILLUSTRATIONS

ILLUSTRATIONS (Cont'd)

ILLUSTRATIONS (Cont'd)

ILLUSTRATIONS (Concl'd)

TABLES

I. CURRENT STATUS

Avco's program accomplishments during the period 11 June through 24 June 1962 continue to reflect the build up in technical activities of the program. Significant factors influencing these accomplishments were the continued structural support efforts on site at NAA/S&ID, the completion of major program plans, and resolution of interfaces with NAA/S&ID.

A. DESIGN

1. Heat Transfer

The primary effort during this reporting period has been on the evaluation of the radiative heating on the spherical face and a comparison of the predicted convective heating distributions with available experimental results.

The equilibrium convective heating has been calculated for NAA specification points 12, 13, 14 and 15 along the 90-degree meridian for NAA re-entry trajectories 1 and 4.

The shock shape and stand-off distances in the plane of symmetry have been determined by the method of Kaatari (NASA TN D860).

The radiative equilibrium heating was computed along the zero meridian on the spherical face for the NAA re-entry trajectories 1 and 4. The initial approach methods and procedures for the radiative heating are based on the works of Kivel and Bailey (Avco-Everett RR-21) for the radiative emissivity of air and Kaatari (NASA TN D-860) for the shock stand-off distance and shock shape.

The study of foreign gas injection and species radiation in laminar boundary-layers is continuing. The full equilibrium multicomponent equations are being studied and prepared for programming.

The Apollo shock tube tests to measure convective heat transfer rates were begun on 15 June 1962 and are continuing.

The radiative heat-transfer models were placed on order during this reporting period and delivery is promised for 15 July 1962, at which time these tests will begin .

The models required for the shape variation experiments are being fabricated by the vendor. Initial delivery is promised for 15 July 1962, at which time testing will begin.

2. Thermodynamic Analysis

The evaluation and modification of analysis techniques is progressing according to schedule. Selection of a final design analysis procedures will depend upon the results of the ground test program. Modifications to programs 640 (transient surface recession) and 1098 (rapid approximate solution) are being made and program 951 (ablation-in-depth) steady state parametric studies are beginning.

During this period, a limited transient analysis for space flight and lunar environment was initiated using the 640 heat conduction program. In the cases investigated, the attempt was made to calculate gradients through a typical composite heat shield.

An analysis of an area near the hemispherical forecone for minimum temperature (lunar residence) was initiated. In this area of the command module the heat-shield composite consists of ablative material, honeycomb structure, and insulation with some finite space between the pressure vessel and the insulation. The net heat-transfer effects may be affected considerably by this lack of a conducting path to the pressure vessel.

Additional calculations concerning the effects of heating multiplier on the structure temperature have been completed.

A trajectory study for the leeward side (low heat-flux region) has been completed. A second trajectory analysis for the windward side was started. Additional materials such as Avcoat X3000, and other charring plastics are being studied using rapid screening techniques.

A revision of the heat-shield thickness requirements will be made to reflect new (current) material properties.

In this reporting period, new molecular constants were calculated for the $x^1\Sigma_g^+$, $A^3\Sigma_u^+$, $B^3\pi g$ and $C^3\pi u$ electronic states of the N_2 molecule, as well as the $x^3\Sigma_g^-$ and $B^3\Sigma_u^-$ electronic states of the O_2 molecule. The procedure was exactly that used for the NO calculations described in the preceding two biweekly progress reports. The new constants are based upon the most recent spectroscopic data.

3. Structural Studies

A number of stress analyses of the substructure and the ablator panels have been completed or are in process of completion and are reported in detail in Section IVA3 of this progress report.

A detailed structural development test plan is being formulated. To date a part of this program has been written for the evaluation of bonded ablator panels at a cold soak down to -260° F. Various bonds designed for cold temperature applications will be investigated. The first specimens are ready for test.

The test data for a 2-tile bonded panel subjected to a quartz lamp test and a single tile bonded panel subjected to a 600° F soak test are being evaluated.

Avcoat II turbulent tubes were machined and thermocouples installed, but work was stopped due to NAA/S&ID elimination of Avcoat II from the Apollo program. Fabrication of Avcoat 5019 and 5026 is in process.

A detailed test plan for mechanical vibration tests has been formulated. Instrumentation preparations (checkout, scaling, etc.) of an 18 x 12-inch test panel have been made, and the specimen is ready for test.

4. Engineering Design

The design personnel, who visited NAA, returned 16 June 1962. The amount of design information obtained resulted in gaining knowledge of NAA/S&ID problems. Spacecraft layout information should be available at S&ID about 9 July and this will be the basis of further discussion.

No information was available at this time as to the procedure S&ID will require of Avco in the preparation and maintenance of interface control drawings.

While at S&ID, drawing SK-6-14-62 showing various fastener schemes was prepared and two copies were given to S&ID for their information.

The major effort has been the preparation of the following drawings. These drawings will be evaluated by the aero, thermo and applied mechanics disciplines for review and comments in preparation for a reference design selection.

LA-4149, Revision C--heat-shield geometry and thickness
LA-4179--tile edge treatment
LA-4180--access panel - bonded tile
LA-4181--access Panel - unbonded tile
LA-4157, Revision A--aft compartment - unbonded tile

a. Aft Compartment

Design studies continued on the "radial wedge" design (LA-4165) resulting in the addition of a compensating spring to ensure float during the thermal cycle while at the same time insuring positive attachment to the substructure. This design offers possible tile replacement advantages and elimination of holes at the tile corners.

Studies were also made and are continuing on a method of free edge restraint for each end item split line.

b. Crew Compartment

A layout study is in process showing a revised arrangement for unbonded tiles. The purpose of this layout is to investigate the problem of mechanical fastener location in order to eliminate interference with stringers and other reinforcements located on the inside surface of the outer structure.

Another layout is in process studying the problems of rocket-motor installation and removal.

A layout study (LA-4162) showing a spring-loaded closure panel was completed and also a layout (LA-4163) showing a proposed solution to a crew window cover.

c. Forward Compartment

A flat pattern layout of the forward compartment showing tile arrangement and cutouts required for various doors is being prepared based on present NAA information.

A preliminary design investigation of the aft compartment tile arrangement using tiles one square foot in area has been initiated and is currently in progress.

During this report period, the Specifications and Standards Section completed incorporation of Apollo Program documentation requirements into the Avco RAD drafting manual.

5. Flight Test

A flight test program to define requirements for qualification of the heat shield was prepared and presented to NAA/S&ID on 25 June 1962. Justification and recommendations with regard to such a program was given to NAA/S&ID personnel on that date both in the form of a rough draft document and in the course of discussion. This information was presented in response to a request from NAA/S&ID by TWX MA14691, and, it is understood will be used by NAA/S&ID in a re-evaluation of the present flight test program.

B. MATERIALS DEVELOPMENT AND EVALUATION

1. Materials Development

Emphasis during the past two-week period has been more on development and investigation of processing variables. Twenty-five 12 x 12 inch panels of the prime candidate X5026-22 were produced.

A direct correlation has been obtained between mixing temperature and panel density. The higher the mixing temperature, the lower the density.

Panels containing a higher percentage of reinforcement (silica and/or glass fibers) have been molded and submitted for evaluation in the OVERS arc. A panel containing silica microballoons in place of the phenolic microballoons was also molded and submitted.

Processing studies carried out in the Baker-Perkins mixer indicate that panel density is directly proportional to mixing time.

A vacuum drying process has been developed which removes up to 7.5 percent volatiles from the phenolic microballoons. Larger batches are to be processed so that vacuum dried microballoons can be used in making 12 x 12 inch panels. Microscopic examination shows no detrimental effects other than a darkening in color as the results of more complete cure.

Air flotation drying of the microballoons at J. O. Ross was cancelled because of the danger of fire or dust explosion when the balloons are heated in air to 350°F. Sufficient capacity was not available for supplying an inert heated gas.

The affect of molding temperature on peak exotherm was determined for the X5026-22 formulation.

A dry blended system was made up and molded to demonstrate the feasibility of this method of processing.

Cylindrical specimens of Avcoat 5019 have been prepared from which at least three 15-inch long turbulent pipe specimens can be machined. Flat 9 x 9 x 0.5-inch panels of Avcoat 5019 are also being prepared.

Work on Avcoat II was terminated on 14 June 1962. This report covers the status of the work accomplished during the four days of this reporting period when work was performed.

a. Avcoat II Evaluation

The test specimens for analysis of physical and thermal properties were radiographed and inspected for flaws. The specific gravity of k, C_p, and arc samples was determined.

b. Epon 872 Evaluation

Three 18 x 3-inch diameter castings of Epon 872 cured with BF_3-monoethylamine were made and submitted to the machine shop for fabrication of turbulent arc tubes.

c. Genamid 2000 Evaluation

The tensile test results of three Avcoat II formulations cured with different ratios of Genamid 2000 were returned from Physical Test. The results appear in the analysis section of this report.

Samples of commercial adhesives of several categories have been received for evaluation; additional supplies have been ordered. These categories include: silicones, silicone-epoxy, nitrile-phenolics, epoxy-phenolics, epoxy-nylons, and epoxy-anhydrides. Silicone polymers, as a class, are expected to offer considerable potentiality for adhesive bonding of heat-shield material to Apollo substructures and to withstand the effects of extreme low temperatures and elevated temperatures. Existing silicone polymers are rated to withstand 500°F for 200 hours and temperatures as low as -120°F. The extent that these limits can be extended will be determined by physical and environmental tests.

A series of screening specimens were made to evaluate Dow-Corning silicone elastomers at the temperatures of dry-ice-acetone mixture (approximately -80°F), and at liquid nitrogen temperatures (-320°F).

These specimens consisted of bonding cleaned strips of 15-7 PH stainless steel 0.020-inch thick and 1 inch wide x 4 inches long to 1-inch cubes of cleaned and primed X-5026-22 material. DC 1200 primer was used on both substances and DC 4000, DC 601, and DC 731 silicones were used to bond the two materials.

The peel resistance of DC 731 is superior to the other two silicones at 75°F, -80°F, and -320°F. DC 601 is relatively weak at 75°F, but increased in peel resistance at -80°F and -320°F. DC 731 is brittle at -320°F, but the specimen had appreciable resistance to fracture; failure was rapid when it occurred. Separation was adhesive failure at the primer/adhesive interface at the metal side of the bond.

Blocks of X-5026, 4 x 4 x 1 inches thick were bonded to 15-7 PH S.S. honeycomb for NDT evaluation and environmental exposure tests at low temperatures with the above silicone elastomeric adhesives. DC 4000 resin requires partial cure before bonding and the resultant non-uniform gel coat resisted flow and caused large void areas. The application of external pressures to the system may eliminate these voids to a degree.

Environmental test specimens, required for structural test, instrumented with strain gages, consisted of stainless steel panels (Type 304), 18 x 4 x 0.25 inches, and blocks 12 x 4 x 1 inches of X-5026-22, were bonded to both surfaces. Epoxylite 5403, epoxy adhesive, was used and the stainless steel was cleaned and primed before bonding. Duplicate specimens were made.

A second set of specimens were made using DC 1200 primer and DC 731 silicone adhesive as the bonding agent.

Six 12 x 12 x 1/2-inch tiles of Avcoat X-5026 were shipped to NAA/S&ID on 15 June 1962.

Certain reportedly stable paints, paint components and coatings for surface optical property control have been obtained and others have been ordered. Screening tests to eliminate those components that are unstable toward vacuum, ultraviolet radiation, ascent heating and aging have begun. The first series of tests will check the effect of vacuum (10^{-6} to 10^{-7} torr) on the white light reflectivity and weight of candidate materials. The white light reflectivity will be measured before and after testing with a photovolt reflectometer that has demonstrated the ability to differentiate between shades of white and colors.

Evaluation of solutions and combinations of solutions for substructures surface preparation has continued during this reporting period. Primary work involved was the determination of the most effective method of etching 15-7 Mo stainless steel. In addition to the standard procedures, the Dalic Process was also used to evaluate and compare various solutions.

Char layer analyses and degradation studies of X-5026 formulations are continuing. A procedure for significantly reducing the amount of inorganic impurities in Harcure A was developed.

Additional continuously-weighed decomposition runs have been made at 350, 600, 700, 800 and 900°C on X-5026-22. The apparatus has been disassembled to allow substitution of a tungsten helix in place of the stainless steel helix previously used. This new helix has a lower temperature coefficient of its modulus of rigidity and hence will be less sensitive to room temperature fluctuations. This will allow the longer time runs necessary at lower temperatures to be made.

The heating and measurement apparatus for the free evaporation of decomposition gases from the surface of X-5026 has been completed. The kinetics of the thermal decomposition of this material is being examined.

Per instructions received from NAA/S&ID all evaluation of Avcoat II type materials has been terminated.

Evaluation of X-5026 formulations by physical tests is continuing. Tiles of the current reference X-5026 formulation have been inspected and supplied to various groups for use in adhesive bonding, particle impact, mechanical fastener and structural programs.

Effects of the following defects on mechanical properties are under investigation: a) Microballoon segregation, b) Fiber clumps, and c) Density variations.

During this reporting period a total of 43 tiles of X-5026 were ultrasonically and radiographically inspected. The majority of these were variations from the reference formulation which will be used to investigate the effects of various components on char strength and physical and mechanical properties.

A program for the measurement of dielectric properties and their correlation with density, etc., has been initiated.

Some of the X-5026 formulation variations have been found to be highly attenuating in ultrasonic tests.

A second series of X5026-29 have been arc tested in the low enthalpy Model 500 arc. These data are presently being reduced, but the brightness surface temperature and emitted radiation as a function of enthalpy are reported.

The samples that have been cut from the parallel and transverse directions of a plate of X-5026 material have been arc tested in the Model 500 arc and the data are in the process of being reduced, as are the two groups tested during the previous two-week period. A test has been performed to determine the ablation products by means of a probe which collected the gaseous products in the vicinity of the ablating surface.

A minor modification has been put into the data reduction computer program, so that the arc enthalpy is now referenced to absolute zero.

Screening tests in the OVERS arc facility (i.e., low flux, long time high enthalpy task) are continuing in an effort to determine the char characteristics of Avcoat 5026. A series of tests have been performed in the OVERS arc on materials designated as follows: 5026-22, 5026-23, 5026-29 and 5026 (old system) in which Harcure A, a plasticizer, has been purposely omitted from the formulation. All tested samples produced char layers containing both horizontal and vertical cracks. Samples evaluated at the low heat fluxes (15 to 60 Btu/ft^2sec) had char layers which contracted.

Analysis of the Avcoat X5026-22, Sample T temperature data (given in the 29 May 1962 Bi-Weekly Progress Report) was continued to determine temperature-variable effective thermal conductivity and specific heat. Results for thermal conductivity have been obtained for the heat-conduction model which assumes thermal conductivity is constant from room temperature to 250°F and linear from 250 to 1000°F and that specific heat is constant at 0.42 Btu/lb-°F.

The temperature data for the OVERS run of X5026-22, Specimen S has been reduced. It was intended to heat this specimen with a heat flux of approximately 60 Btu/ft^2-sec which is considerably larger than the 20 Btu/ft^2-sec applied previously to Specimen T, Avcoat X5026-22. Unfortunately, Specimen S was improperly centered in the OVERS arc, and consequently the specimen was not uniformly heated and the temperatures in Specimen S did not rise as high as in Specimen T. The slopes of the temperature histories of Specimen S have been calculated. Effective thermal diffusivities for Specimen S, Avcoat X5026-22 have been obtained using program 1077. Even though Specimen S was not heated uniformly its diffusivity values (0.0029 to 0.0053 ft^2/hr) are approximately equal to those calculated for Specimen T (0.0022 to 0.0058 ft^2/-hr).

A correct check-case was obtained using program 1105 which can be utilized to calculate as functions of temperatures the properties thermal conductivity and specific heat from transient temperature measurements. Further improvements for improving convergence and reducing machine time are currently being programmed.

Additional calculations were made for surface temperature and heat conducted into the specimen ($\dot{q}_{cond}$) from the OVERS test with the Avcoat X5026-22, Specimen T. (The heating conditions were q_{cw} = 20.5 Btu/ft^2-sec with H_s = 5000 Btu/lb.) These calculations differ from those reported in the last biweekly progress report by being based on data reduced at intervals of two seconds. Calculations previously reported utilized data reduced at ten-second intervals. Calculations were made for two assumptions of initial temperature distribution. In one case, a uniform distribution of initial temperature was assumed, while in the second case, the initial temperature distribution was based on a curve fitted through the thermocouple readings of temperature at the start of the test. The effect of these assumptions on the surface temperature and heat flux was discernible only in the first few time steps. A summation was made of the total heat flux into the specimen including values for radiation and transpiration. These results were from 3 to 9 Btu/ft^2-sec below the measured cold wall heat flux.

During the past period work has continued in the areas of low temperature apparatus modification and degradation apparatus assembly. At this time, the low temperature thermal conductivity apparatus is 90 percent completed. The necessary effort to complete this apparatus involves parts which have been ordered and initial calibration runs. The low temperature specific heat remains at the 50 percent completed status because of a minor problem which has developed in the apparatus assembly.

The heat of degradation apparatus has been completed. A schematic of the apparatus is shown in figure 1 . A description of the operation and results of initial calibration are being prepared in report form at present for inclusion in our next biweekly report.

The thermal conductivity of eight sets of Avcoat 5026 samples have been completed during this period. Twelve determinations of specific heat were also completed. Included in the specific heat determinations was a set of four degraded Avcoat 5026-22 specimens. The results of these tests are given in the analysis section of this report.

A mathematical model has been developed to determine the rate of penetrations as a function of skin thickness for micrometeorite impacting the Apollo capsule. From these results, the reliability of the system will be predicted as a function of Avcoat thickness to evaluate whether the proposed design is adequate to defeat the meteoroid hazard.

Avcoat 5026 plates have been ordered and are currently being bonded to aluminum backup plates. A series of tests with glass and aluminum projectiles of mass about 50 to 100 mg are planned at velocities around 20, 000 ft/sec. These results will be used to predict penetration scaling laws in terms of projectile material for stony meteoroids.

The two sets of optical property samples (Avcoat 5026-Ap113-73F and P) have been measured during the past period. The data is being prepared for IBM key-punching and submission to a small computer program which will provide corrected data.

There is attached a flow diagram (Fig. 1a) to indicate the present and proposed scheme of optical property data reduction. The present scheme requires mechanical data reading which is converted to typed raw data by the electrotyper. It is then, manually key punched and submitted to the program. The proposed scheme will eliminate all manual operations and provide direct IBM punch card output. The latter scheme will allow a greater accumulation of data which will be required to establish measurement accuracy, data reliability, and statistical analysis to detect variations due to material formulation variations.

Tasks initiated include the following:

a. IBM 1620 computor programs for statistical analysis of material property measurements,

b. Definition of reliability criteria in terms of failure success,

c. Development of math model for reliability estimation, and

d. Generation of time phased flight profile.

Task in process include a) Survey of past structural reliability demonstration techniques, and preliminary trade-off of cost versus techniques requirements.

a. Tasks Initiated:

1) Investigation of analytical procedures including sampling selecting of techniques for deriving final material physical and thermal properties for Apollo ablative materials.

2) Support a designed program for an investigation of optimum adhesives, surface preparations, joint designs and fasteners for the bonding and/or fastening of ablative material in the Apollo program.

b. Tasks Completed:

1) Analysis and estimates of some physical and thermal properties of an experimental Avcoat 5026 type ablative material for preliminary design purposes.

2) Analysis of Avcoat II casting process for reproducibility and consistency with physical and thermal property estimates for back-up procedural experience to be applied to Apollo material evaluation test programs.

A rough draft of the test procedure portion of the General Environmental Criteria is completed and being reviewed.

A preliminary test method for radiographic inspection of Apollo heat-shield tiles, Avco at X-5026, was developed and released to quality control for initiation on test panels.

The End-Item Test Plan, RAD-SR-62-110 and the Procedure for Control of Inspection, Measuring and Test equipment RAD-SR-62-106 have been completed and submitted to NAA/S&ID. One two-inch thick brazed honeycomb test panel has been received for evaluation and radiography. The corresponding test method for 1/2-inch thickness is, therefore, being rewritten in coordination with material engineering.

Material Engineering has submitted probable sources of supply on base materials. Existing documents and procedures are being reviewed to assure vendor surveillance up to the requirements of NCP200-3.

The Qualification Test Program Plan RAD-SR-62-99 (Part IIA) has been completed and submitted to NAA/S&ID. A test plan is being prepared to help develop and qualify Avcoat X5026 as an ablative material. The plan calls for exposing samples to temperature, humidity and altitude conditions and determining the hyperscopic and tensile properties.

Mechanical vibration testing of a 12-inch by 18-inch substructure panel was temporarily delayed as vibration exciters were not available. The equipment is being set up once again and the instruments calibrated.

C. MANUFACTURING

1. Tool Design

a. Master Facility Tools

Tool designs of the forward and crew compartment master facility tools await appointed release to tool manufacturing per schedule.

b. Other Tool Designs

All other tool designs are progressing as scheduled. Preliminary tool design study continues in areas of needed tooling.

2. Tool Manufacturing

The rough base structure for the aft compartment master facility tool has been completed, is normalized, and awaits coordination with NAA/S&ID furnished master tooling as scheduled.

3. Tool Coordination

a. NAA/S&ID Supplied Tooling

The master facility tool, for the aft compartment, supplied by NAA/S&ID, has been received in good order and is in temporary storage awaiting scheduled coordination purposes.

4. Facilities

No input.

D. ADMINISTRATION AND DOCUMENTATION

During this period a major effort of planning documentation was completed and submitted to NAA/S&ID. The completed reports and plans are as follows:

1. RAD-MS-62-68 "Program Plan for Apollo Boilerplate Flight Test"

2. RAD-SR-62-115"Apollo Heat Shield Program Plan"

3. RAD-SR-62-113 "Apollo Heat Shield Test Plan"

4. RAD-SR-62-112 "Apollo Heat Shield Quality Assurance Program Plan"

5. RAD-SR-62-111 "Facilities Plan for Apollo Command Module Heat Shield Ablative Panels"

6. RAD-SR-62-106 "Apollo Heat Shield Procedure For Control of Inspection, Measuring, and Test Equipment"

7. RAD-SR-62-99 "Apollo Heat Shield Reliability Plan--Part IIA Qualification Test"

8. RAD-SR-62-110 "Apollo Heat Shield End-Item Test Plan"

9. RAD-M-62-2 " "Work Statement For Apollo Command Module Heat Shield Ablative Panels"

10. RAD-SR-62-117 "Phase I Bi-Weekly Progress Report" Period, 28 May to 10 June 1962, Dated 12 June 1962

11. The "PERT TWX Bi-Weekly"

12. "Monthly Financial Report"

13. "Monthly TWX Financial Report

In addition the following still motion picture photographic documentation was made and submitted to NAA/S&ID: a) Fabrication of low temperature ablative material cylindrical samples by the impregnation and rolling method, b) Fabrication of high temperature ablative material cylindrical samples by machining and bonding method, and c) Exterior views of the Lowell facility.

II. PROBLEMS AND ACTIONS

The problems presented in this section are those which threaten to impair program implementation in accordance with schedule requirements. The decisions, inputs, or other actions required to resolve each problem area are presented. This section does not attempt to identify all areas that require further definition, clarification, and/or coordination but rather those areas requiring action within the immediate future.

A. DESIGN

1. Heat Transfer

No reply has been received from NAA with reference to the items discussed at the May 16 and 17 meeting. Nor has NAA commented on the discrepancies pointed out in the previous biweekly progress report between the heat-transfer predictions of NAA and Avco.

The main problems in the study of species radiation from the boundary layer continue to be material properties, ablation products and computer program modifications. Some data on material properties has been obtained. Some simplified theoretical approximations for other properties are being developed.

2. Thermodynamic Analysis

Lack of data previously requested in biweekly progress reports is beginning to affect not only the thermal design effort but also the analytical studies associated with heat-shield reliability. Urgently needed are complete definitions by NAA/S&ID of the following:

a. Ascent and abort trajectories

b. Drogue and parachute deployment sequence to include descent velocities from an altitude of 100, 000 feet to impact.

3. Structural Studies

a. Problem

Stresses and deflections of substructure and ablator panels under combined temperature and load conditions cannot be properly computed due to lack of knowledge of time sequence of pressures and rigid body loads for ascent abort, and re-entry conditions.

b. Action

Request has been made to NAA/S&ID to supply this information.

4. Engineering Design

a. Problem

Interface control procedure must be established by NAA/S&ID.

b. Action

Request has been made to NAA/S&ID.

The following information is still required from S&ID:

a. Heat-shield penetration control drawing

b. Details of forward compartment structure

c. Details of aft compartment corner

d. Details of spring-loaded doors

e. Details of crew compartment windows and escape hatch

The above information has been requested from NAA/S&ID.

B. MATERIALS DEVELOPMENT AND EVALUATION

1. Materials Development

The problem of fissuring and weakness of the char layer under low flux heating conditions continues to receive top attention.

Additional investigation has shown that the phenolic microballoons lose approximately 7 percent volatiles when heated in argon or when heated in a vacuum and that the volatiles are mostly water. The most significant step to correct this situation is to vacuum dry the microballoons. This has been initiated.

Longer post cures may be required. Panels in different stages of post cure have been submitted for chemical analysis to determine the percent residual volatiles and their identification: (anhydride, acid, expoxide, water, etc.)

The volatile content may be reduced by reducing the amount of phenolic microballoons.

The impregnator is urgently needed for the processing of Avcoat 5019 materials. A hand process is currently being used.

Existing silicones may not have sufficient elasticity at -260°F or strength to withstand thermal and mechanical forces present in the full scale vehicle. Modification of existing silicones may be required. The use of a foamed structure at the glue line will be of benefit. Samples of silicone resin that foams in place have been received and foam sheet stock ordered.

X-5026 heated to above the temperature at which degradation begins gives off copious amounts of volatile products. Since the toxicity of these gases has not been determined, mechanical properties tests at high temperatures have been discontinued temporarily. Hoods and exhaust ducts have been requested to vent these gases from tensile machines and permit testing in the higher temperature ranges.

2. Materials Evaluation

The purchase of test equipment for carrying out the objectives of this phase of the program is being held up and awaits approval of request for special test equipment.

Some difficulty is still being encountered in covering the enthalpy range uniformly. By properly adjusting the air flow this range can be completely covered.

Design on the new radiation simulation system, which will have a higher heat-flux capability and which will produce a more uniform heat flux than the present system, is about 60 percent complete. Purchase of the long head time and items for the radiation simulator; e. g. , parabolic minors, etc. , is being held up pending the approval of the request for special test equipment.

3. Quality Assurance

The purchase of test equipment for carrying out the objectives of this phase of the program is being held up and awaits approval of request for special test equipment.

NAA's requirements on random vibration input are not yet defined. Vibration exciters and temperature chambers are not available to the extent needed to meet the test time schedule.

C. MANUFACTURING

Load time for acquiring production support facilities, needed immediately to equip and install ablative panel pilot plant for scheduled operation, is tightening. Need for approval by NAA/S&ID, facilities list, is the only applicable action at this time.

D. ADMINISTRATION AND DOCUMENTATION

1. Documentation Requirements

a. Problem

Report requirements are being amended in accordance with documents of later issue that have not been established in the procurement specification or letter contract.

b. Action

All correspondence and reports by NAA/S&ID and Avco should contain as an attachment any reference that has not been previously established especially if in any way the scope or costs of the definitive contract are affected.

2. Revisions of Documentation

a. Problem

In anticipation of required program changes, it is necessary that the Avco planning documents previously submitted to NAA/S&ID to be consistent with the definitive contract in order that program changes may be reflected in an approved set of planning documents.

b. Action

A plan for a sequential revision by Avco, NAA/S&ID, and joint review and NAA/S&ID approval of all plans needs to be established. Revision of specific plans should be initiated just prior to others consistent with scheduled program implementation activities.

3. The following plans and reports should be completed.

a. Revised application for facilities consistent with the NAA/S&ID/Avco joint review.

b. Revised special test appendix to reflect the discussion and agreements of the above facilities review and the revised STE format presented by NAA/S&ID.

c. Submittal of biweekly PERT reports and phase I biweekly progress report.

d. Application for special tooling.

e. Plan for revision of Avco planning documents to be consistent with the work statement of the definitive contract.

III. FORECASTS

This section presents a forecast of the significant events which are expected to occur during the next biweekly reporting period.

A. DESIGN

1. Heat Transfer

During the next period it is planned to make further comparisons betwen the predicted and experimental results.

The analysis of the heating along the windward meridian will be evaluated for angles of attack of 28 and 30 degrees.

A literature survey will be started to review the theoretically predicted emissivities of air. At present the available results include Kivel & Bailey (Avco-Everett RR-21), Breene, et al. (GE R61SD020), and Thomas (JAS April 1962) who has computed the air emissivities based on the absorption coefficients of Meyerott, et al. (AFCRC - GRP 68).

The boundary-layer program will be further modified to account for multi-component species. This problem will probably span several reporting periods. The properties study will continue and some preliminary formulations will be developed and used.

An analysis of the heat transfer to the separated flow region will be initiated.

Experimental total (convective plus radiative) heating data will be obtained from the Avco shock tube test facility. This data will be factored into the analysis as soon as possible.

2. Thermodynamic Analysis

Continued emphasis will be placed on evaluation of the charring ablation thermal analysis techniques. On receipt of additional ground test information, the evaluation will be changed as required.

During the coming report period, more detailed transient calculations for orbital and space flight conditions will be made using a newly developed space flight and orbital temperature digital computer program. Modifications to the computational processes will be made as required.

An analysis of the cold temperature area in a hemispherical forecone will be undertaken.

The effect of the heat input variations will be further investigated by extending the analysis to other vehicle locations and machine programs.

Work during the next period will be primarily aimed at re-evaluation of present re-entry heat-shield design to account for material property and heating variations or revisions.

Preliminary analysis of various regions of the body where 2 dimensional heat flow problems may exist will begin. Initially, this study will consist of analyses of attachment schemes.

Work will continue toward calculating the influence of radiative heating on charring plastics.

3. Structural Studies

The analyses described in section IVA3 will be continued and additional analyses started to define critical stress and strain conditions for the heat shield.

Work will be continued on formulation of the detailed structural development test plan, especially for ablator panels attached by mechanical fasteners and for bonded panels subjected to heating.

Analyses will be started to evaluate a reference heat-shield design, which will be presented during the next reporting period.

Analyses will be made to determine mode shapes and frequencies of the vibration test panels in order to correlate testing and analysis of the specimens. Mechanical vibration tests will be started if test equipment is made available. Honeycomb panels measuring 24 x 36 inches will be ordered for vibration tests.

Test plans for shock testing will be written, as well as plans for acoustic testing at an outside facility.

Avcoat 5019 and 5026 turbulent tubes will be fabricated during the week of 25 June. Tests are scheduled to begin on 2 July.

4. Engineering Design

Representation by the Avco Design Section should be at NAA/S&ID starting on or about 9 July.

It is planned to prepare a preliminary reference design during the early part of July. (This will not include tile arrangement.) This will enable both S&ID and all Avco sections to continue their analysis on a common basis until new test information is available.

The "radial wedge" tile design will continue to be studied for feasibility.

Heat-shield fairing optimization studies will continue as new thickness values are received.

Tile arrangement and fastener conceptual studies will also continue.

Design investigation of the one square foot tile vehicle will continue.

B. MATERIALS DEVELOPMENT AND EVALUATION

1. Materials Development

a. More large batches will be made to establish optimum density at the higher mixing temperatures.

b. Studies on mixing and molding variables will continue.

c. Sufficient phenolic microballoons will be dried by the new vacuum process to mold 12 x 12-inch panels.

d. Different post cures will be evaluated.

e. Work will continue on development of formulations having lower mass loss in the arc.

1) Higher fiber content.

2) Lower microballoons.

f. Work will be started aimed at developing a dry blended molding material.

No additional honeycomb panels have been received from NAA/S&ID. Therefore, no panel shipments will be made in the next period.

Physical test specimens, including peel type, will be made. Environmental test panels for Applied Mechanics will be processed, using representative adhesives. Literature survey of low and high temperature resistant adhesives will continue.

Preliminary tests on candidate paints and components will continue with initial emphasis on the effect of vacuum on optical properties. The effect of ultraviolet radiation, ascent heating, and aging will subsequently be evaluated.

Analysis of the continuously weighed decomposition runs will be completed during the next period.

Work outlined above will continue during the next reporting period. A preliminary correlation between density and ultrasonic velocity will be prepared.

More tests will be conducted; some with a high speed motion picture camera taking pictures of the front surface to visually see if shearing of the charred surface occurs. A measure of the reflectivity of the charred 5026 material will be obtained from 0.2 to 2.75 microns enabling an estimate of the true temperature to be made.

A number of OVERS test samples (approximately 20) have been prepared. All samples are variations of 5026-22 in which various ingredients have been omitted from the formulation in order to determine if any of these are the cause of the char instability observed in low flux testing. These samples are to be evaluated in the next reporting period.

Design of the experimental apparatus will be continued during the next reporting period.

Two specimens each of Avcoat X5026-22, Avcoat X5026-23 and Avcoat X5026-29 have been instrumented and will be tested on the OVERS arc facility in the coming reporting period. If the temperature data is reduced in time, the analysis of this data will be begun for effective thermal properties, char characteristics, and surface temperature.

A calculation is in progress to evaluate the ability to predict emissivity of the surface using the results of computer program 958. Input for this program is being generated using computer program 640. Internal temperature histories are being obtained for a hypothetical case in which the emissivity of the sample has been assumed. It is assumed that a pulse of heat is transferred to the sample, and then the end heating is discontinued, the sample cooling by radiation. Program 958 will be used, employing these temperature histories as input, to determine the surface temperature and the end heat flux in the cooling process. Evaluation of this procedure will be based on the ability to approximate from these results, the value which was initially assumed for the emissivity.

It is planned to continue testing of Avcoat 5026 formulations submitted for evaluation. It is planned to have the results of thermal conductivity measurements of degraded Avcoat 5026.

It is also planned to have the description of the operation and initial results obtained from the degradation calorimeter.

Several impact tests should be accomplished within the next reporting period. Some of the results of the theoretical analysis should also be finished during the next reporting period.

It is anticipated that computer programs for analysis of material property data will be completed within the next two weeks along with the survey of Structural Reliability Prediction.

The test procedure portion of the environmental criteria will be finalized and conform to any later information received.

A sweep-and-step resonance survey of the 12 x 18-inch substructure panel will be started shortly. The finished panel-adapting fixture is scheduled for delivery in mid-July.

C. MANUFACTURING

1. Tool Design

a. Master Facility Tools

Forward and crew compartment master facility tool designs will be released to tool manufacturing when the schedule requires.

b. Other Tool Designs

All other established tool designs, and continued tool design studies, will progress as scheduled.

2. Tool Manufacture

Coordination of the in-process aft compartment master facility tool with the NAA/S&ID furnished control master will start and progress to schedule.

IV. ANALYSIS

A. DESIGN

1. Heat Transfer

Many problems have arisen in the comparison of NAA and Avco heating predictions. The discrepancy between NAA and Avco heating predictions along the 90-degree meridian appears to be inconsistent. For the case of trajectory 1, Avco's prediction is approximately twice that of NAA. For the case of trajectory 4, this is reversed and NAA heating is higher than Avco's prediction. In order to obtain a better understanding of the discrepancies both longitudinal and circumferential heat-transfer distributions are shown in figures 1b and 2. The experimental data shown from Langley should be increased by approximately 15 percent due to the fact that the data is under hot wall conditions and must be divided by the recovery factor to be compared with cold wall data. When this is done the comparison between Avco's predictions and experimental results is good. This cannot be said of NAA predictions.

In order to determine if there is a trajectory where the heating can be turbulent, local Reynolds numbers were calculated for trajectories 2, 3, 5, and 6 and the results are shown in figures 3 through 6. Only during the latter part of the trajectory, where the heating is low, does the flow become turbulent.

The cold wall, convective heating has been calculated for points along the 90-degree meridian for two re-entry trajectories (points designated by NAA as 12, 13, 14 and 15 and trajectories designated by NAA as 1 and 4). Heat transfer to these points was obtained in the following manner.

Heating was calculated using the reference enthalpy method for the Apollo shape at 0 degree angle of attack having the pressure distribution at 33-degree angle of attack as determined from JPL test data. This approach gives the correct external flow at the points and only the surface distant from the stagnation point to points along the 90-degree meridian would be in error. However, there should be little difference between the surface distance from the stagnation point to points along the 90-degree meridian at 0-degree angle of attack and at 33-degree angle of attack.

Figures 7 through 14 show the cold wall, convective heating for a wall temperature of 5000°R. Also shown on these figures is the heating obtained by NAA for a wall temperature of 5000°R.

Circumferential convective peak heat distributions for the rear portion of the body are presented in figures 15 through 18. Also shown on these figures is the heating obtained by NAA.

The method of Kaattari has been used to calculate the shock shape in the plane of symmetry. This shape and previous results for shock detachment at the stagnation point have enabled calculation of shock detachment and slope at several stations of interest on the blunt face of the vehicle.

To give an indication of the accuracy of the results the shockwave angle versus body azimuth angle is shown in figure 19. It compares Kaattari results with measurements of schlieren photographs of wind tunnel tests. The agreement is about as good as that previously shown for stand-off distance at the stagnation point.

The radiative equilibrium heating was computed for the NAA specification points 2, 3, 4 and 5 along the zero meridian on the spherical face for the NAA re-entry trajectories 1 and 4. The time histories of the radiative heating are given in figures 20, 21, and 22.

For the initial approach the empirical curve fit to the Kivel and Bailey tables of radiative emissivity of air has been combined with the results of the shock detachment distance as a function of stagnation density ratio resulting in the following approximation:

$$q_r = 131\, K^1 \frac{\rho_\infty/\rho_o}{\rho_s/\rho_o}\left(\frac{\rho_{field}}{\rho_o}\right)^{1.15}\left(\frac{T_{field}}{10^4}\right)^4 \rho^{4.35\left(\frac{T_{field}}{10^4}\right)}$$

where K^1 is the slope of the shock detachment distance normal to the body at the point in question as a function of the stagnation density ratio.

ρ_{Field} and T_{Field} - refer to the temperature and density at any point in the field (constant in a given slab)

The semi-infinite slab assumption was used throughout the analysis. The slab has been assumed to be tangent to the body point in question. Since the properties vary normal to the body the arithmetic mean radiation between the body surface and shock wave has been assumed. In essence the field has been divided into two slabs with slab 1 possessing the properties behind the shock wave and slab 2 possessing the properties of the body surface.

The shock shape was determined by the method of Kaatari. The equilibrium conditions behind the shock were solved at the maximum radiation heating points in the trajectories. The radiative heating ratios determined at these points were assumed to be constant for the remainder of the trajectories.

The existing boundary layer program will be modified to solve the species continuity equation. This involves programming the continuity equation and coupling it with the present momentum and energy equations. The required changes are fairly extensive but not difficult conceptually.

The majority of the properties will probably be found by using the hard sphere molecular model. This will not be accurate for all species, but it is simple and requires a minimum of data. The only information needed is the molecular weight and the collision cross section. The Eucken correction for the conductivity can be applied quite simply.

The experimental convective heat transfer data thus far obtained are given in figures 2, 23 and 24.

The stagnation point heat transfer rate measurements at zero degrees angle of attack are shown in figure 23 where it can be seen that the theory of Fay and Riddell[1] is in good agreement with the data. Figure 24 shows the forebody heat transfer rate measurements obtained at zero-degree angle of attack. The theory of Kemp, Rose, and Detra[2] is in good agreement with the experimental data.

Preliminary forebody data obtained at 33-degree angle of attack along the windward-leeward plane are shown in figure 2, where it can readily be seen that the heat-transfer rate reaches a maximum in the vicinity of the 33-degree angle of attack stagnation point and decreases steadily with increasing body distance. At present there is insufficient data to exactly determine the 33-degree angle of attack stagnation point; however, it is expected that this point will be defined during the next reporting period.

---

[1] Fay, J. A. and F. R. Riddell, Theory of Stagnation Point Heat Transfer In Dissociated Air, Journal of the Aeronautical Sciences, Vol. 25, No. 2 (February 1958) pages 73-85.

[2] Kemp, N. H., P. M. Rose, and R. W. Detra, Laminar Heat Transfer Around Blunt Bodies In Dissociated Air, Journal of the AeroSpace Sciences, Vol. 26, No. 7 (July 1959) pages 421-429.

2. Thermodynamic Analysis

The modifications to the 640-heat conduction program for transient orbital temperature responses have been completed and the program is being checked out. This program makes it possible to calculate the temperature response at a station on a rotating or non-rotating cylinder or cone subject to radiant (solar heating) and one-dimensional heat conduction normal to the surface.

Modifications to the 640-surface recession program are in the early stages of programming. The nature of these modifications were reported in the previous biweekly progress report.

Calculations are in progress to determine the heat shield thickness using the charring ablation program (Program 951). As previously reported, the calculations will cover a range of Q_c = 500 to 40 Btu/ft^2 and will be used to determine possible weight savings by comparison with programs 640 and 1098. No conclusions or comparisons of great detail will be presented until the study is more nearly complete. At the present time roughly 50 percent of the calculations are finished.

Transient lunar or space flight environmental gradients were calculated using a typical thickness of Avcoat 5026. Two conditions were considered to exist before the initiation of minimum temperature environment: 1) maximum steady state temperature conditions for a vehicle orientation such that the sun's rays impinge at a 35-degree angle with the surface heat shield and 2) a typical ascent gradient at the end of boost flight. These results will be combined with other calculations and presented in the next biweekly report.

The analysis of safety factor requirements continued, particular emphasis was placed on the effects of total heat input evaluation errors. Figures 25 and 26 demonstrate the significance of heating on design structure temperature.

It is apparent that small changes in thickness cause large changes in the rear temperature. That is, a slight over design would not result in a large weight penalty for the blunt face area, but a slight under design would be extremely severe in its effect on rear temperature.

The preliminary comparison of Avcoat X-3000 on the conical forebody and blunt face was completed. The comparisons of this material with other candidate ablators are presented in figures 27 and 28.

Values for the molecular constants computed for the $x^1\Sigma_q^+$, $A^3\Sigma_u^+$, $B^3\pi_g$ and $C^3\pi_u$ electronic states of the N_2 molecule, and the $x^3\Sigma_g^-$ and $B^3\Sigma_u^-$ states of O_2 are shown in Table I.

Cubic (and quartic) parabolae were fitted to these data, adjusted by a least squares technique, and the new molecular constants so obtained were tabulated. Table I lists the molecular constants obtained for both cubic and quartic fits to the experimental data. The maximum deviation of the experimental data from these curves is as shown.

The potential energy function for the $x^3\Sigma_g^-$ state of the O_2 molecule is shown in figure 29. The exact RKR points are shown by the squares, and the two analytic forms of the potential function are shown by the labelled curves. The potential function which shall be used for this state is shown by the dot-dash curve. As can be seen, the latter passes through the RKR points in the region where experimental data exists, and is intermediate to the two analytic forms of the potential function. The fits obtained have been unsatisfactory, so far, due to prohibitively large residuals in the logarithms of concentration.

Work started on calculations of wave functions of the vibrational levels in the various electronic states of the principal radiating constituents of heated air. The particular molecule currently being analysed is NO. The calculation involves obtaining the eigenvalues and eigen functions of the Schrödinger equation for each electronic state, using the "exact" values of the potential energy functions.

The eigen value to this equation are those corresponding to the experimental values of energy levels previously reported. For levels beyond this region, an eigen value search technique has been perfected which permits rapid zeroing-in on the required values. A technique for rapidly obtaining the eigenfunctions corresponding to these levels has also been perfected; and evaluation of the wave functions is proceeding. The wave functions so obtained and the overlap integrals computed from them will represent a significant improvement over anything previously published on the subject due to use of exact potential functions and the most recent spectroscopic information. Previous tabulations are incomplete and are based upon the approximate Morse potential energy function. They are also without the benefit of the most recent data on molecular constants.

TABLE I

MOLECULAR CONSTANTS

STATE	MAX. DIFF.	ω_e	$\omega_e x_e$	$\omega_e y_e$	$\omega_e z_e$
N_2	-5.11622834×10^{-1}	2.35755966×10^{3}	$+1.40877626\times10^{1}$	-1.66381861×10^{-2}	
$X^{\prime}\Sigma_g^+$	-3.40733496×10^{-1}	2.35732246×10^{3}	$+1.39464717\times10^{1}$	-3.42738247×10^{-2}	5.87854621×10^{-4}
N_2	2.81722988×10^{-1}	1.46020456×10^{3}	$+1.36052262\times10^{1}$	-3.48658697×10^{-2}	
$A^3\Sigma_u^+$	2.53226255×10^{-1}	1.46051762×10^{3}	$+1.38524719\times10^{1}$	6.23518794×10^{-3}	-1.82671367×10^{-3}
N_2	3.32726850×10^{-1}	1.73403101×10^{3}	$+1.42892276\times10^{1}$	-2.04032807×10^{-2}	
$B^3\pi_g$	3.06298813×10^{-1}	1.73429885×10^{3}	$+1.44487701\times10^{1}$	-4.89510317×10^{-4}	-6.63792348×10^{-4}
N_2	8.57143090×10^{-1}	2.03438786×10^{3}	$+1.62057143\times10^{1}$	-2.44285714	
$C^3\pi_u$	2.05714089×10^{-1}	2.03652536×10^{3}	$+2.08107143\times10^{1}$	-1.92857123×10^{-1}	-3.00000002×10^{-1}
O_2	4.98122090×10^{-1}	1.57987779×10^{3}	$+1.16196923\times10^{1}$	5.28656119×10^{-3}	
$X^3\Sigma_g^-$	3.38396740×10^{-1}	1.48053913×10^{3}	$+1.19782658\times10^{1}$	4.59845002×10^{-2}	-1.23327088×10^{-3}
O_2	5.06109561	7.04864309×10^{2}	$+9.25896282$	-3.00575054×10^{-1}	
$B^3\Sigma_u^-$	1.74436308	7.00337987×10^{2}	$+6.68946491$	-6.06063578×10^{-1}	9.69804837×10^{-3}

3. Structural Studies

During the reporting period the analyses described below were conducted or are in process of being performed.

a. Parametric Study of Mechanical Properties Required for Bonded Ablator Panels in Cold Environment

Parametric studies were completed dealing with mechanical properties required for bonded Avcoat 5026 ablator panels subjected to a cold environment with the outer surface of the ablator at a temperature of -260°F and a linear temperature of 43°F per inch through the thickness of the heat shield. The assumptions used in the analysis were described in the progress report of 12 June. The results are shown in figures 30 through 32, where required 5026 tensile strength, multiplied by a factor 7, is plotted against ablator modulus of elasticity for various values of coefficient of expansion. Each figure is valid for a fixed value of Poisson's ratio. The geometry for which these curves apply is shown in figure 30. Other ablator thicknesses were analyzed, but the most severe stresses were found for a 0.2-inch ablator. The factor n is intended to represent the effect of additional stresses imposed on the ablator by substructure restraints such as stringers, frames or rings. A value of n equal to unity means that the only ablator restraint comes from thermostructural interaction between the ablator and the honeycomb substructure. It was estimated, rather arbitrarily, that the additional restraints will approximately double the ablator stresses, and consequently the n value reflecting this case is equal to 2. This situation is found on the crew compartment but not the aft compartment. The curves shown in figures 30 through 32, compared with preliminary Avcoat 5026 properties (see pages 83 and 84 of 31 May progress report), indicate that it will be possible to obtain the required property combinations for Avcoat 5026.

Similar analyses are being performed for Avcoat 5019 and for the Epoxylite 5403 bond.

b. Buckling of Unbonded Ablator Panels During Re-entry

Analyses were performed to determine mechanical fastener spacing required to prevent buckling of an unbonded ablator panel surrounded by adjacent panels with no initial gap between the panels. Two Avcoat 5026 panels were analyzed: (1) a 12 x 12 x 1-1/2-inch panel located at point 1 on the Command Module and (2) a 12 x 12 x 1 inch panel located at point 5. The substructure for both cases was equivalent to an 0.060-inch sheet of PH 15-7 Mo(TH 1050) sheet, corresponding to a honeycomb with 0.030-inch face skins. Thermal thrusts in the ablator resulting from the heating encountered on trajectory 1 were computed as functions of time and are plotted on the curves marked N_T in figure 33 for point No. 1 and in figure 34 for point 5. The curves labeled N_{CR1} represent a panel with a mechanical fastener in each corner buckling as shown in the upper sketch of figure 35. The curves labeled N_{CR2} represent a panel with five mechanical fasteners, one in each corner and one in the center of the panel, buckling as shown in the lower sketch of figure 35. Buckling was predicted using temperature-dependent material properties varying through the thickness of the ablator. For the panel with five mechanical fasteners the finite-difference method was used to obtain the critical thrust. The temperature gradients used in these analyses were those predicted from NAA/S&ID heating curves furnished in the Apollo ablator panel procurement specification.

The intersection of the critical curves with the thrust curve indicate the times in the trajectory when buckling will occur. For point 1 a 4-point attachment scheme will buckle at time equal to approximately 800 seconds, just prior to the second heating pulse, whereas a 5-point attachment scheme will buckle at time equal to 950 seconds, soon after the second heating pulse. For point 5 the 4-point scheme will buckle at time equal to 400 seconds, after the first heating pulse, whereas the 5-point scheme will buckle at time equal to 600 seconds, still after the first pulse but prior to the second. The critical curve for a panel with 8 fasteners, one at each corner and a symmetrical arrangement of 4 fasteners near the center of the panel, was obtained after figures 33 and 34 were drawn. This curve also intersects the thrust curve. These results show that an unbonded zero-gap design is impractical. Analyses are being performed to determine the relief afforded by various gap sizes. From these analyses new N_T curves will be drawn and an assessment made of the practicality of a 5-fastener design with a reasonable gap size.

For the attachment schemes discussed above, all mechanical fasteners except one must be capable of supplying only radial resistance to panel motion relative to the substructure, with the one fastener supplying radial and shear resistance. Fastener loads are determined from the radial component of the edge thrusts. Plots of the radial load are shown in figures 36 and 37 for the two panels described above, expressed in lb/in.^{2} of panel surface area. Fastener loads are obtained by multiplying this pressure by 144 in.^{2} and dividing by the number of fasteners.

c. Substructure Stress Analyses

Various stress analyses of the substructure were conducted by Avco personnel at NAA/S&ID and at Avco in order to define critical stress and strain conditions for the heat shield. The results of these analyses are being evaluated at Avco and will be presented in the next progress report. The purpose of this section is to describe the analyses completed and in progress.

1) Aft compartment heat shield

a) Effect of stiffness of Torus on Toroidal Stresses and Spherical Plate Stresses

A preliminary evaluation of the effect of toroidal corner stiffness of the torus was varied, and the resulting discontinuity stresses computed for the abort loading condition on the aft compartment. For these analyses it was assumed that the aft compartment heat shield is supported by a uniform line load at the torus-sphere junction rather than at four points. This assumption was made because analytical tools are available to handle this problem and because this approach will give an indication of the order of magnitude of the effect produced by the torus.

An IBM solution of this same problem is being run at Avco in order to check the hand calculations performed at NAA/S&ID.

b) Aft compartment heat shield analyzed as plate supported at four points

An analysis was performed of the aft compartment heat shield for the abort condition by treating the spherical plate as a circular flat plate supported at four points and loaded with a uniform pressure. Bending effects will be felt primarily near the edges. The effect of the torus, however, is not reflected in this analysis. Results obtained from this study will include deflections, moments, and stresses in the spherical plate.

c) Outer region of aft compartment analyzed as a flat ring bending out of its plane

An analysis was conducted of the outer region considered as a flat ring supported at four points and bending out of its plane and twisting due to an applied uniform pressure and a uniform line shear applied along the inner edge of the ring. The deflected shape of the ring was assumed and the unknown coefficients in the deflection equation determined by minimizing the potential energy of the system. For a uniform load of 5.6 psi (pressure plus inertia) and a uniform shear of 160 lb./in., the maximum deflection of the outer region, assuming 0.060-inch face skins and a 2-inch honeycomb depth, was 0.839 inches.

d) Outer region of aft compartment analyzed as a shallow spherical shell restrained by inner spherical shell

An analysis is in progress treating the outer region of the aft compartment as a shallow annular spherical shell supported at four points and loaded with a uniform pressure plus a membrane load from the central region of the aft compartment, with this central region also applying elastic reactions to deflections of the outer annular region. The effect of the torus is temporarily being ignored in the analysis. The purpose of this analysis is to obtain stresses and deflections which can be compared with corresponding values from the analysis which treats the aft compartment as a flat plate supported at four points along the edge.

e) Membrane solution for aft compartment under unsymmetrical external pressure

In order to estimate the stresses and deflections of the aft compartment heat-shield substructure under unsymmetrical external pressures, a spherical membrane solution is being generated.

d. Crew Compartment Heat Shield

1) Longitudinal thermal interaction stresses-inner and outer structures

Longitudinal thermal interaction stresses in the forward region of the crew compartment were computed, taking into account relative longitudinal extensional stiffnesses of the inner and outer structures. If the interaction stresses between forward and crew compartment are assumed to be uniformly distributed, margins of safety are high, as shown in figure 38. However, if the stress concentrations in the forward compartment are accounted for, these margins are considerably reduced. As an estimate of this effect, it was assumed that the stress distribution at the junction of the forward and crew compartments was as shown in figure 39, producing the loads shown in figure 40. This effect produced negative margins in the crew compartment, indicating that a gap may have to be placed between the forward and crew compartments.

2) Circumferential thermal stresses in forward region of crew compartment

Circumferential membrane and bonding thermal stresses in the crew compartment heat shield were computed assuming that the honeycomb shell is a ring on 21 supports, with the deformation of the RTV at the stringers relieving the restraints imposed by the stringers when the heated shell attempts to expand. These analyses, although completed, are being checked, since greater bending flexibility was found as compared to a previous estimate.

3) Stresses and deflections due to unsymmetrical external pressures

In order to estimate the stresses and deflections of the forward region of the crew compartment under the unsymmetrical external pressures encountered during abort tumbling, a conical membrane analysis is being performed, temporarily ignoring the presence of stringers. Once the deflections are known, effects of stringer reactions will be incorporated into the analyses to account for support provided by the stringers.

4) Thermal buckling of a typical crew compartment maintenance panel

A buckling analysis of a typical crew compartment maintenance panel was performed to determine if floating fasteners must be used to connect the panel to the vehicle. The geometry used and results obtained are shown in figure 41. The allowable compressive stress, which is the stress at which panel buckling occurs, intersects the applied stress curve at a temperature of 330°F. This indicated that, since a higher temperature will be encountered during re-entry, floating fasteners will be required, since substructure buckling may damage the ablator.

5). Deflections and stresses in a typical crew compartment panel under external pressure

An analysis was performed to determine the load stresses and deflections induced in a typical panel in the aft region of the crew compartment. The panel was assumed to be flat and simply supported. The results indicate that large margins of safety exist under the pressures encountered during abort tumbling if the structure is assumed to be at room temperature.

6) Thermal interaction stresses and deflections in crew compartment at junction of crew and aft compartments

An analysis was made to determine the stresses and deflections in the crew compartment due to thermal expansion of the aft loaded with a radial edge load imposed by the aft compartment. Because of the slotted holes in the crew compartment frames in this region, it was assumed that the frames furnish no resistance to edge deflection of the crew compartment. The analysis will determine the station at which moments reduce to zero, indicating the point at which slotted holes can be replaced by fixed fasteners.

e. Forward Compartment Heat Shield

1) Longitudinal stresses

If no gap exists between forward and crew compartments, longitudinal thermal expansion of the crew compartment will stress the forward compartment heat shield substructure. Since the forward compartment is tied to the inner structure at four locations, stress concentrations like those indicated in figures 39 and 40 will result, and local reinforcement may be required. Definite conclusions cannot be made until the temperatures are known at the time of forward compartment jettison. The problem can be overcome, however, by using a gap between forward and crew compartment

2) Bending Interaction Stresses at Junction of Forward and Crew Compartments

An analysis is being made of the bending stresses induced in the forward compartment due to radial thermal expansion of the crew compartment heat shield. The forward compartment structure is being analyzed as a cone loaded with an edge radial load.

4. Engineering Design

Discussion of sketches and drawings completed or in process is given in the current status section of this report.

Integration of Apollo Documentation Requirements into Avco RAD drafting procedures has been accomplished.

Further preliminary reviews and discussions of the specification plan have been conducted. Until definitive contract information is available, it is not possible to establish firm baselines nor to prepare detailed specifications.

B. MATERIALS DEVELOPMENT AND EVALUATION

1. Materials Development

a. Determination of Volatiles in Phenolic Microballoons

Fifty gram samples of phenolic microballoons were heated in a vacuum of 5 mm. of Hg.

Batch No.	Heating Time	Average Mantle Temperature °C	Average Pot Temperature °C	Percent Volatiles
C281-E	6 hrs. 45 min.	173	150	5.7
C	4 hrs.	170	150	7.6

The greatest percent of the volatiles appeared to be water. Some formaldehyde was detected.

The treated balloons were inspected under the stereo microscope to determine whether the treatment caused rupturing. It was found that no rupturing resulted.

The balloons as compared to the untreated were much darker in color and slightly enlarged. Both the untreated and treated balloons were very resilient.

By use of a Fisher-Johns melting-point apparatus and the microscope, the balloons were brought slowly and then rapidly from room temperature to 150°C and studied. It was found that in neither case did the balloons rupture or become sticky. Thus, the heat treatment should in no way adversely affect the balloon.

A sample of microballoons was similarly heated in Argon. Percent weight loss was about the same and the main product was again water. However, there was a measurable amount of phenol. Since this sample was from another lot of microballoons, it would be that it contained free phenol instead of free formaldehyde. Union Carbide claims that the balloons contain no free formaldehyde, but 0.6 to 0.85 percent free phenol.

b. Effect of Mixing Time on Density

To check the effect of mixing time on density, the Baker-Perkins mixer was used to make up 3500-gram batches of X-5026-22 for molding into 12 x 12-inch panels. Three batches were made up with mixing times of 1/2, 3/4 and 1 hour. Each batch was molded in a 12 x 12-inch aluminum mold using the same procedure currently being used to mold the 12 x 12-inch panels of Hobart-mixed X5026-22 material.

Densities, after post cure of the 12 x 12-inch panels fabricated of X-5026-22 material mixed in the Baker-Perkins mixer were as follows:

Mixing Time (Hour)	Postcured Density (gm/cc)
1/2	0.768
3/4	0.900
1	1.160

During the mixing of the material for the above panels, cold water was being circulated through the jacket of the Baker Perkins mixer so that material would hang up on the walls of the mixer to increase the shear on the material being mixed.

Radiographic examination of the above panels showed excessive fiber balls in the 1/2 and 3/4 hour mixed material and high density silica in the one hour mixed material.

The material mixed for 3/4 hour looked similar in consistency to the material mixed in the Hobart and gave a similar molded density. The uniformity of the molded panel, however, was not comparable to the presently produced panels of X5026-22 mixed in the Hobart.

c. Effect of Cure Temperature on Exotherm

The effect of initial cure temperature on exotherm of 6-inch diameter discs, 2 inches thick of X-5026-22 material was determined. The discs were molded at 425 psi with thermocouples imbedded in the center. The following data were obtained:

Mold Temperature (°F)	Peak Exotherm During Molding °F	Time to Peak Exotherm, Minutes
220	363	50
200	359	100
190	221	110

It appears that the X-5026-22 material must be molded at temperatures below 190°F to avoid excessive exotherm during the molding operation.

d. Dry-Blend Process

A dry blended molding material was made up using a solid epoxy resin and hardener with 1/4-inch chopped glass fibers and microballoons. The resin and hardener were ground and passed through a No. 65 mesh screen individually to obtain materials in particle sizes below 210 microns.

The resin and hardener were charged into a twin shell blender and mixed for 5 minutes. The phenolic microballoons were then added and mixing continued for 5 more minutes. The fibers were added next and the whole batch mixed for a half hour. The resulting molding material appeared to be blended fairly well with no excessive fiber clumps.

The material was charged into a 5.34-inch diameter steel mold heated to 250°F and molded at 535 psi pressure for 70 minutes. A thermocouple was imbedded in the part to check exotherm. The temperature rose to a peak of 305°F after 30 minutes. After the 70-minute cure, the part was cooled and removed from the mold. The part had a density of 1.02. Radiographic examination showed some low density areas to be present. A cross section of the part looks fairly uniform.

Paints and coatings with a variety of solar absorptivity/infrared emissivity ratios of from 0.17 to 13.0 have been formulated. Their stability toward the required environment, however, remains to be evaluated.

The results of elemental analysis of different layers of four char samples that have been exposed to a low flux arc for different periods of time are presented in figure 42. Interpretation of these curves awaits results of analysis of arc samples which have been in an arc for equal periods of time. These results will serve to check the reliability of the present data.

Work to date indicates that ultrasonic testing should prove to be the most versatile of the nondestructive techniques for use with X-5026. If, however, the optimum formulation of this material varies significantly from the present formulation, the present ultrasonic equipment may not be usable. In this event special low frequency equipment and techniques will have to be developed.

2. Materials Evaluation

Table II presents approximate surface brightness temperatures, at 0.65 microns (T_O) as measured with a recording pyrometer and the total emitted radiation values (q_r) as a function of enthalpy. The true temperature and the total emissivity may be computed from the spectral emissivity.

TABLE II

SURFACE BRIGHTNESS TEMPERATURES

H/RT_o	T_B °F	q_r Btu/ft^{2}sec
18.6	2070	13.
19.5	----	13.
23.7	2335	12.
31.5	2745	24.
36.8	3600	92.
38.0	3400	58.
43.2	3235	58.
80.0	3690	102.

A series of OVERS screening tests were performed on materials 5026-22, 5026-29 and 5026-23. Figure 43 presents a view of both the tested and untested specimens. All of these specimens were 1-1/2 inches in diameter containing a centrally located test sample (3/4-inch diameter). The centrally located sample and the outer (guard) material were similar. This configuration insures one dimensional heating of the sample. The spacing between the outer and inner sample was 0.003 inch. Figure 44 shows the outer holder (sectioned) and the centrally located sample. One dimensional heating of the inner sample is evident. Figures 45 through 48 present the sectioned view of the untested and tested samples respectively.

Future tests will be aimed at evaluating the behavior of the charred layer under a wide variety of test conditions. Various materials compositions will also be studied.

a. Temperature-dependent values of effective thermal conductivity, k, have been calculated for Specimen T, Avcoat X5026-22. The ordinary transient heat-conduction equation was used as the model and the specific heat was assumed to be constant at 0.42 Btu/lb-°F. The thermal conductivity curve was calculated assuming k to be constant from 100 to 250°F and linear from 250 to 1000°F. These k-values were obtained by satisfying in a least squares sense the temperature measurements given by thermocouples stepped in depth in the sample (numbers 2, 3 and 4); thermocouple number 1 was the driving temperature. The effective thermal conductivity from 100°F to 250°F was calculated to be 0.119 Btu/ft-°F-hr. This value decreased linearly from 250°F to a value of 0.108 Btu/ft-°F-hr at 1000°F. A comparison of the measured and calculated temperatures for thermocouples 2, 3 and 4 is given by figure 49. The RMS difference between these temperatures is 6.0°F.

Thermal diffusivity data obtained from the OVERS arc test for Specimen S of Avcoat X5026-22 is tabulated in Table III. Although the specimen was not centered squarely in the OVERS arc and two-dimensional heating resulted, some information can be obtained from the data.

TABLE III

EFFECTIVE THERMAL DIFFUSIVITIES FOR SPECIMEN S, AVCOAT X5026-22

From Thermocouples No. 1, 2 and 3		
Avg. Temp., °F	Temp. Range, °F	Thermal Diffusivity, ft^2/hr
128	80 - 561	0.0046
251	90 - 752	0.0045
379	136 - 910	0.0042
478	189 - 1042	0.0039
From Thermocouples No. 2, 3 and 4		
Avg. Temp., °F	Temp. Range, °F	Thermal Diffusivity, ft^2/hr
88	77 - 218	0.0053
124	80 - 350	0.0041
181	95 - 465	0.0034
235	120 - 556	0.0029

b. The theoretical treatment by John and Schick[3] of the ablation of carbonaceous charring materials is presented below in modified form. This theory postulates that ablation is caused by oxidation of the surface material, and that the oxidation rate is limited by diffusion of oxygen through the boundary layer gas rather than by chemical kinetics at the surface. The theory forms the basis for calculation of transient ablation rates for graphite and other materials for which only heterogeneous oxidation (solid to gas) occurs. Since the pyrolysis gases from charring plastics compete with the carbonaceous char for the available oxygen, the analysis for these materials is confined to quasi-steady ablation, where the ratio of the rates of gas evolution and surface mass loss is independent of time.

Continued studies and evaluations will be conducted to support the development of additional computational procedures for supplementary existing design and analysis digital computer routines.

The results of thermal property measurements since the last reporting period are as follows:

a. Thermal Conductivity

Material	Thermal Conductivity Btu/hr ft °F at 250°F
Avcoat 5026-22 (AP7, Plate 47)	0.10_6
Avcoat 5026-22 (AP14, Plate 50)	0.10_2
Avcoat 5026-29 (AP65, Plate 40)	0.12_0
Avcoat 5026-29 (AP71, Plate 41)	0.11_6
Avcoat 5026-29 (AP77, Plate 42)	0.11_3
Avcoat 5026-23 (AP83, Plate 52)	0.09_3
Avcoat 5026-23 (AP89, Plate 53)	0.09_3
Avcoat 5026-23 (AP95, Plate 59)	0.09_2

b. Specific Heat (All values based on four measurements)

Material	Specific Heat Btu/lb °F (R. T. to 500°F)
Avcoat 5026-29 (AP64, Plate 40)	0.38_9
Avcoat 5026-29 (AP70, Plate 41)	0.39_4
Degraded* Avcoat 5026-22 (AP43)	0.22_6

*Degraded by heating to 1500°F in argon atmosphere for 1 hour.

[3] John, R.R. and H.L. Schick, Avco RAD-TR-9-(7)-60-11 (22 June 1960). Confidential

In addition to the data reported above, figures 50 through 58 represent in graphical form the experimental thermal properties reported in previous biweekly reports.

Present indications are that our failure reporting and corrective action system meet the requirements of MIL-R-27542.

DEGRADATION ENERGY CALORIMETER

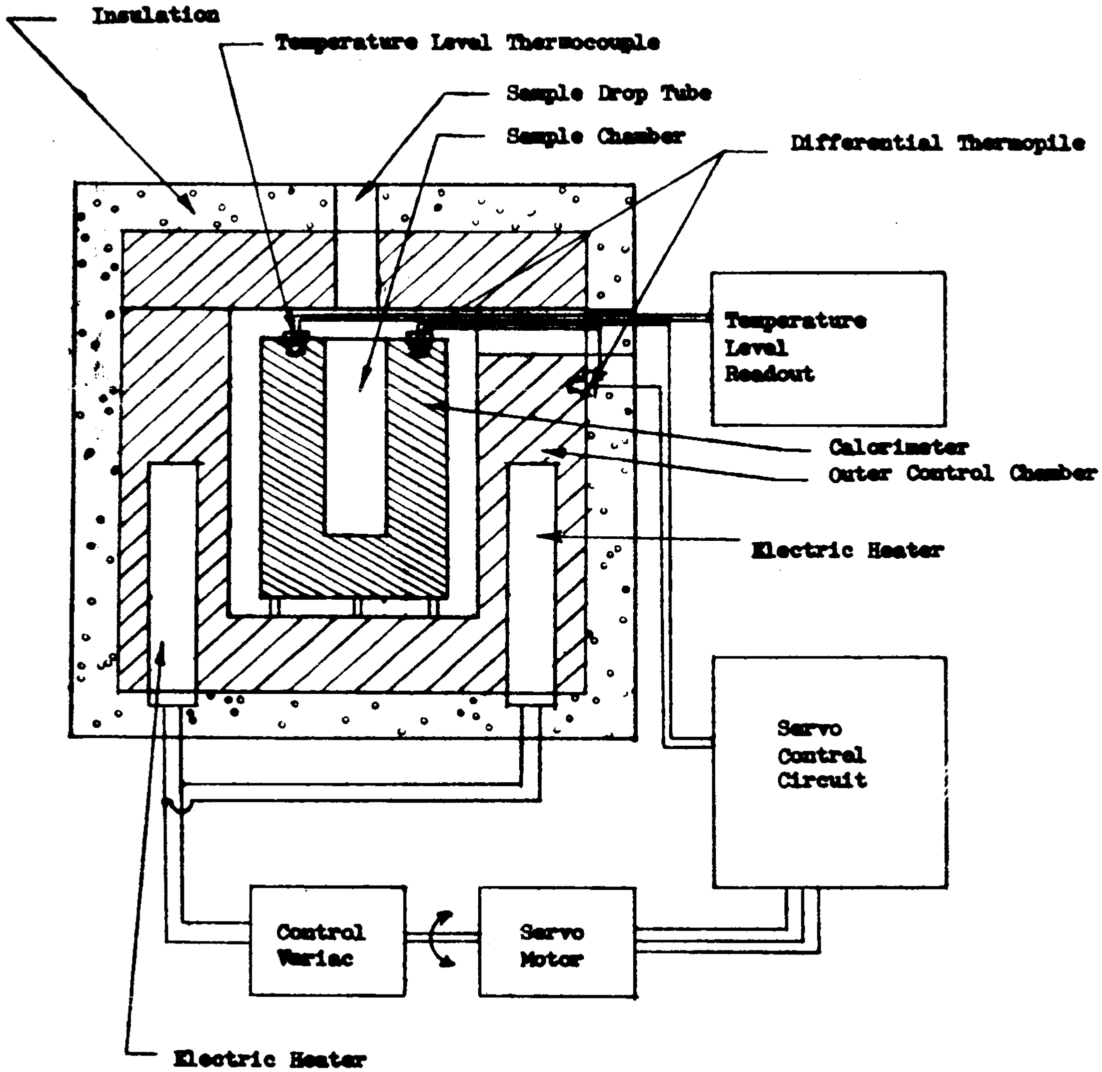

Figure 1

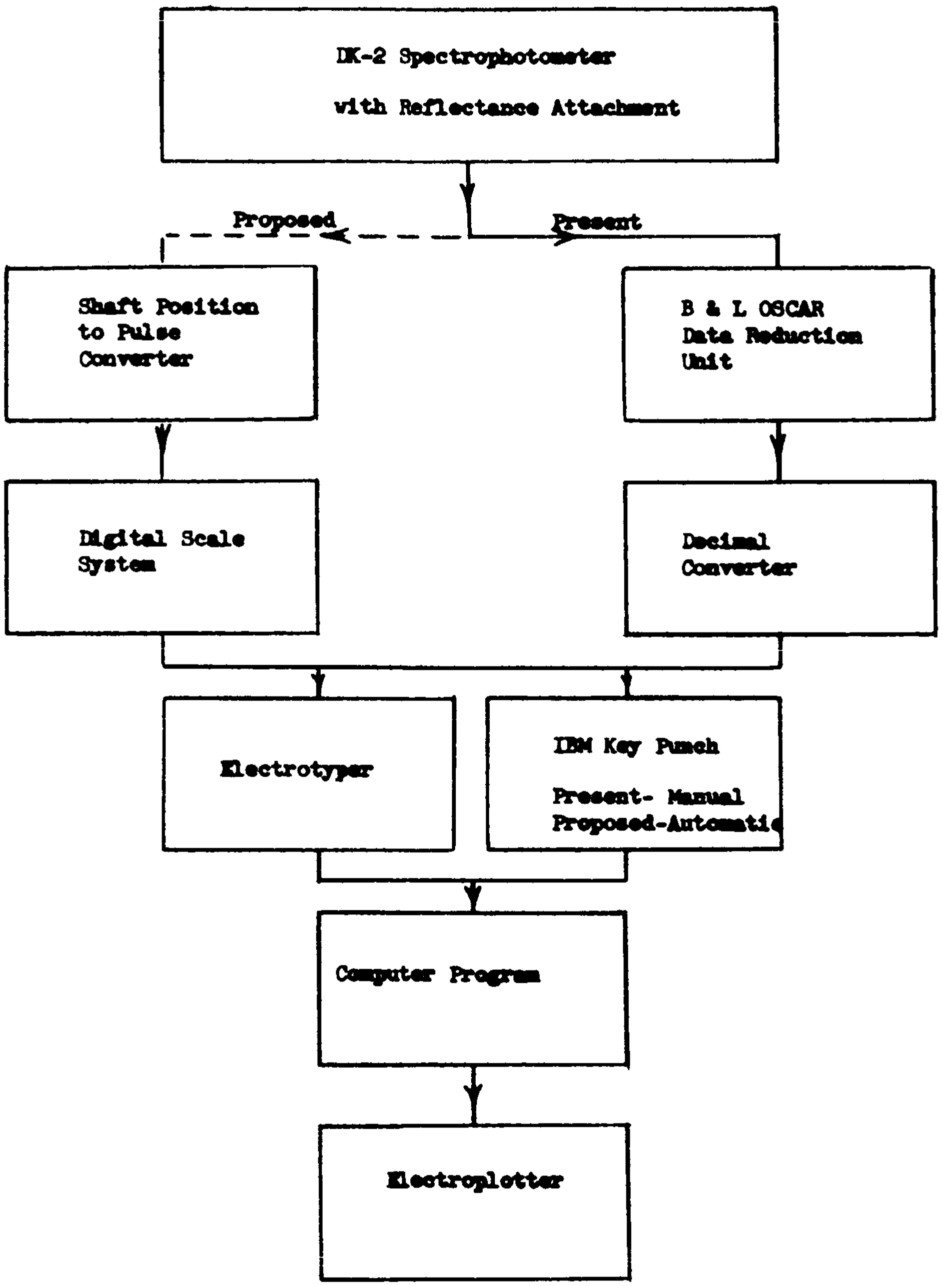

Experimental Optical Property Flow Diagram (0.2 to 2.7 micron wavelength range).

Figure 1A

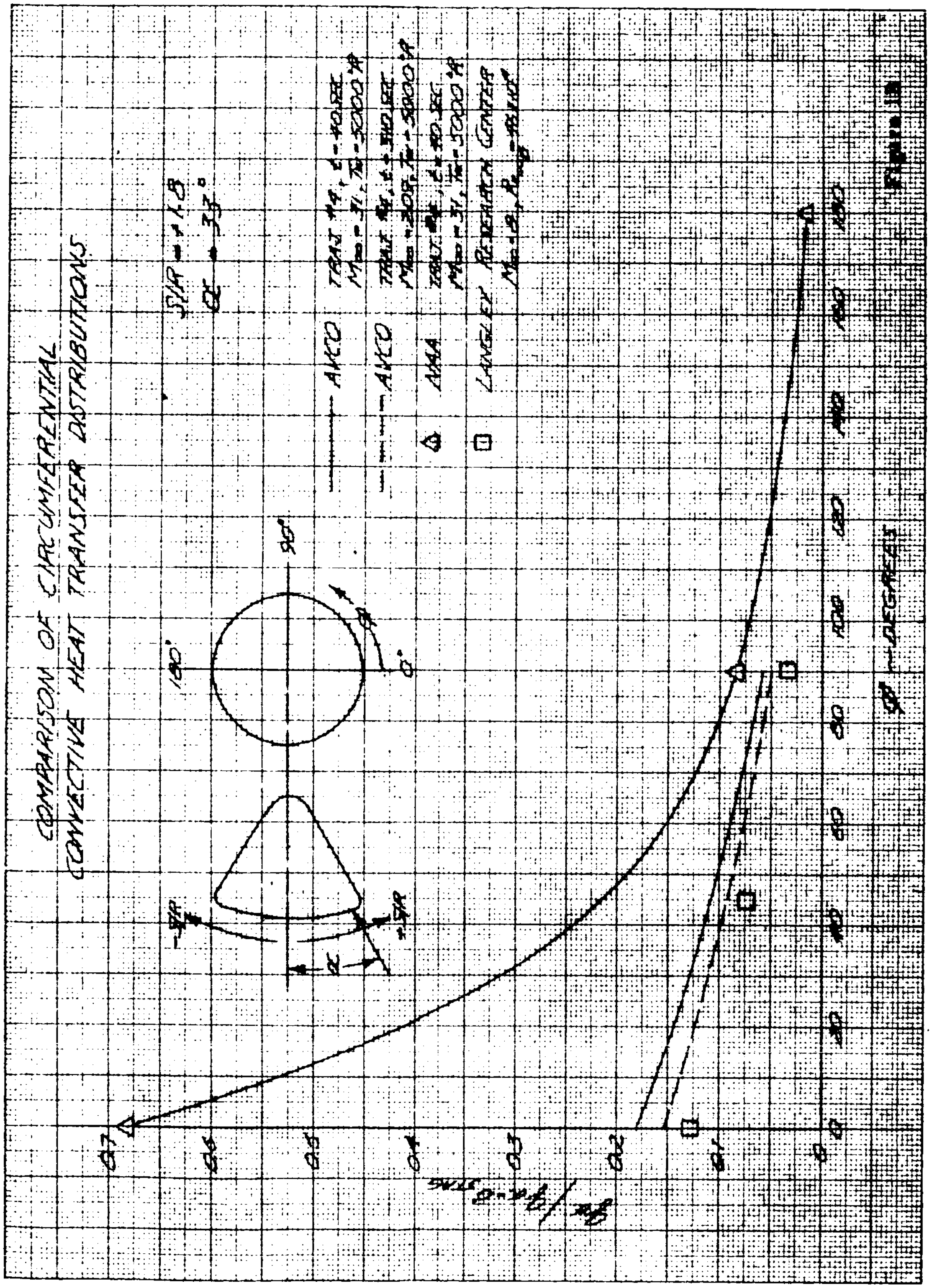
COMPARISON OF CIRCUMFERENTIAL
CONVECTIVE HEAT TRANSFER DISTRIBUTIONS
S/R = +1.8
α = 33°
180°
90°
0°
AVCO TRAJ #4, t = 40 SEC, M∞ = 31, Tw = 5000°R
AVCO
NAA
LANGLEY RESEARCH CENTER
φ — DEGREES

Figure 13

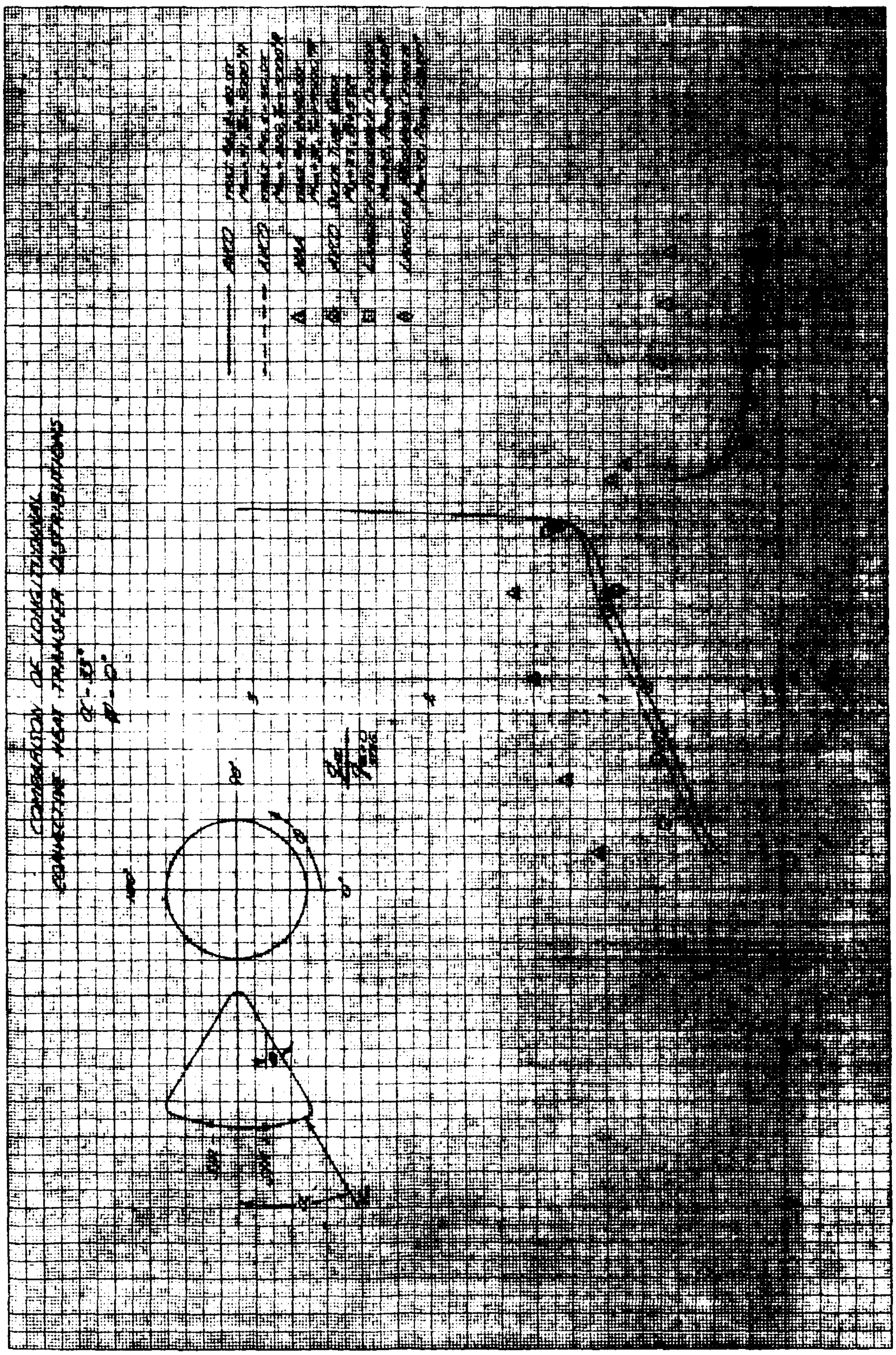
COMPARISON OF LONGITUDINAL
CONVECTIVE HEAT TRANSFER DISTRIBUTIONS

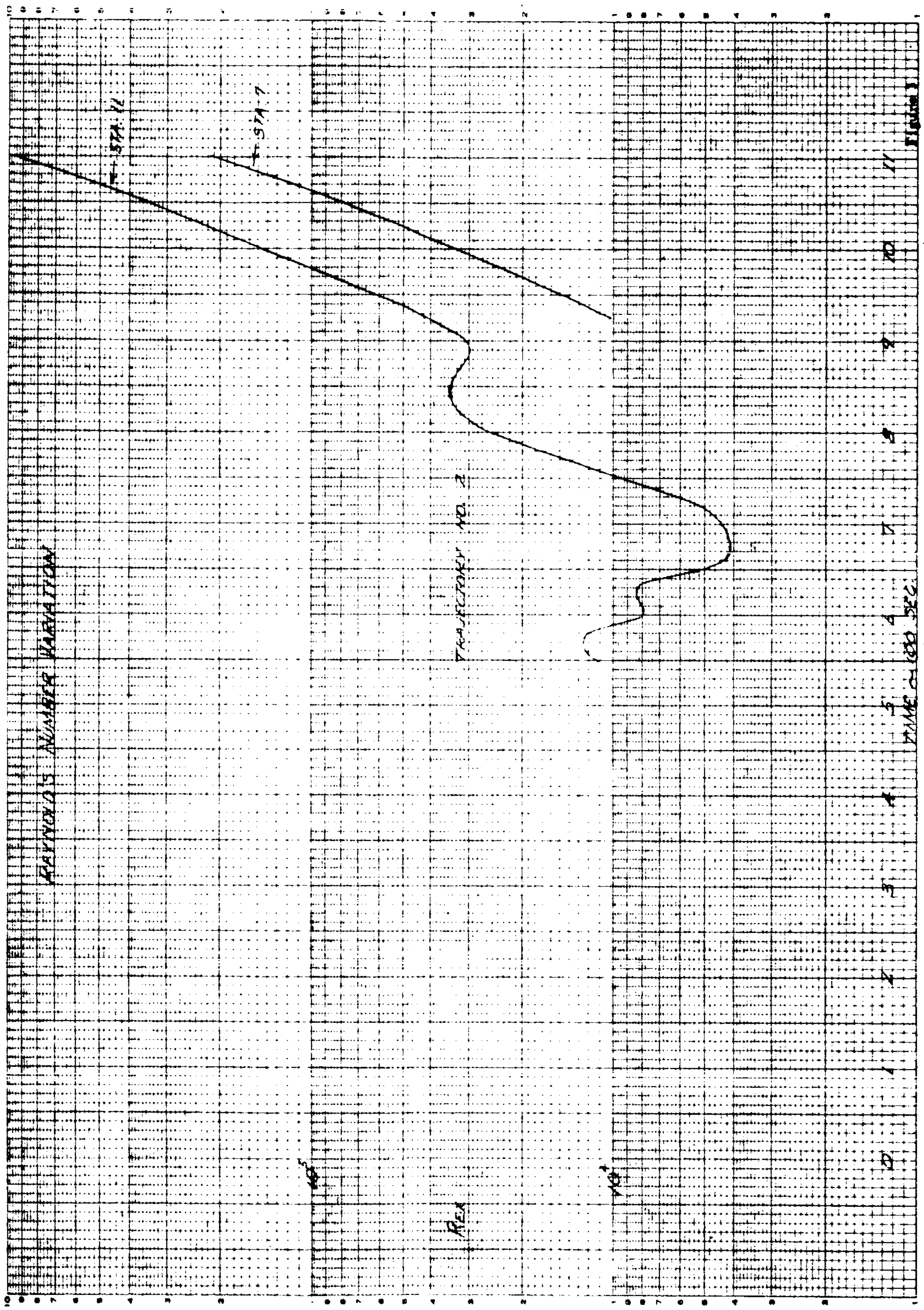
REYNOLDS NUMBER VARIATION
STA. 12
STA. 7
TRAJECTORY NO. 2
TIME ~ 100 SEC
R_{EX}
10^5
10^4

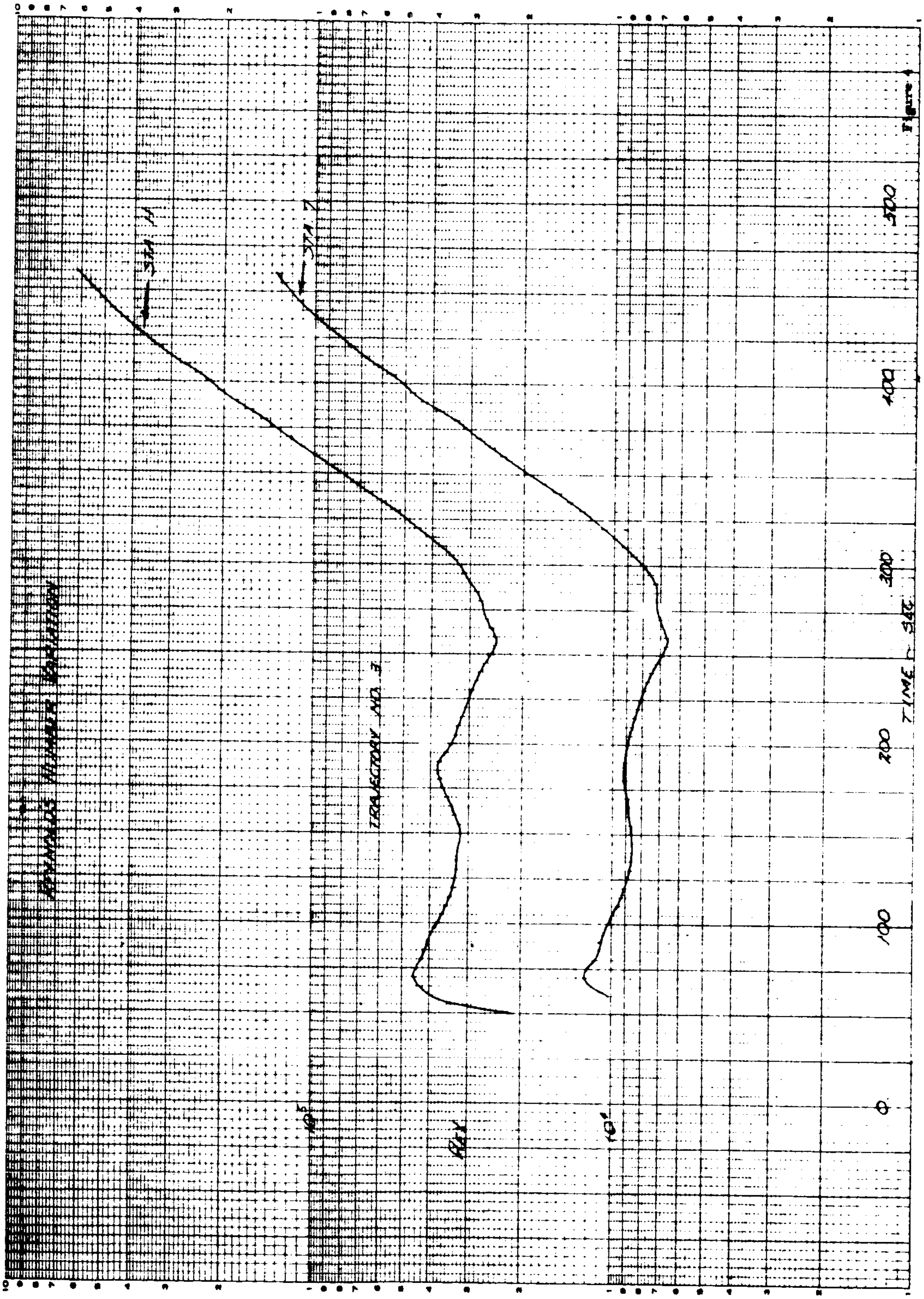
REYNOLDS NUMBER VARIATION
TRAJECTORY NO. 3
STA 11
STA 7
TIME ~ SEC
0
100
200
300
400
500

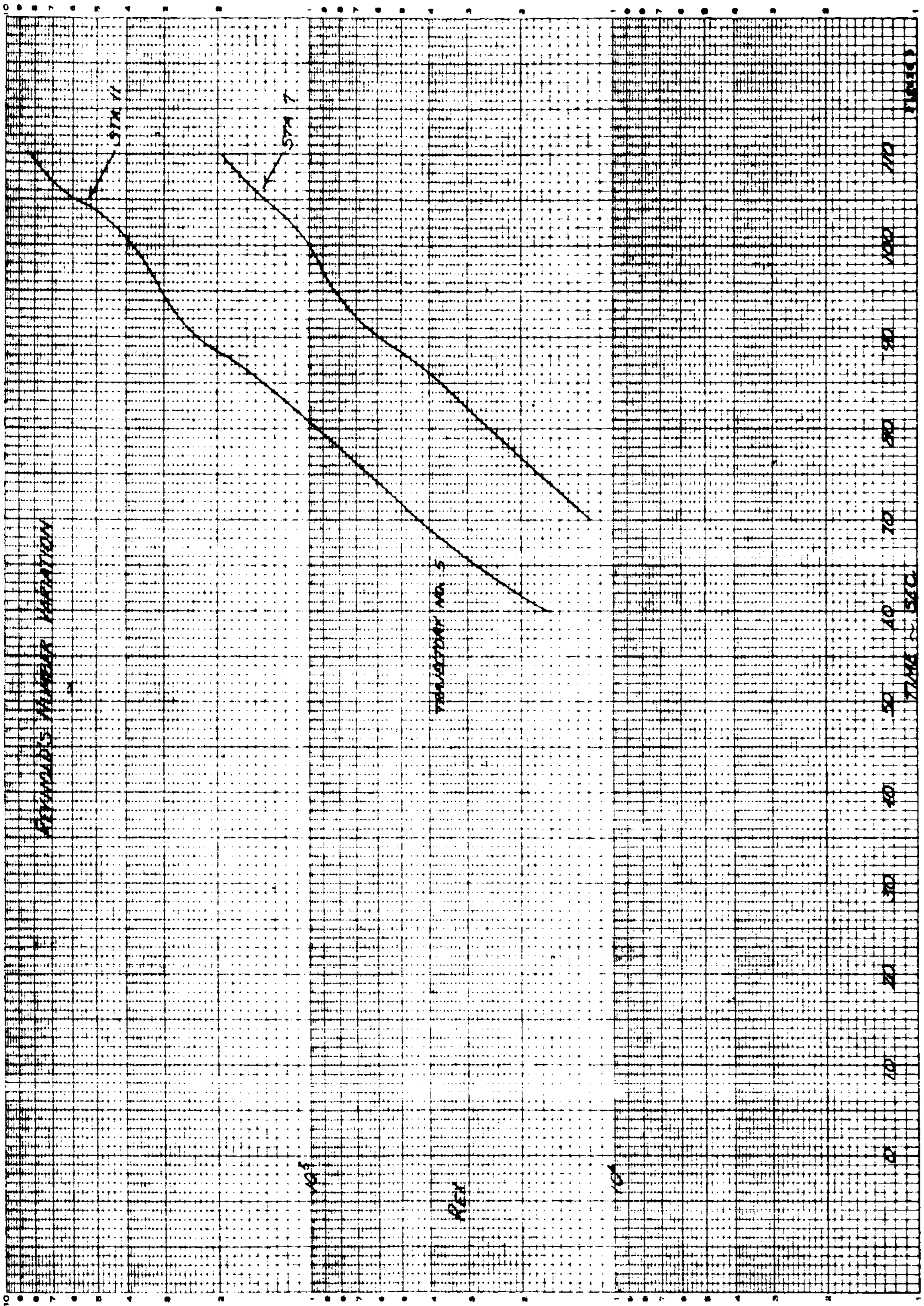
REYNOLDS NUMBER VARIATION
TRAJECTORY NO. 5
STA 11
STA 7
Rex
10^5
10^4
TIME ~ SEC
0
10
20
30
40
50
60
70
80
90
100
110

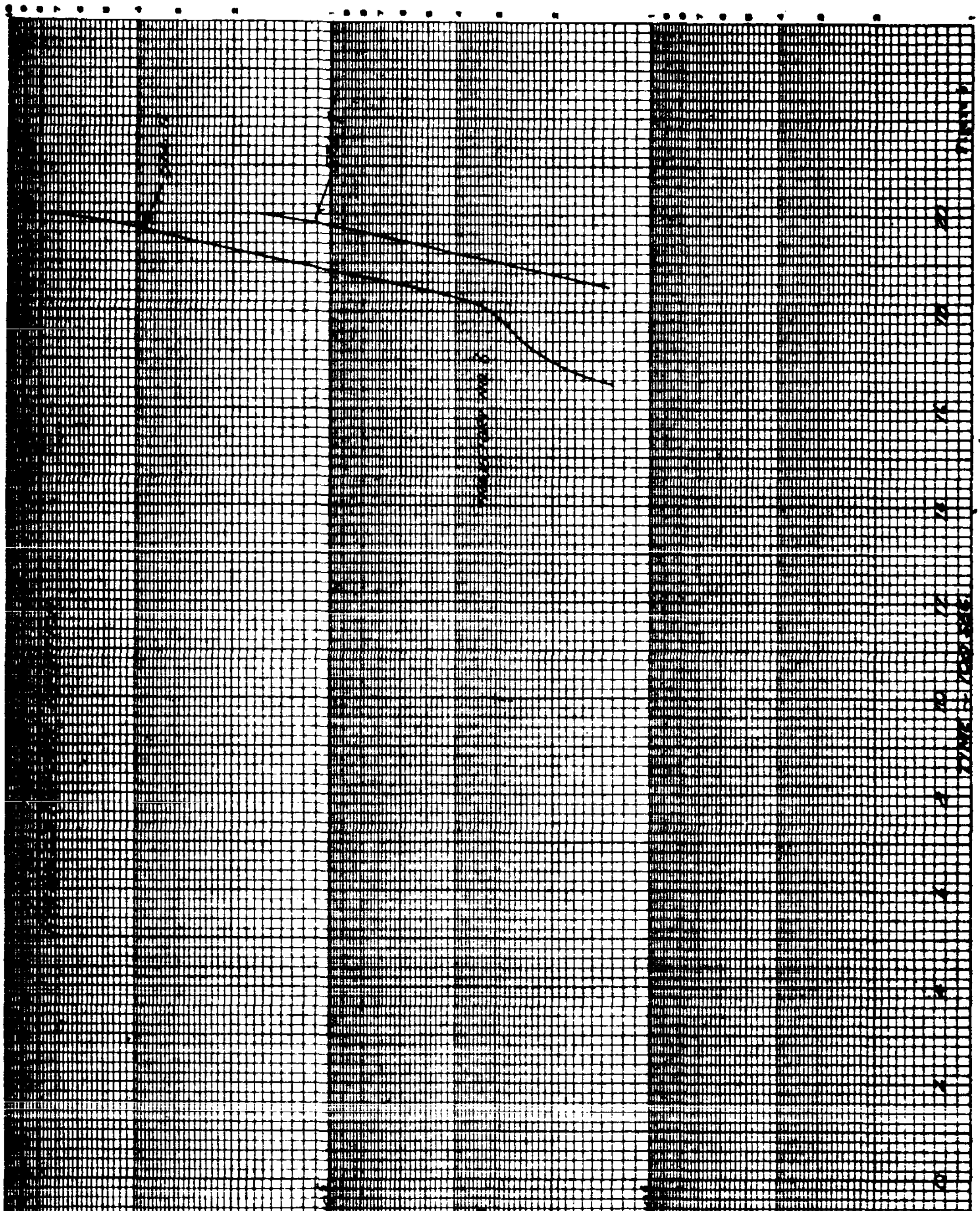

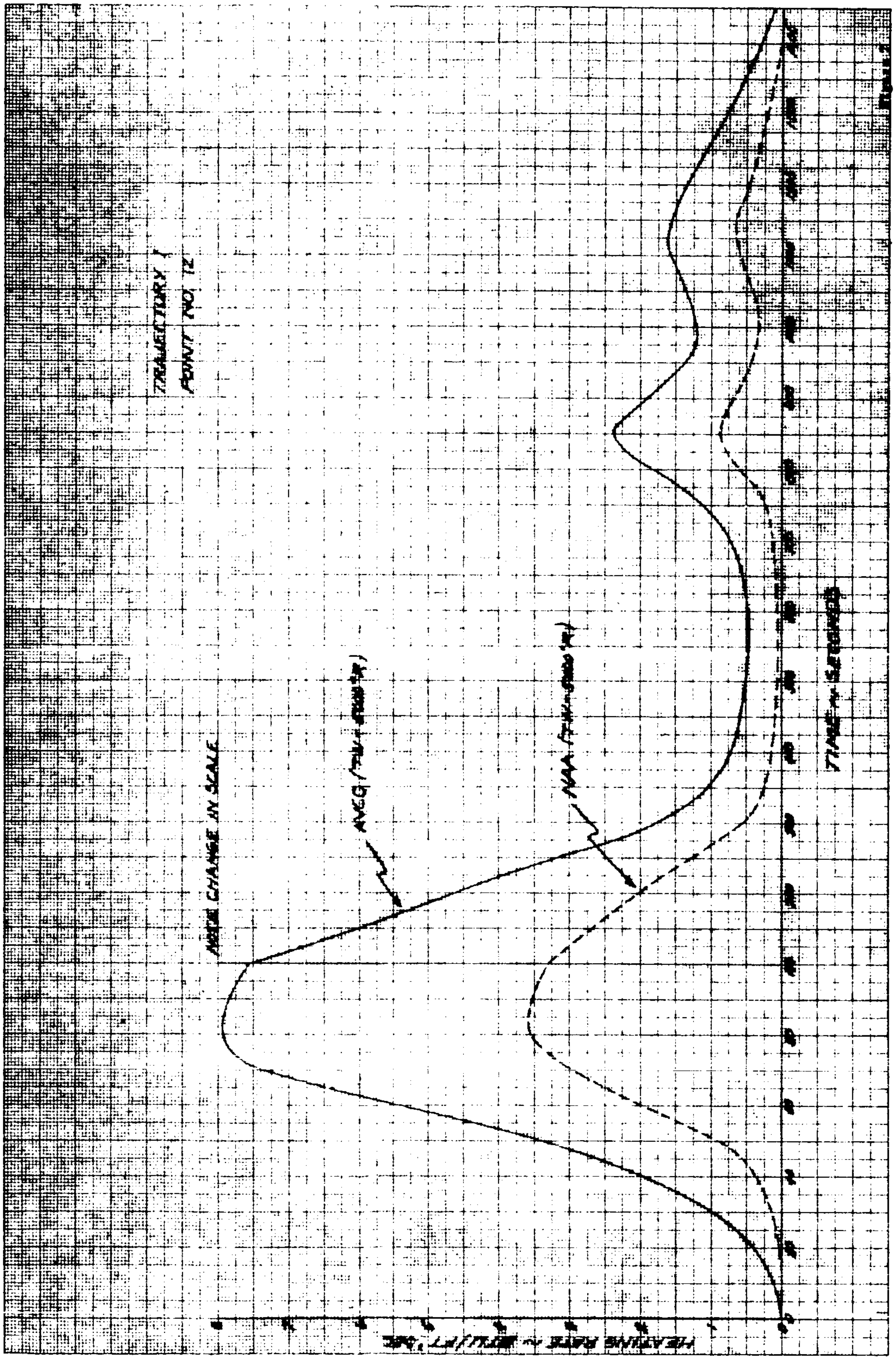
TRAJECTORY I
POINT NO. 12
NOTE CHANGE IN SCALE
TIME ~ SECONDS

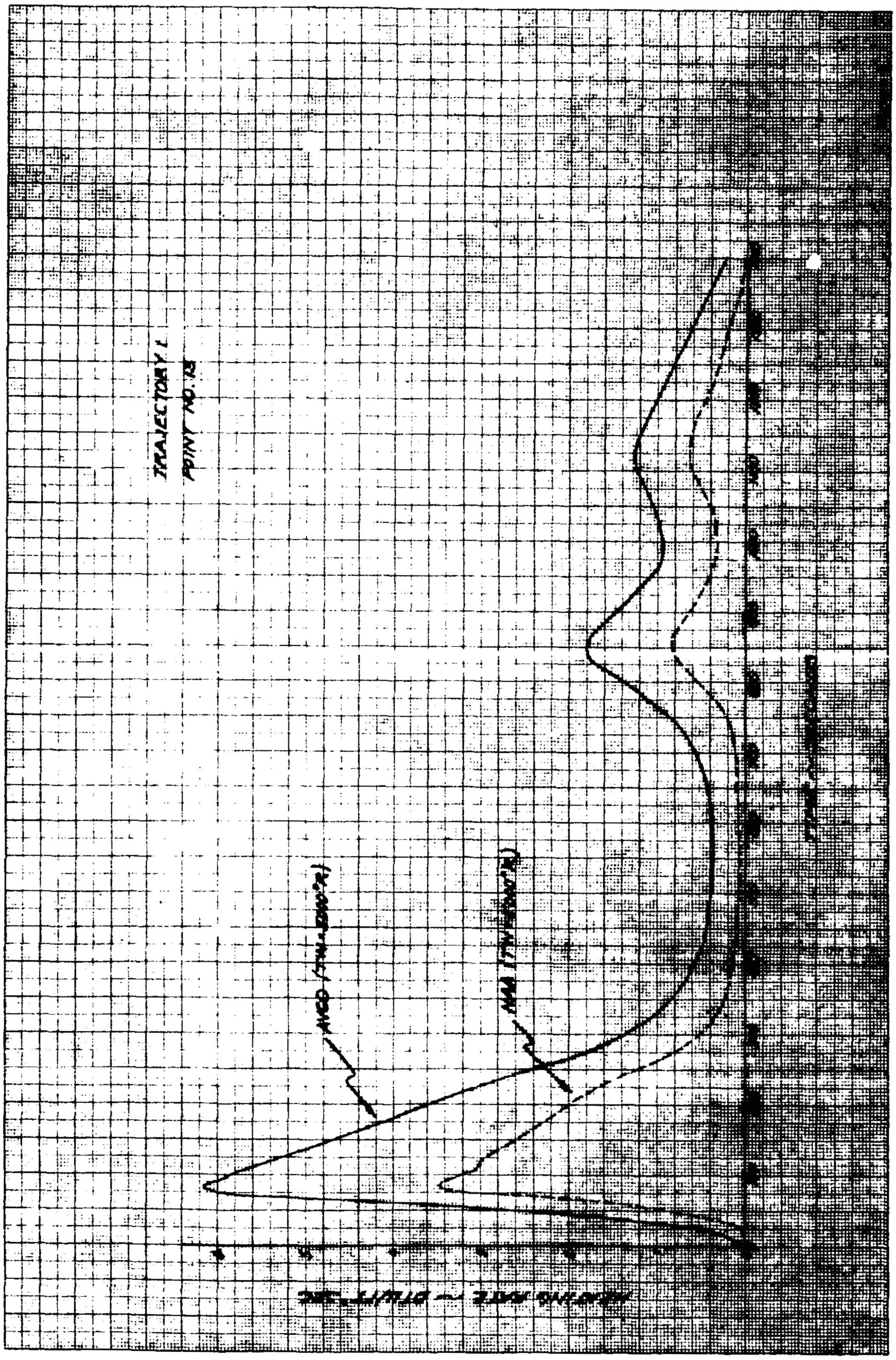
TRAJECTORY I
POINT NO. 13

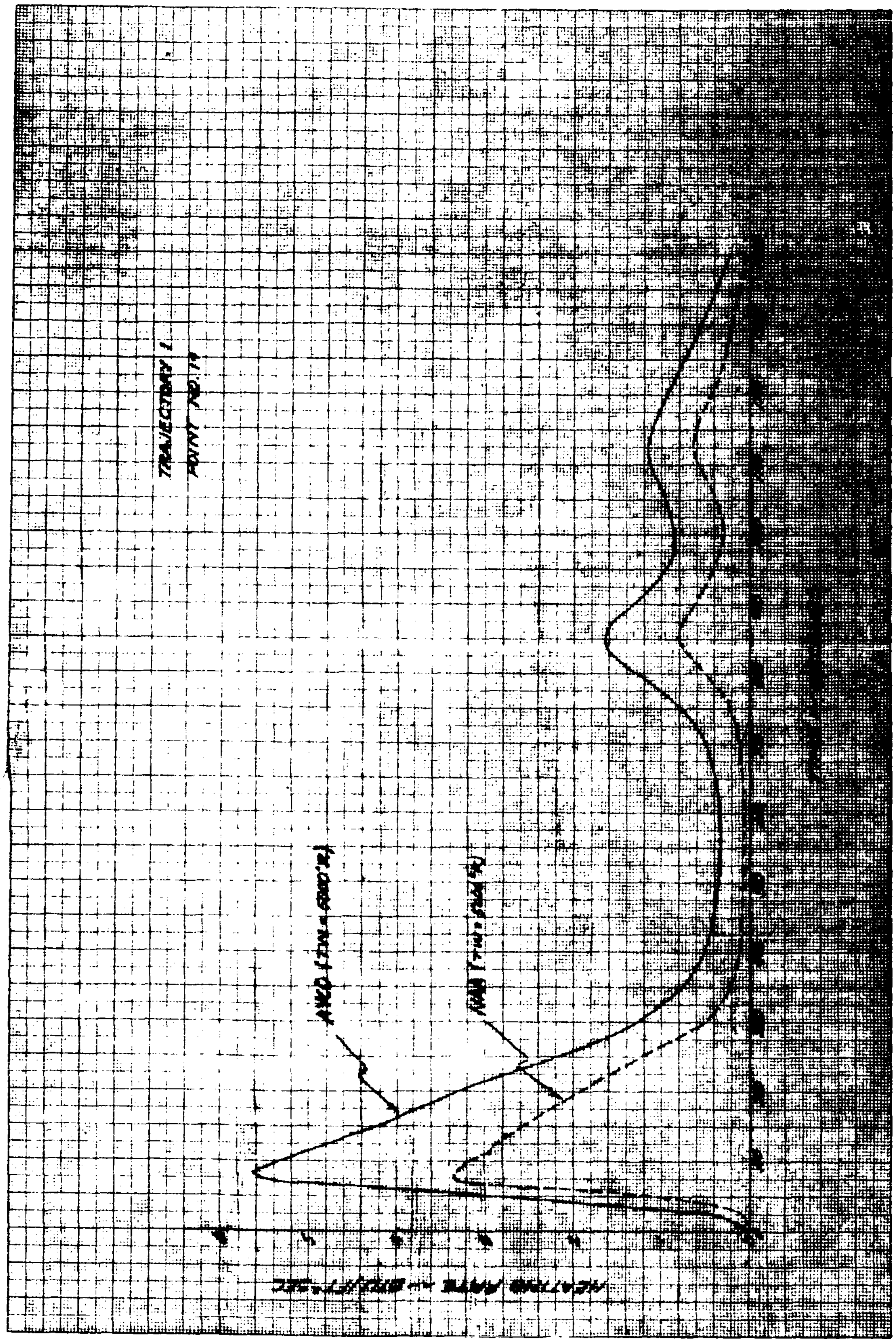
TRAJECTORY I
POINT NO. 14

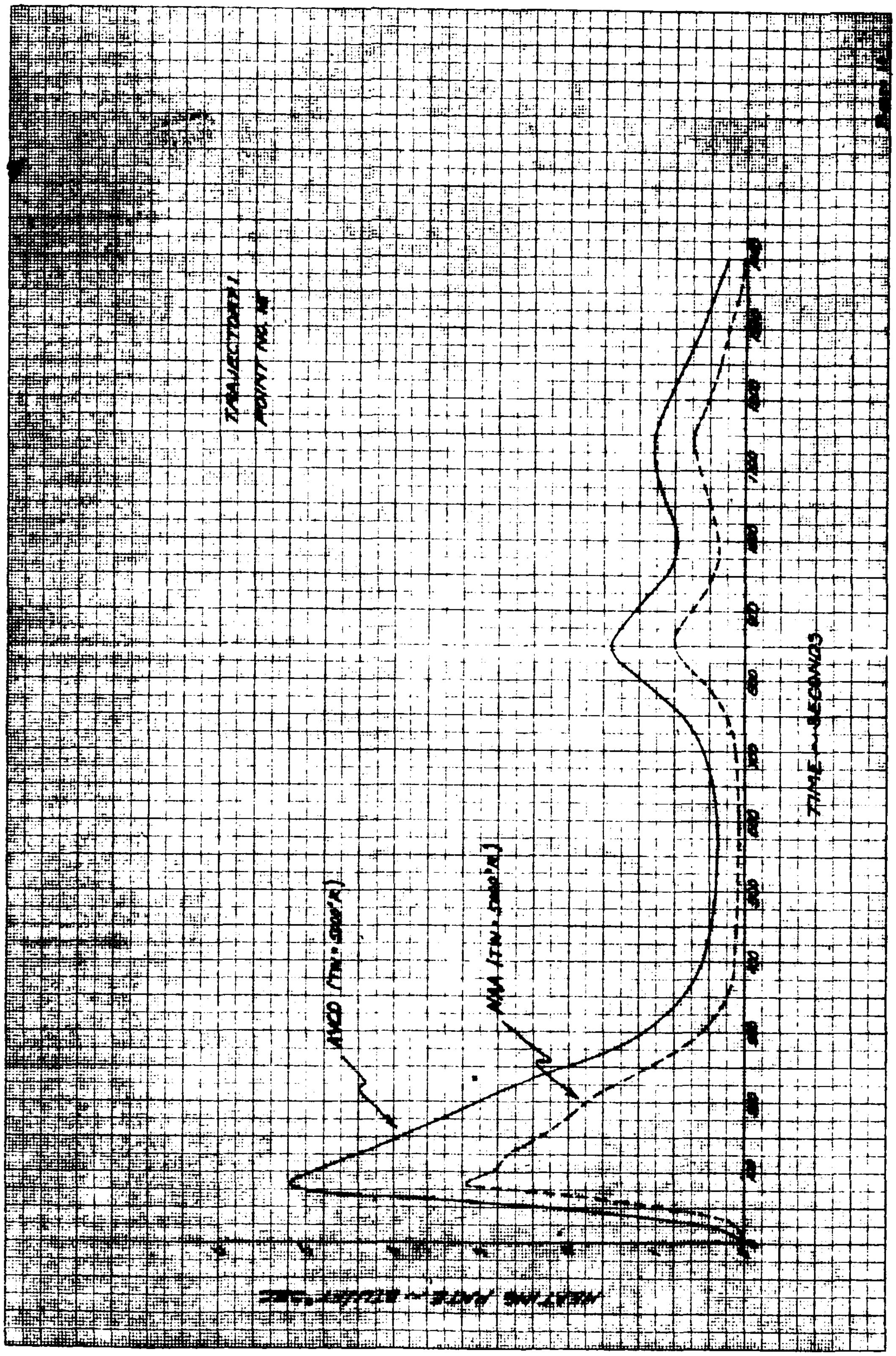
TRAJECTORY I
TIME — SECONDS

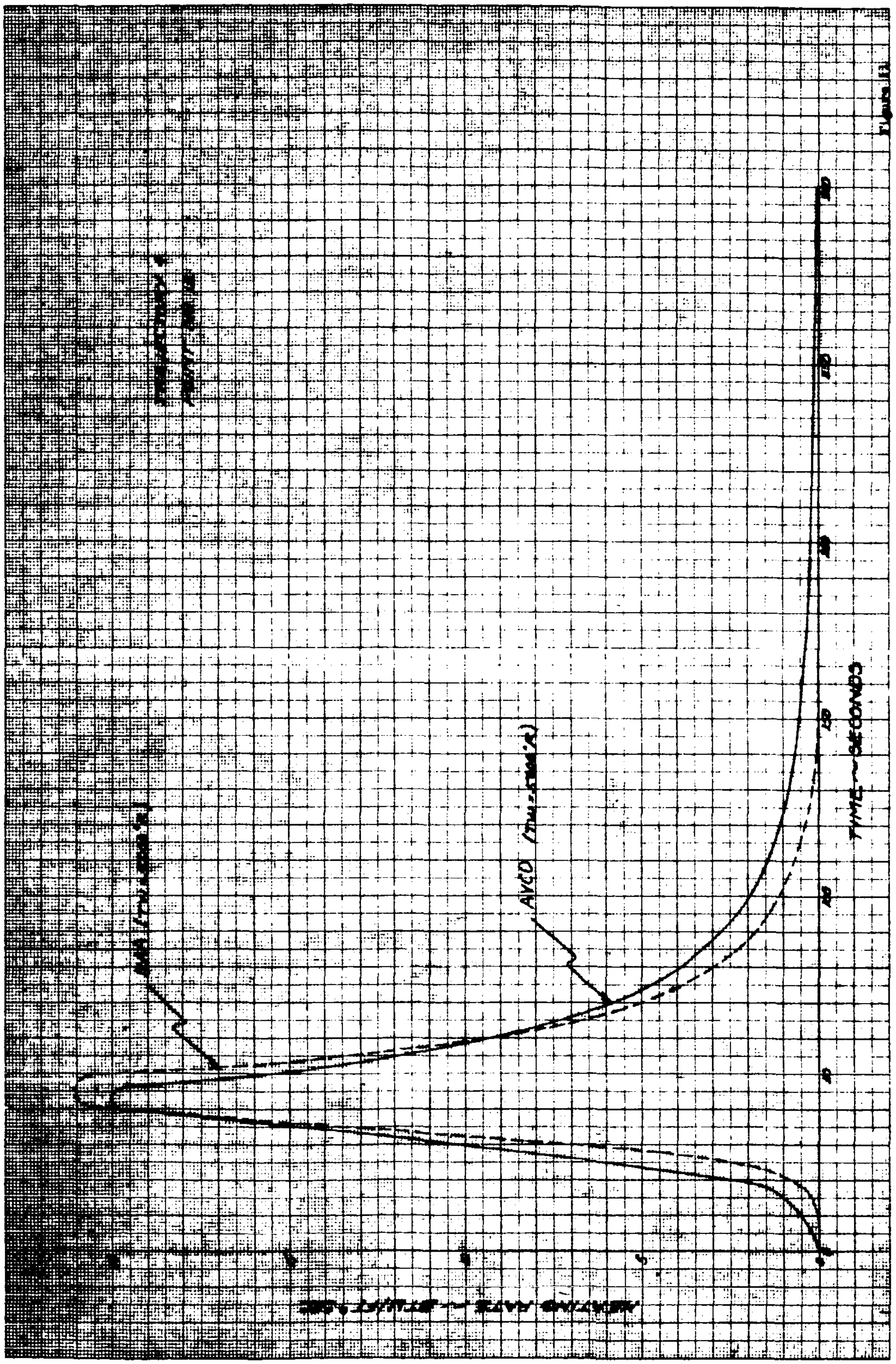
AVCO
TIME ~ SECONDS

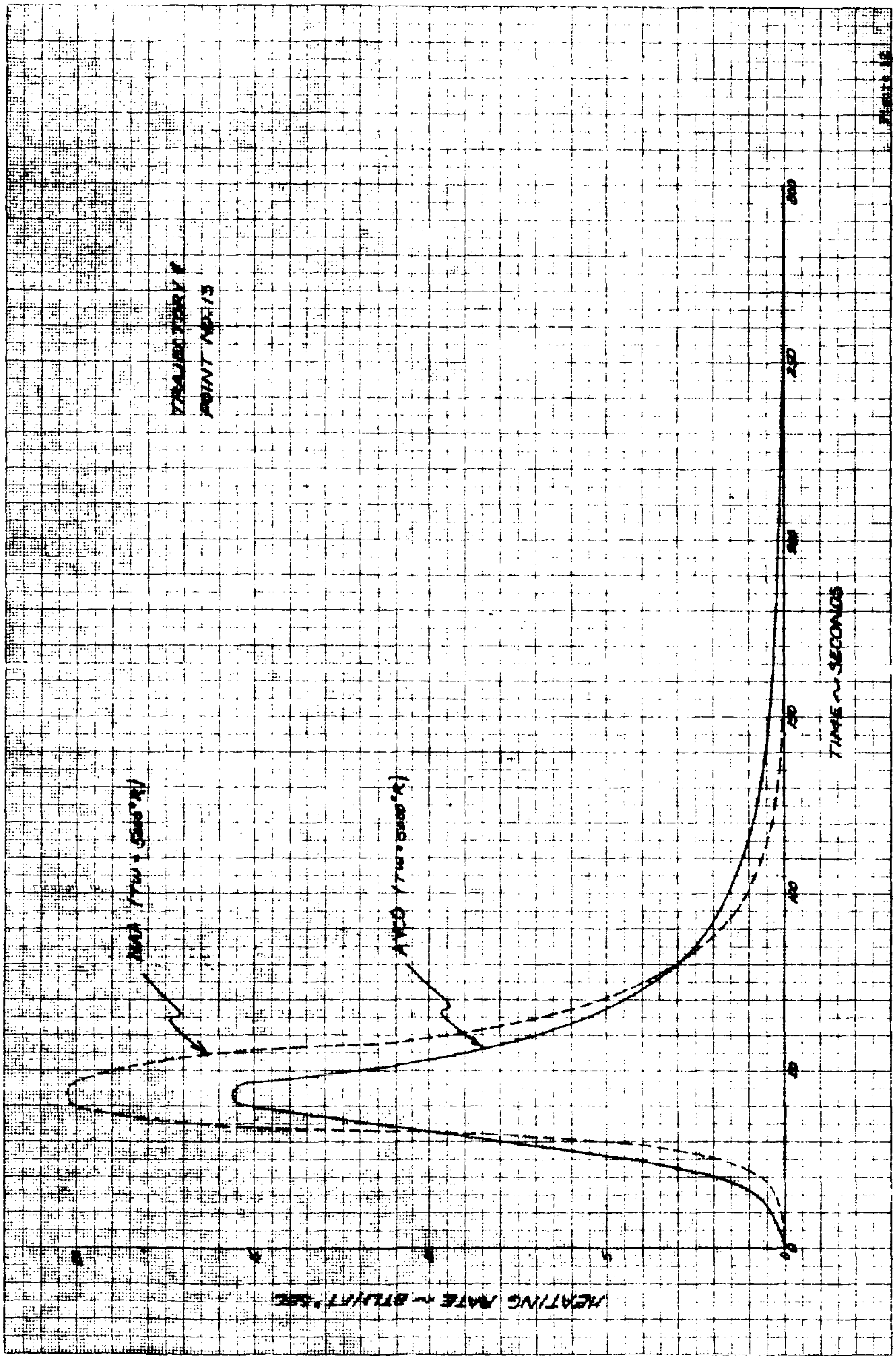
TIME ~ SECONDS
AVCO

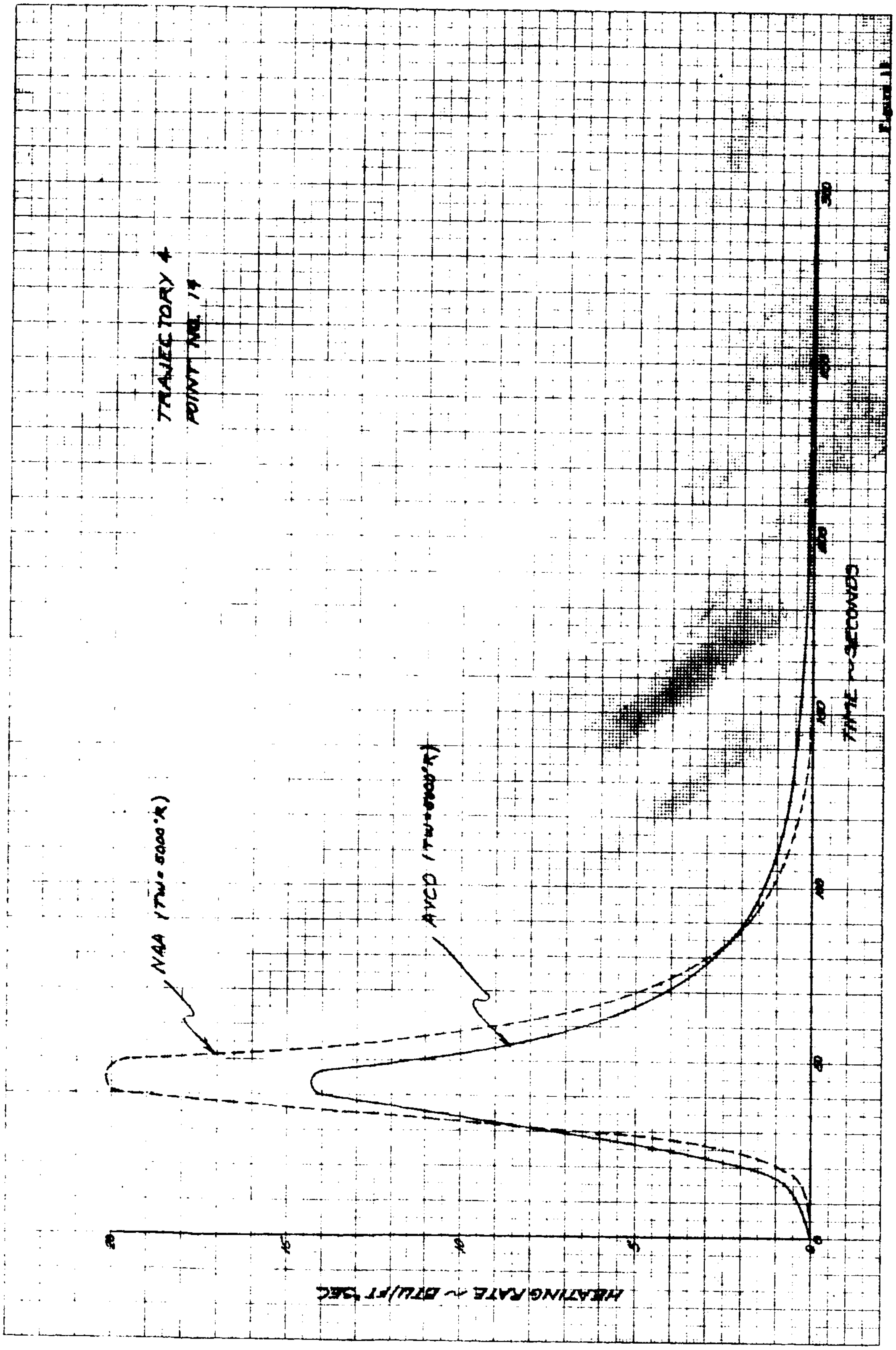
TRAJECTORY 4
POINT NO. 14
NAA (Tw = 5000°R)
AVCO
TIME ~ SECONDS
HEATING RATE ~ BTU/FT² SEC
0
5
10
15
20

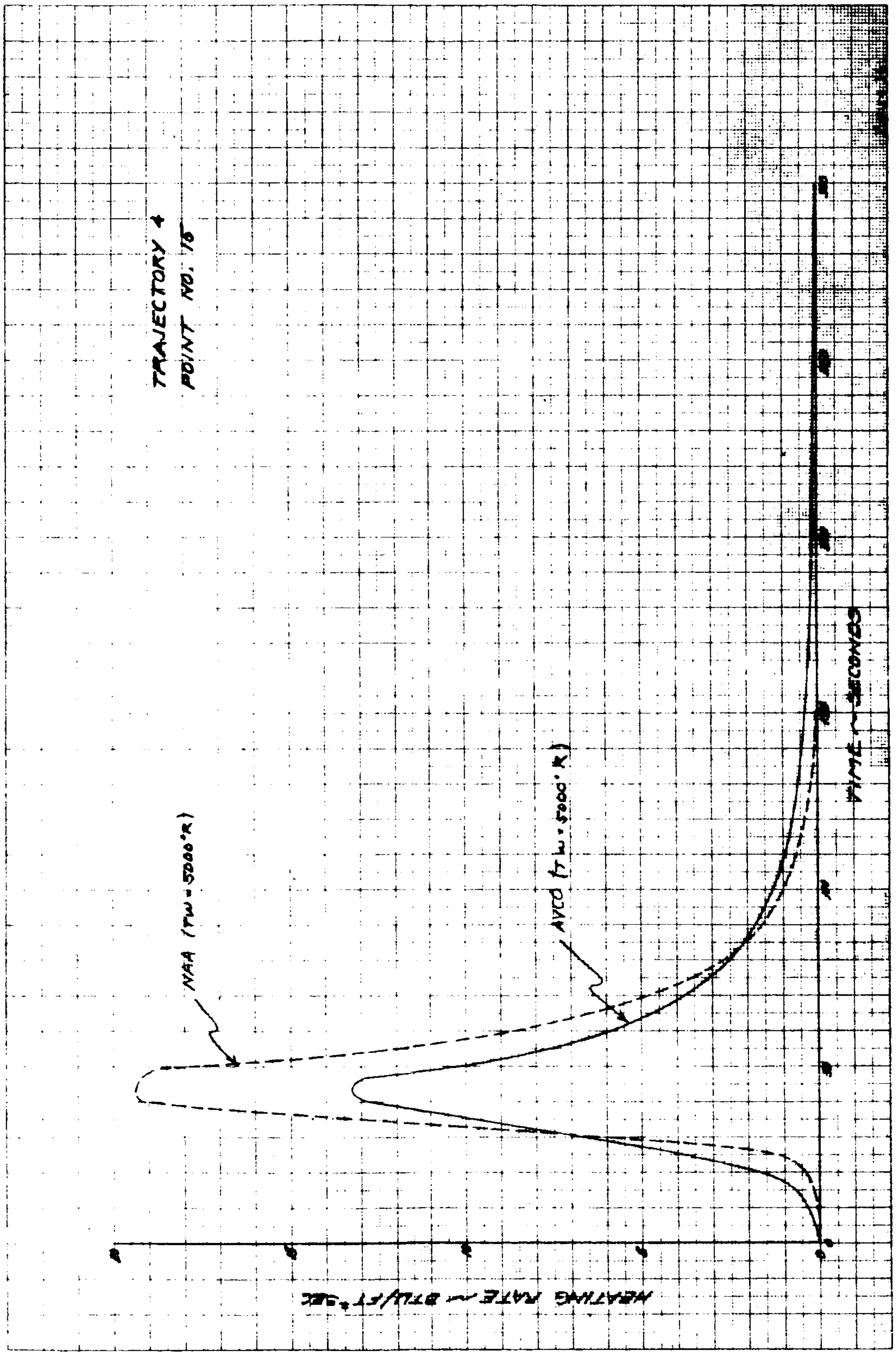
TRAJECTORY 4
POINT NO. 15
NAA (Tw = 5000°R)
AVCO (Tw = 5000°R)
TIME ~ SECONDS
HEATING RATE ~ BTU/FT²-SEC

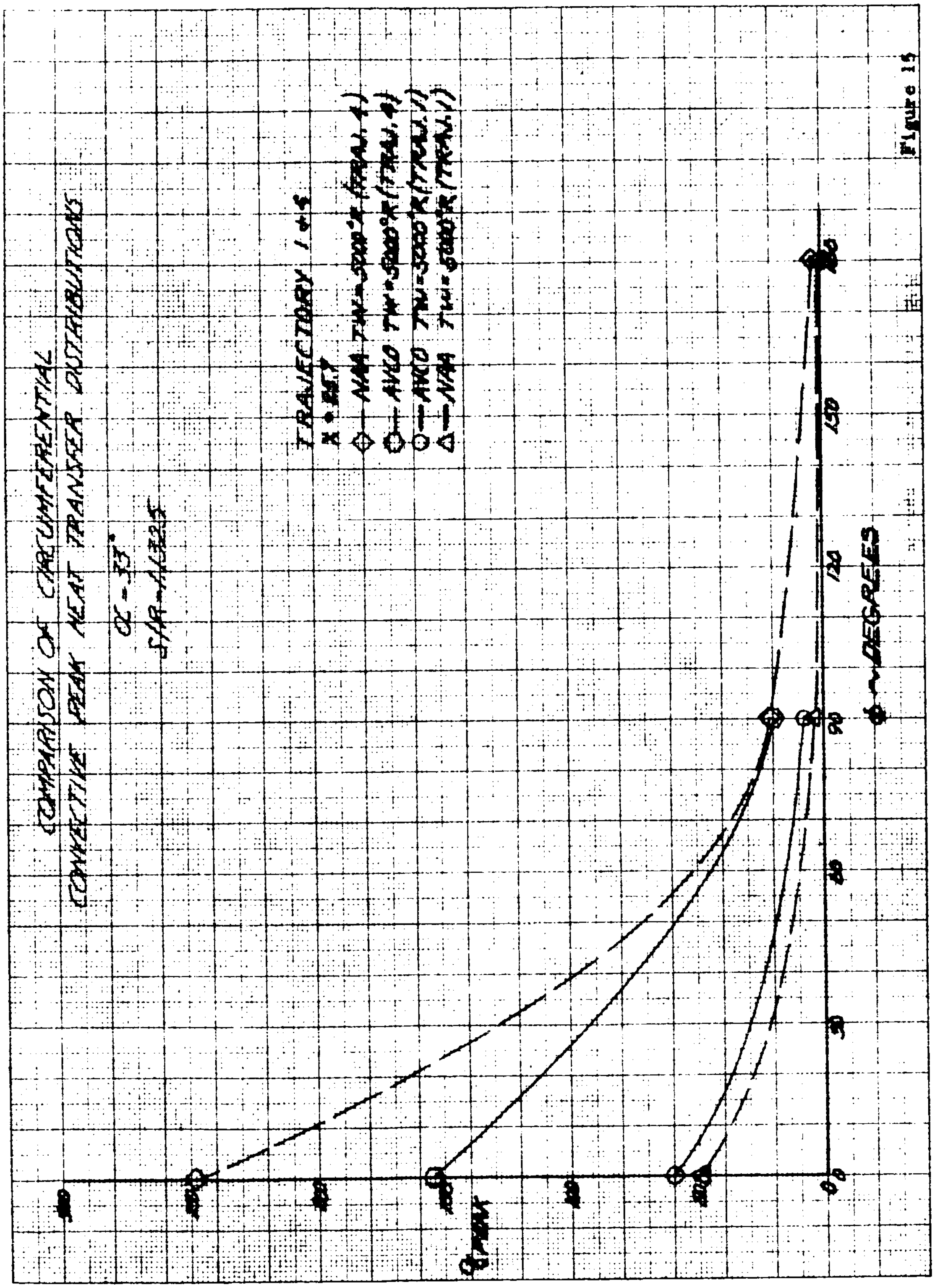
COMPARISON OF CIRCUMFERENTIAL
CONVECTIVE PEAK HEAT TRANSFER DISTRIBUTIONS
α = 33°
TRAJECTORY 1 & 4
X = EST
NAA Tw=3000°R (TRAJ. 4)
AVCO Tw=3000°R (TRAJ. 4)
AVCO Tw=3000°R (TRAJ. 1)
NAA Tw=3000°R (TRAJ. 1)
0
30
60
90
120
150
180
φ ~ DEGREES
q PEAK

Figure 15

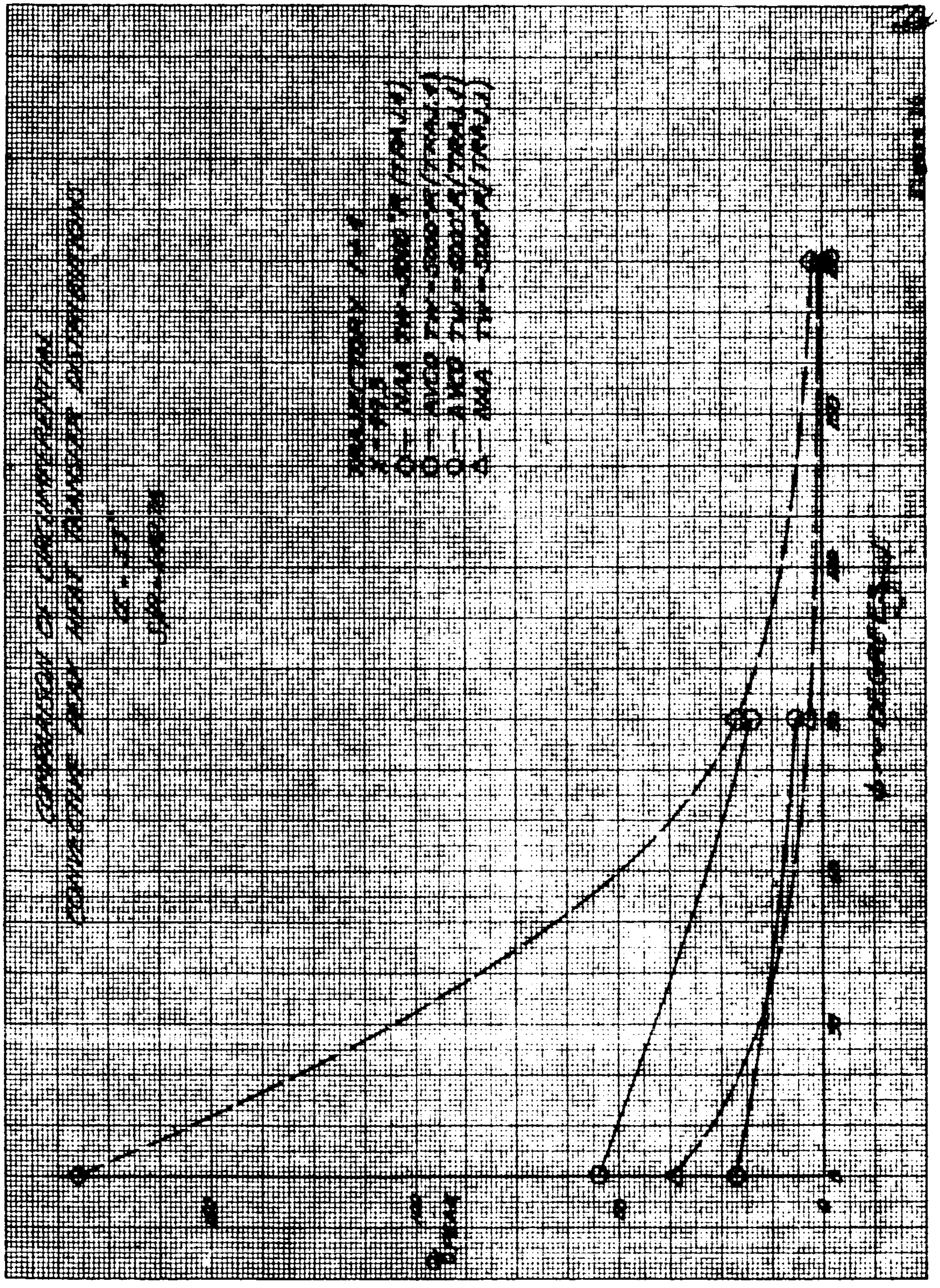
COMPARISON OF CIRCUMFERENTIAL
CONVECTIVE HEAT TRANSFER DISTRIBUTION

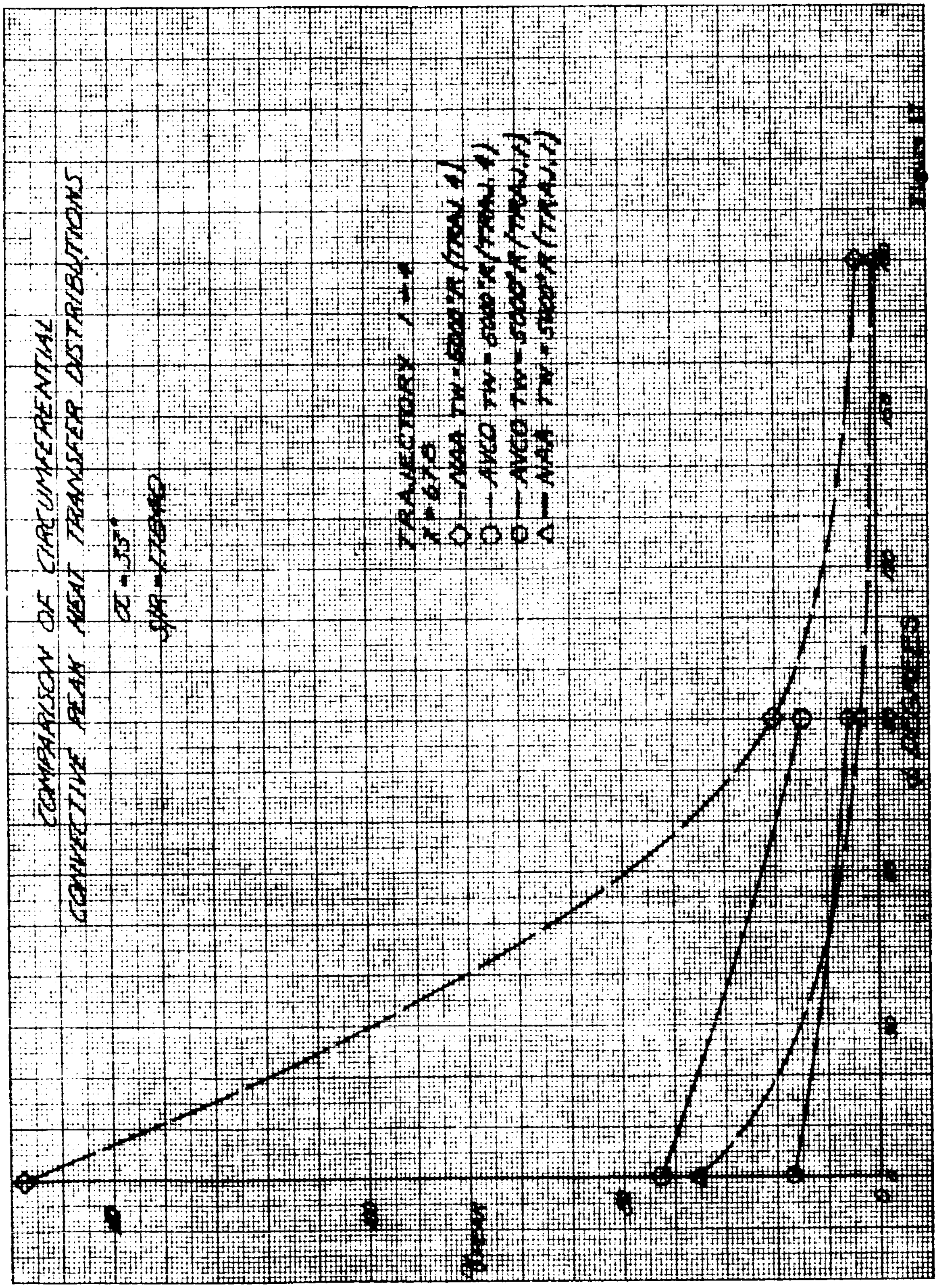
COMPARISON OF CIRCUMFERENTIAL
CONVECTIVE PEAK HEAT TRANSFER DISTRIBUTIONS
α = 33°
TRAJECTORY
NAA
AVCO
AVCO
NAA
φ DEGREES

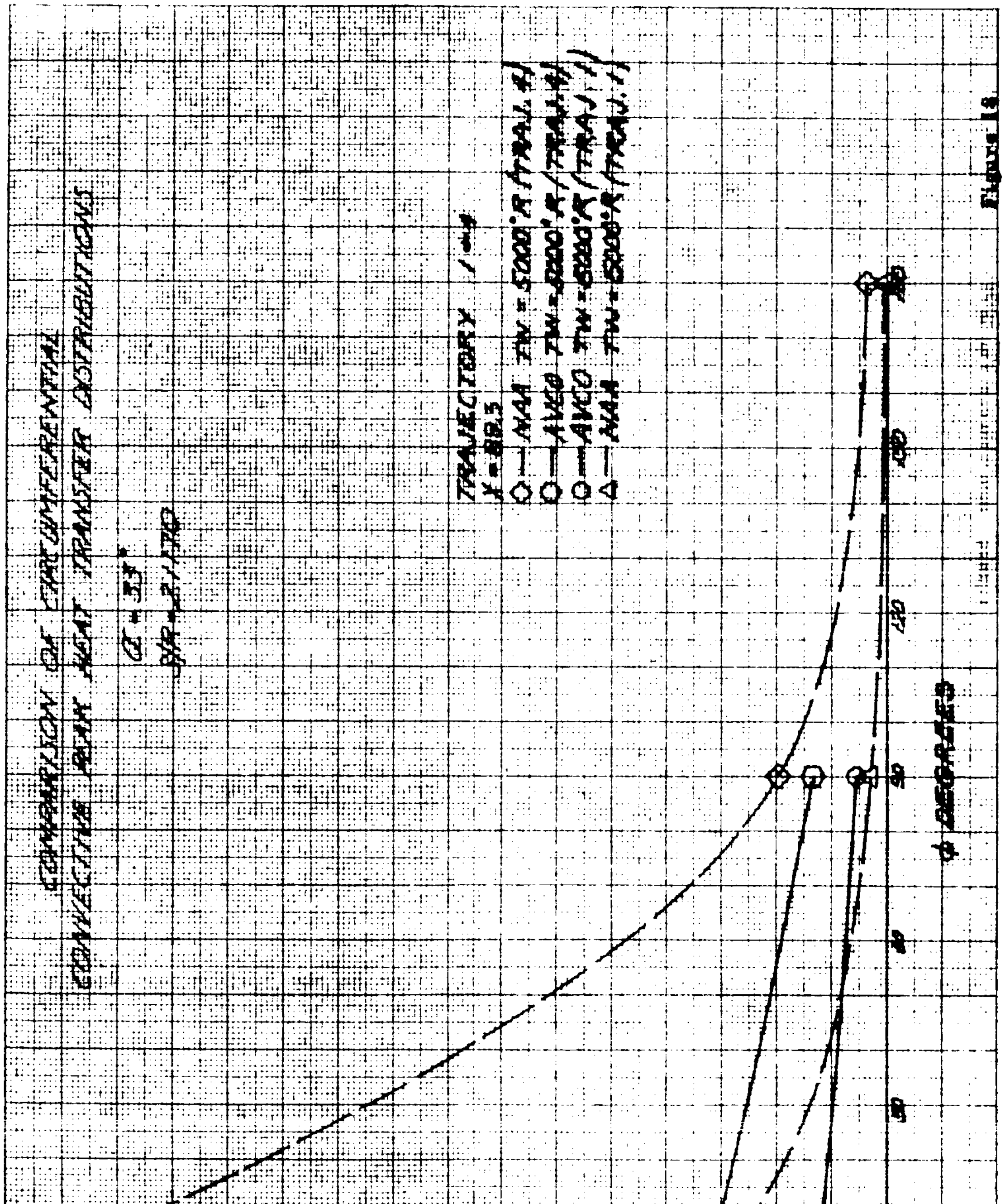
COMPARISON OF CIRCUMFERENTIAL
CONVECTIVE PEAK HEAT TRANSFER DISTRIBUTIONS
TRAJECTORY 1-4
NAA TW = 5000°R (TRAJ. 4)
φ DEGREES
0
90
180

Figure 18

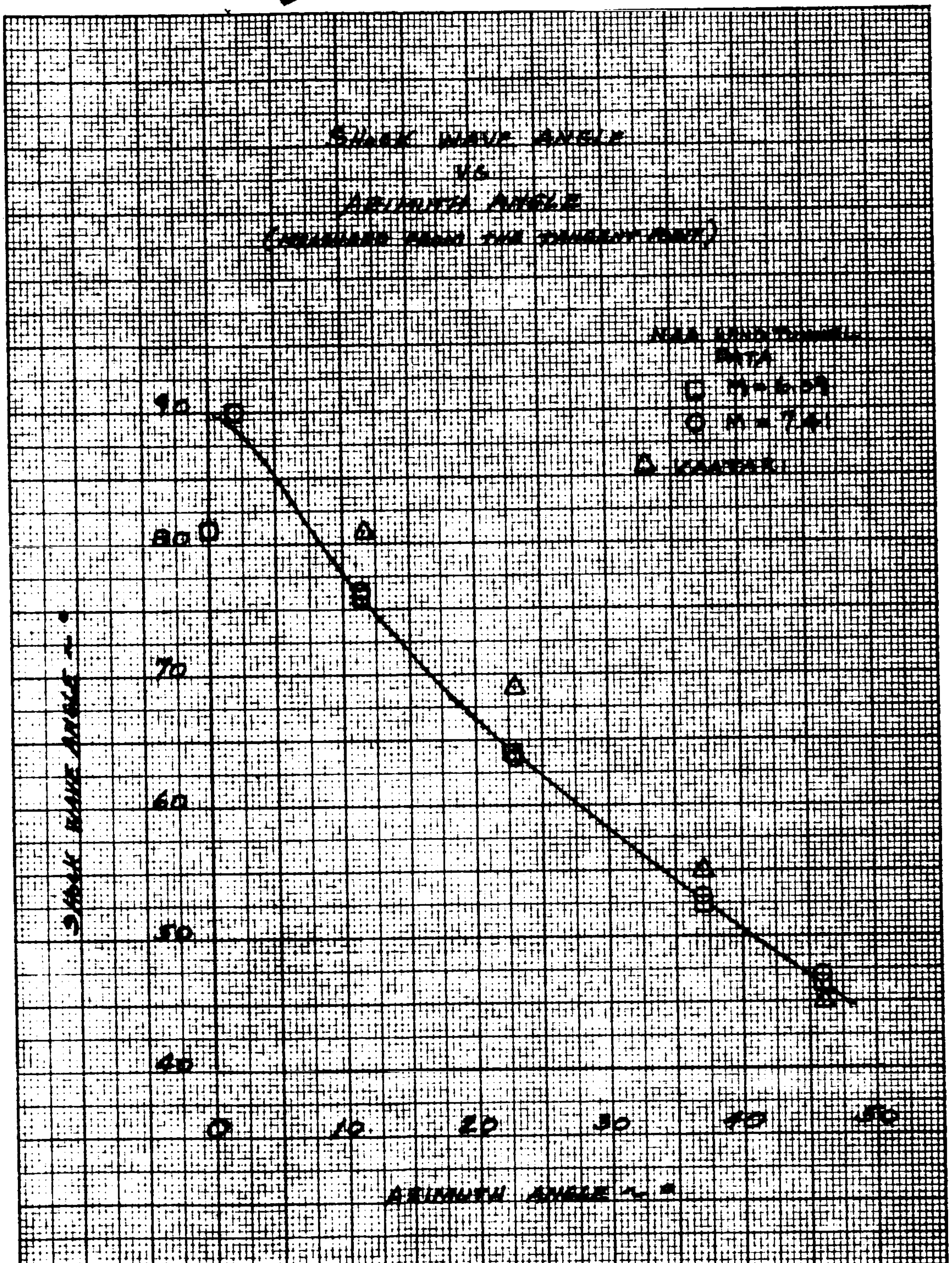
SHOCK WAVE ANGLE
VS
AZIMUTH ANGLE
NAA WIND TUNNEL DATA
90
80
70
60
50
40
0
10
20
30
40
50
AZIMUTH ANGLE ~ °
SHOCK WAVE ANGLE ~ °

Figure 19

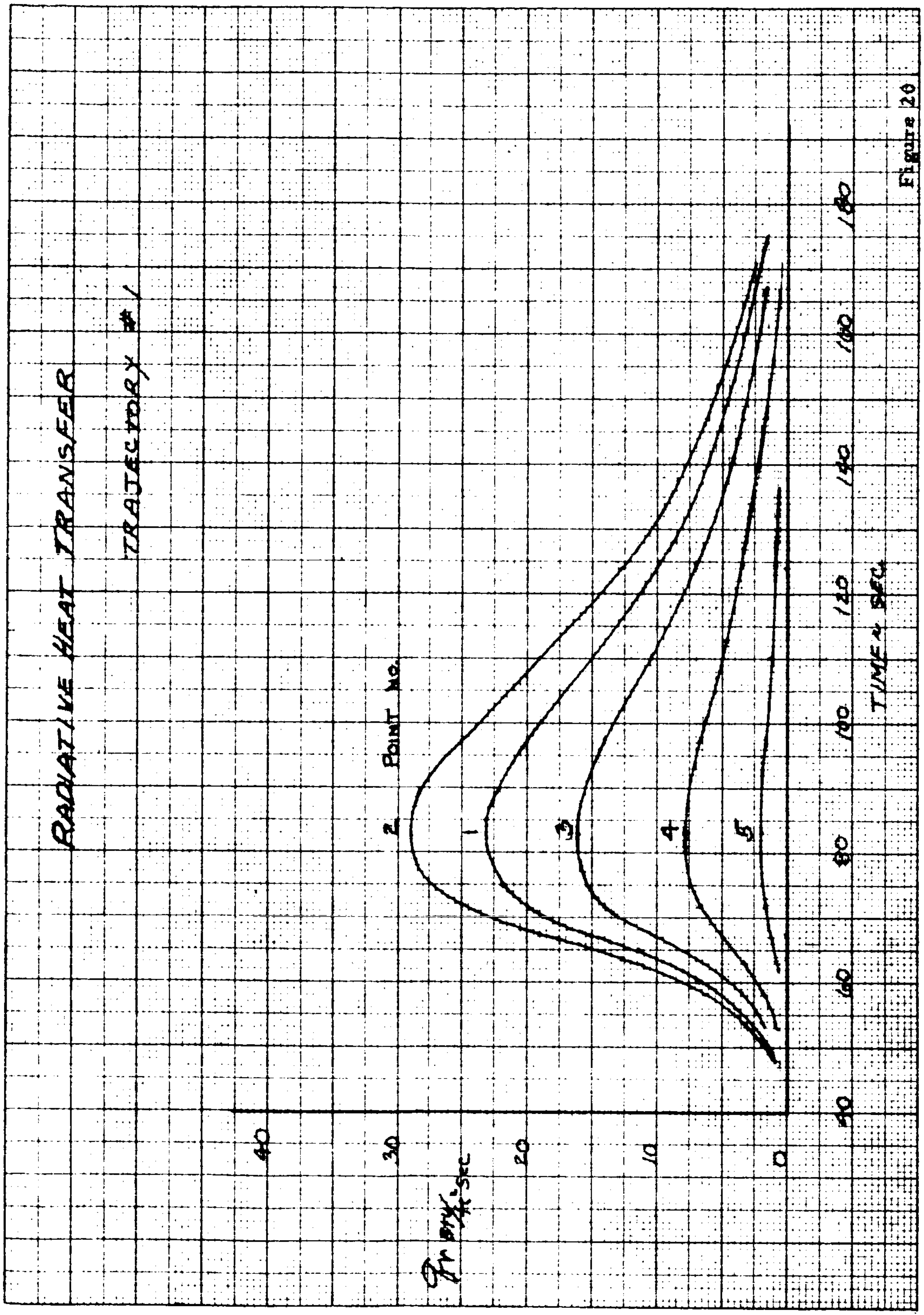
RADIATIVE HEAT TRANSFER
TRAJECTORY #1
POINT NO.
2
1
3
4
5
TIME ~ SEC
40
60
80
100
120
140
160
180
0
10
20
30
40

Figure 20

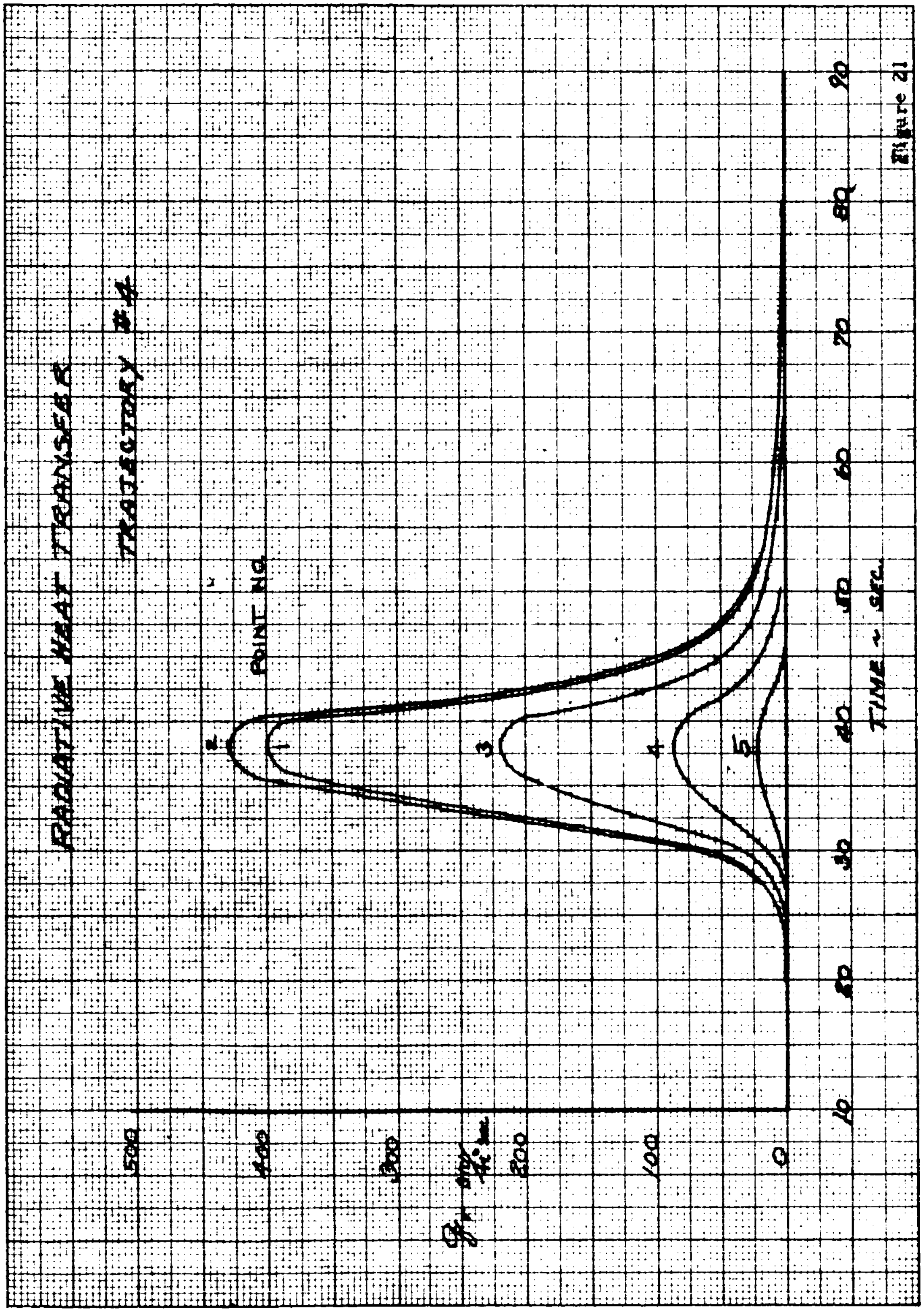
RADIATIVE HEAT TRANSFER
TRAJECTORY #4
POINT NO.
1
2
3
4
5
TIME ~ SEC.
10
20
30
40
50
60
70
80
90
0
100
200
300
400
500

Figure 21

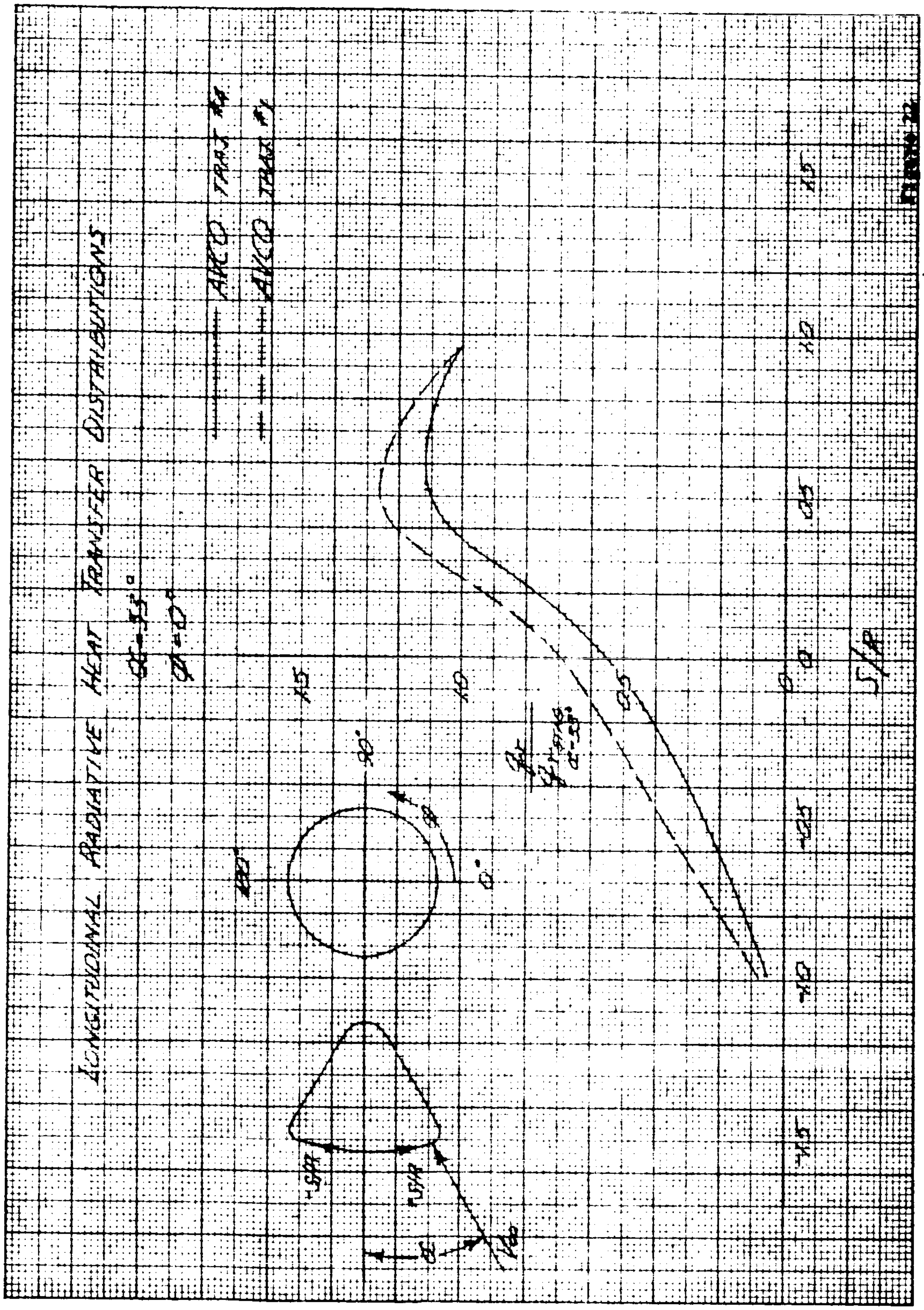
LONGITUDINAL RADIATIVE HEAT TRANSFER DISTRIBUTIONS
α = 55°
Φ = 0°
AVCO TRAJ #4
AVCO TRAJ #1
180°
90°
0°
Φ
-S/R
+S/R
α
V∞
q_r / q_r STAG α=55°
1.5
1.0
.05
0
-1.5
-1.0
-0.5
0
.05
1.0
1.5
S/R

Figure 22

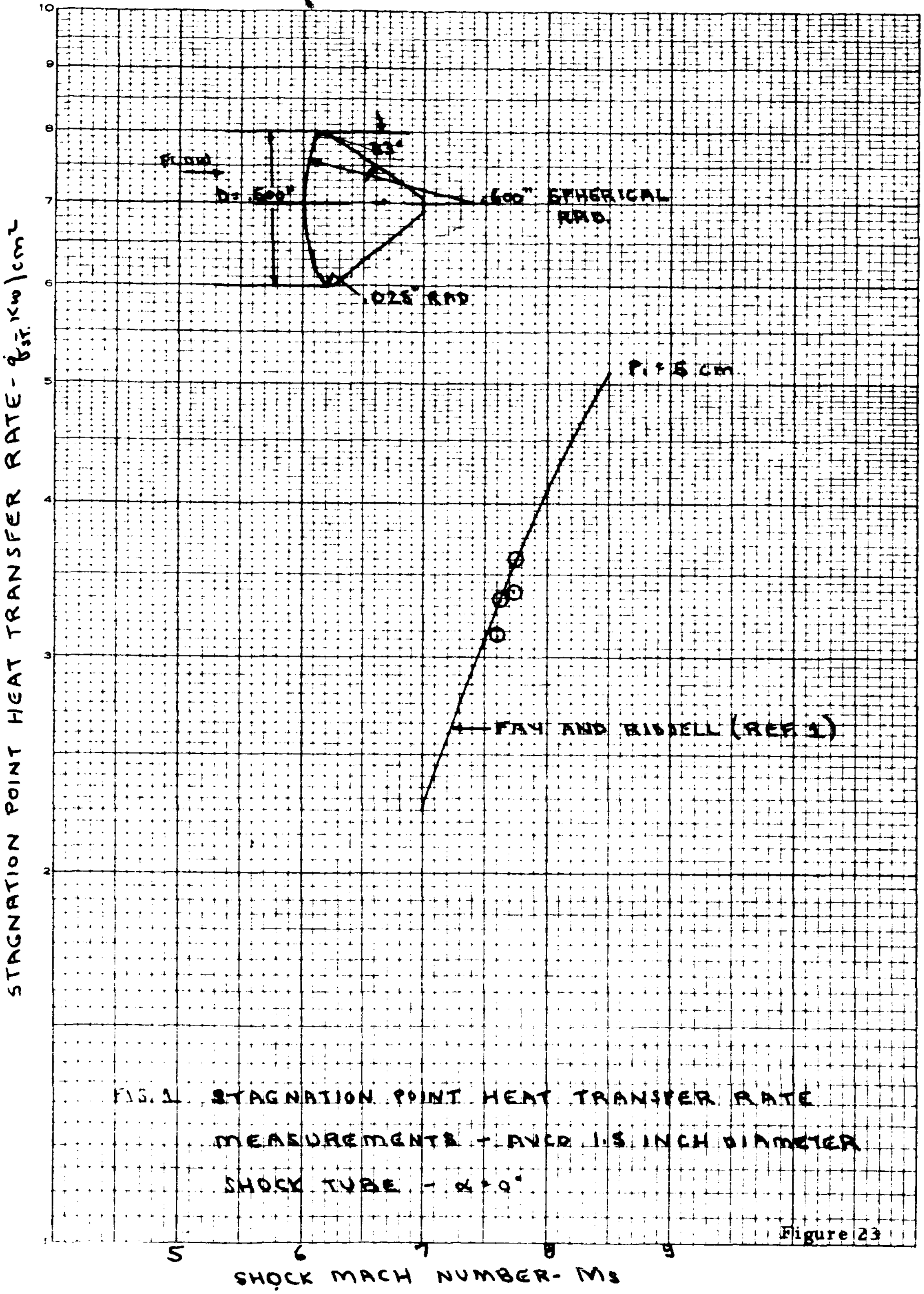

FIG. 1 STAGNATION POINT HEAT TRANSFER RATE MEASUREMENTS - AVCO 1.5 INCH DIAMETER SHOCK TUBE - $\alpha = 0°$

Figure 23

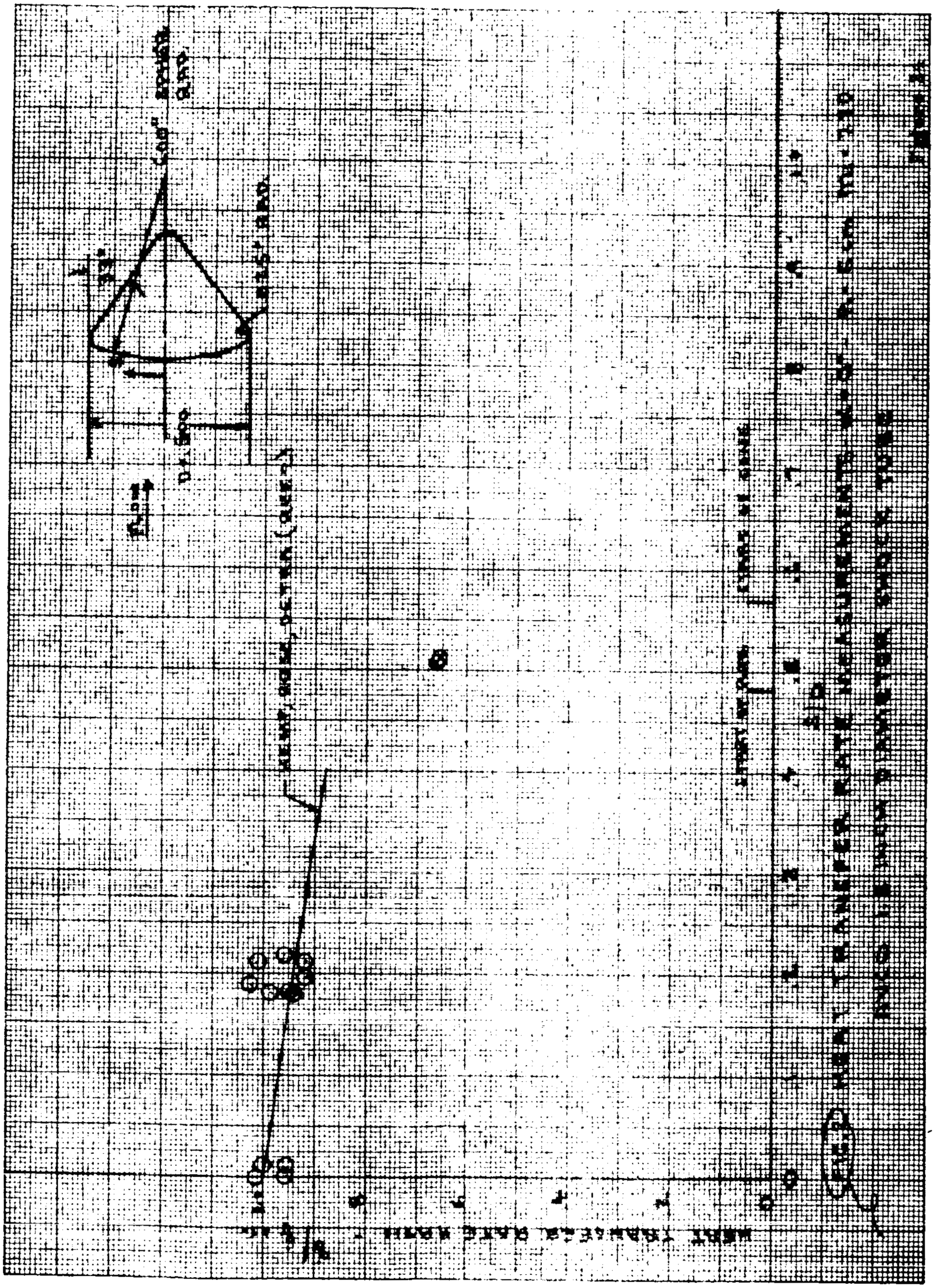

FIG. 2 HEAT TRANSFER RATE MEASUREMENTS
AVCO 1.5 INCH DIAMETER SHOCK TUBE

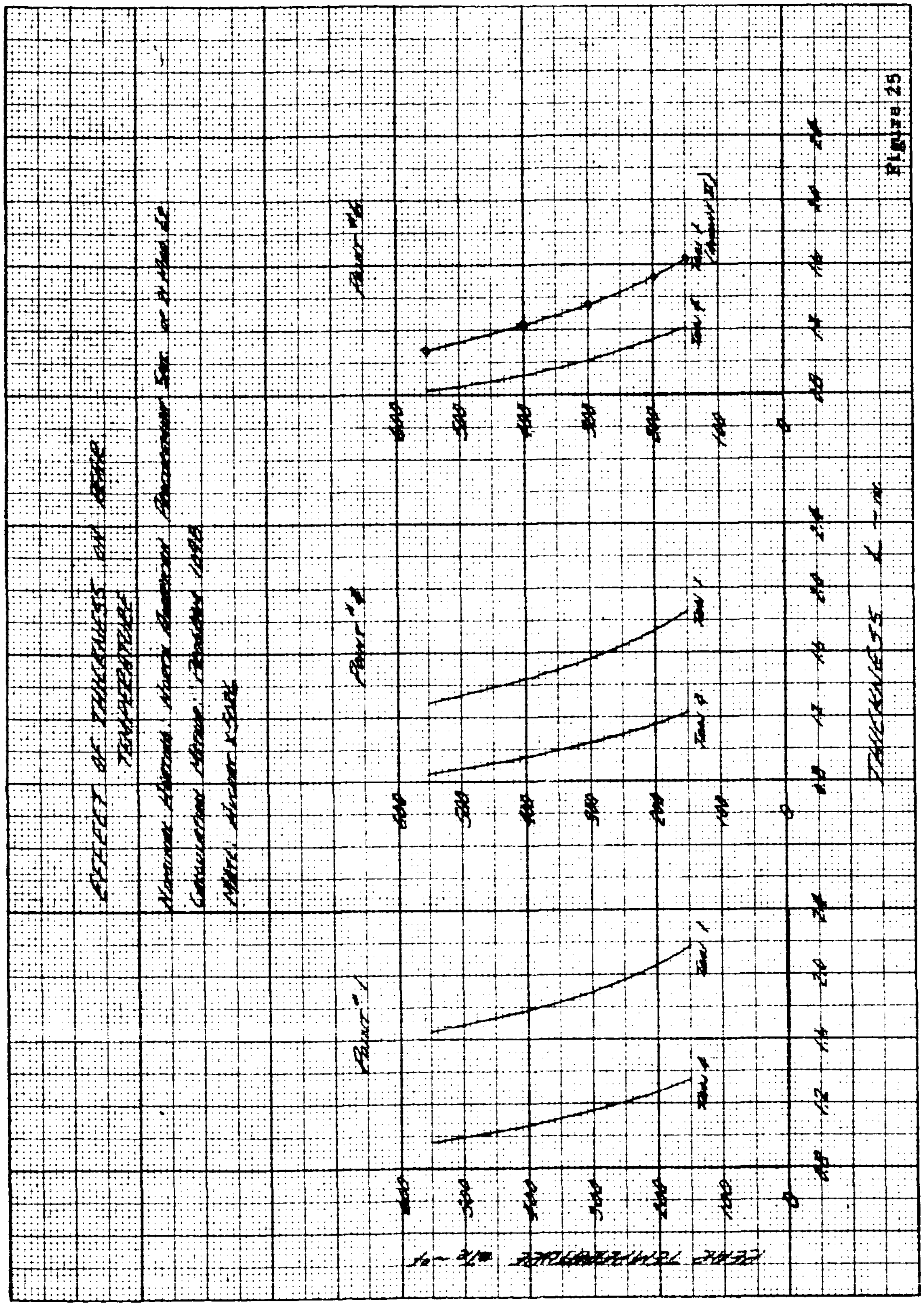
EFFECT OF THICKNESS ON
TEMPERATURE
600
500
400
300
200
100
0
0.8
1.2
1.6
2.0
2.4
THICKNESS
Figure 25

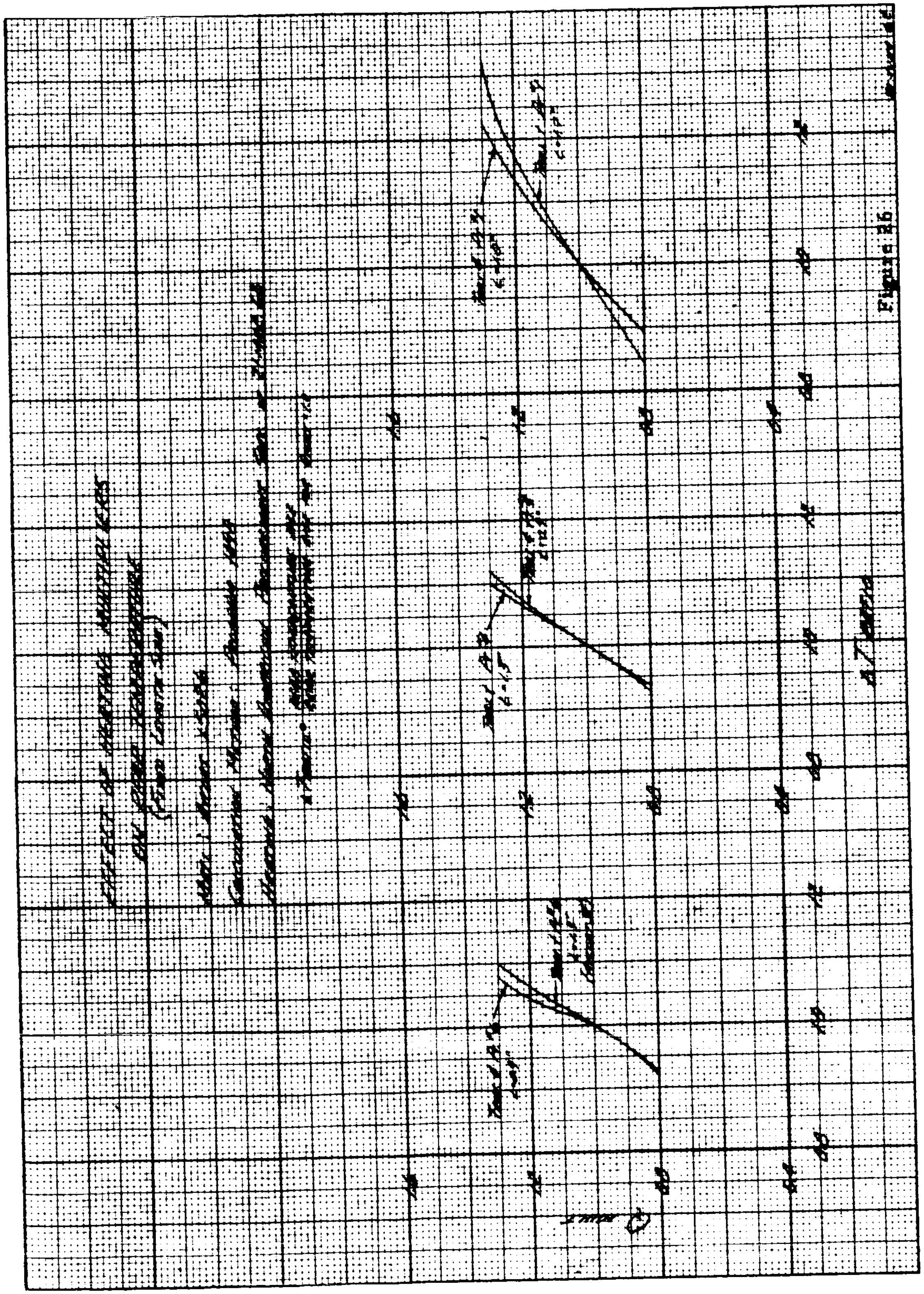

Figure 26

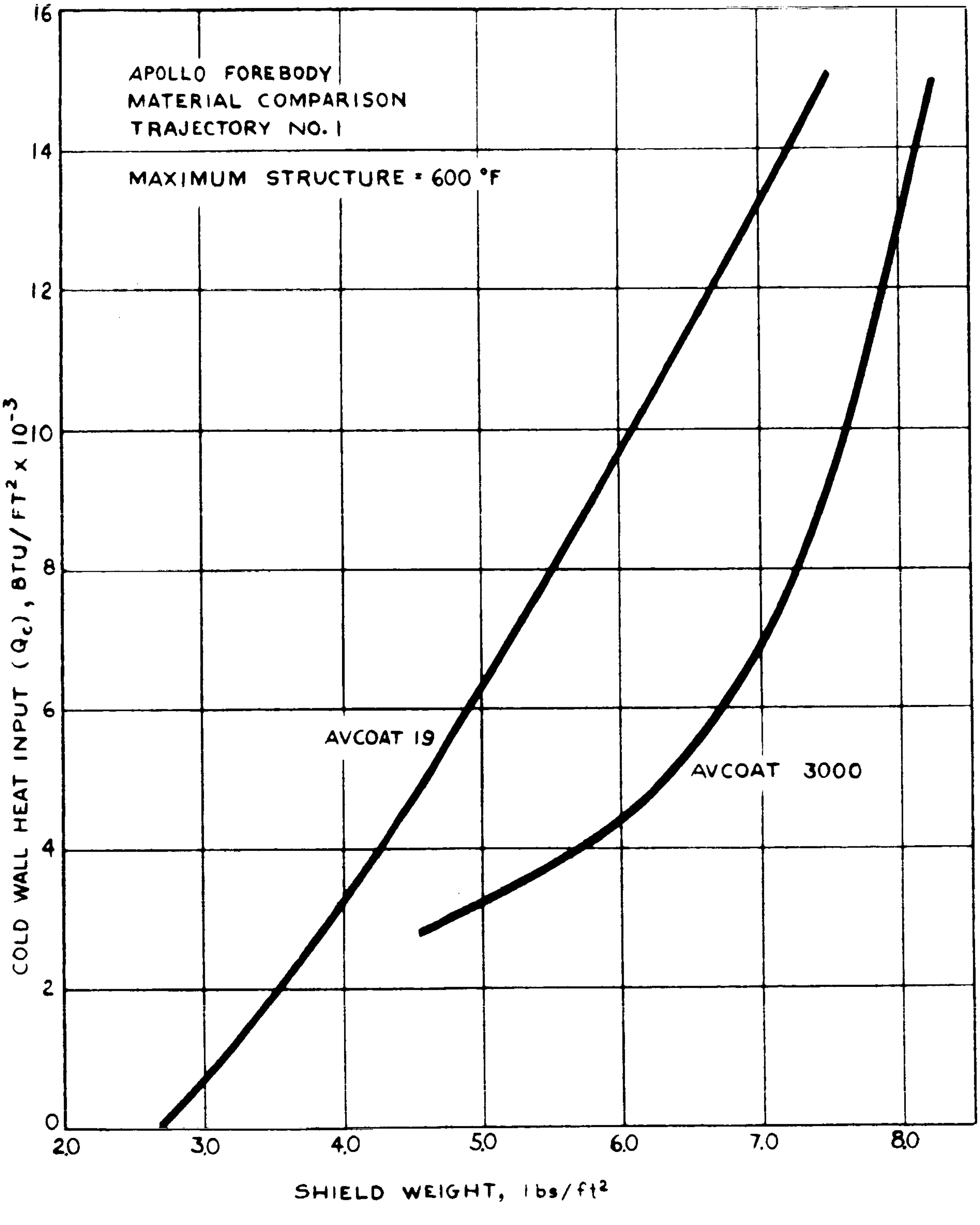

Figure 27 APOLLO FOREBODY MATERIAL COMPARISON -- TRAJECTORY 1

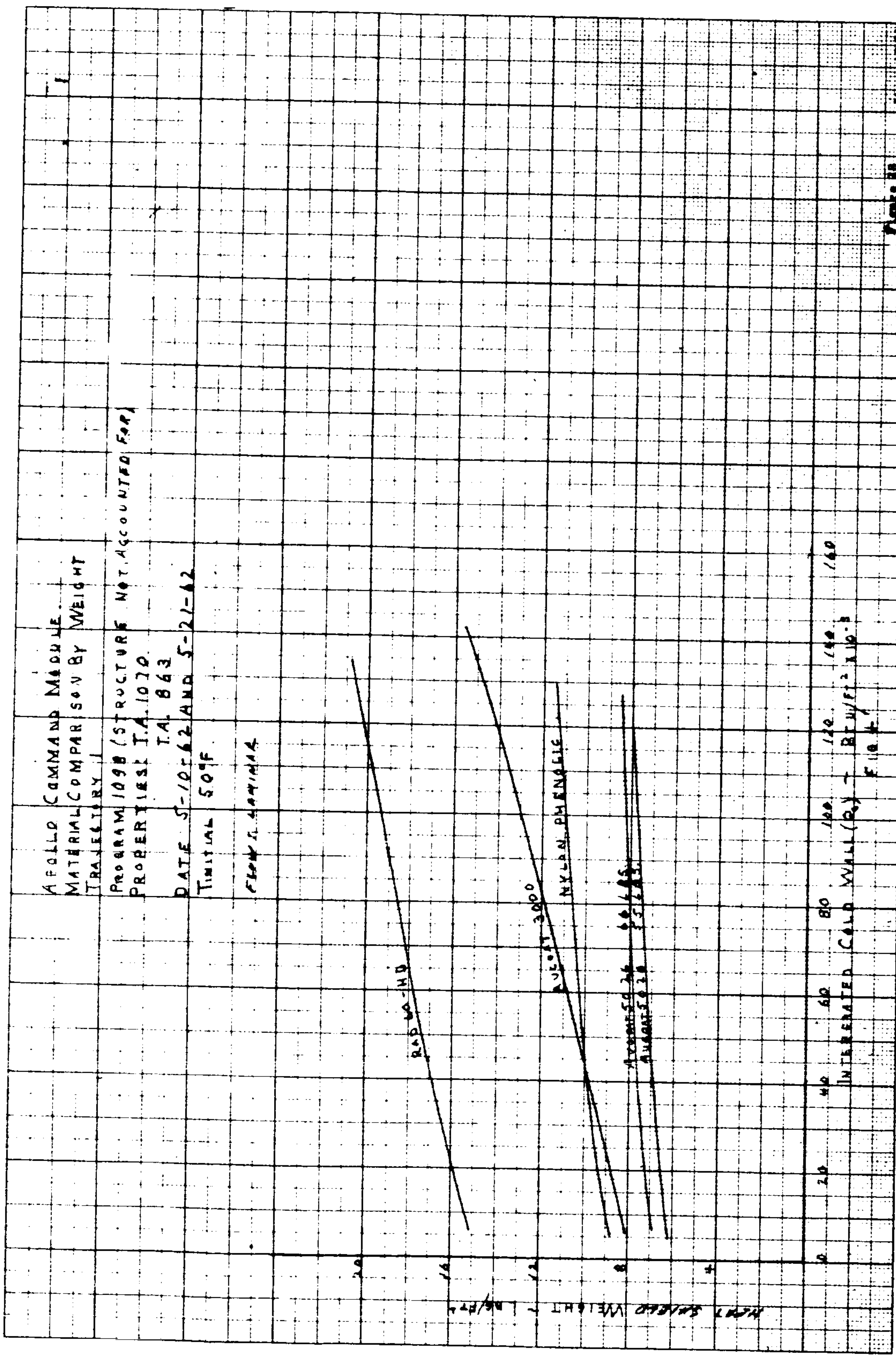

APOLLO COMMAND MODULE
MATERIAL COMPARISON BY WEIGHT
TRAJECTORY I
PROGRAM 1098 (STRUCTURE NOT ACCOUNTED FOR)
PROPERTIES: T.A. 1070
T.A. 863
DATE 5-10-62 AND 5-21-62
T INITIAL 50°F
FLOW IS LAMINAR
RAD XX-HD
AVCOAT 5026
AVCOAT 5026
NYLON PHENOLIC
INTEGRATED COLD WALL (q) ~ BTU/FT² x 10⁻³
HEAT SHIELD WEIGHT ~ LB/FT²
0
20
40
60
80
100
120
140
160
4
8
12
16
20

-75-

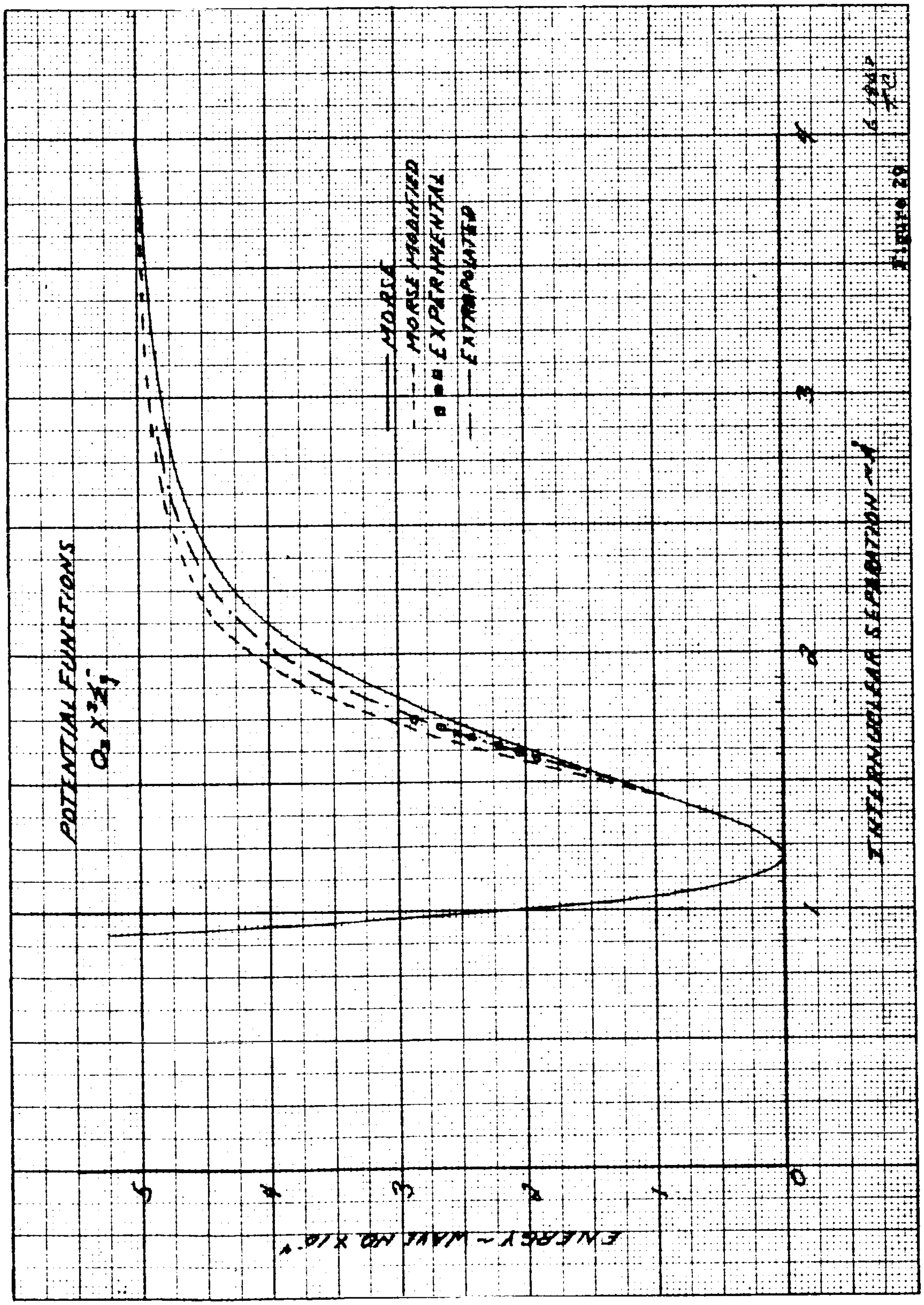

POTENTIAL FUNCTIONS
$O_2\ X^3\Sigma_g^-$
MORSE
MORSE MODIFIED
EXPERIMENTAL
EXTRAPOLATED
INTERNUCLEAR SEPARATION ~ Å
ENERGY ~ WAVE NO x 10^4
0
1
2
3
4
5
Figure 29

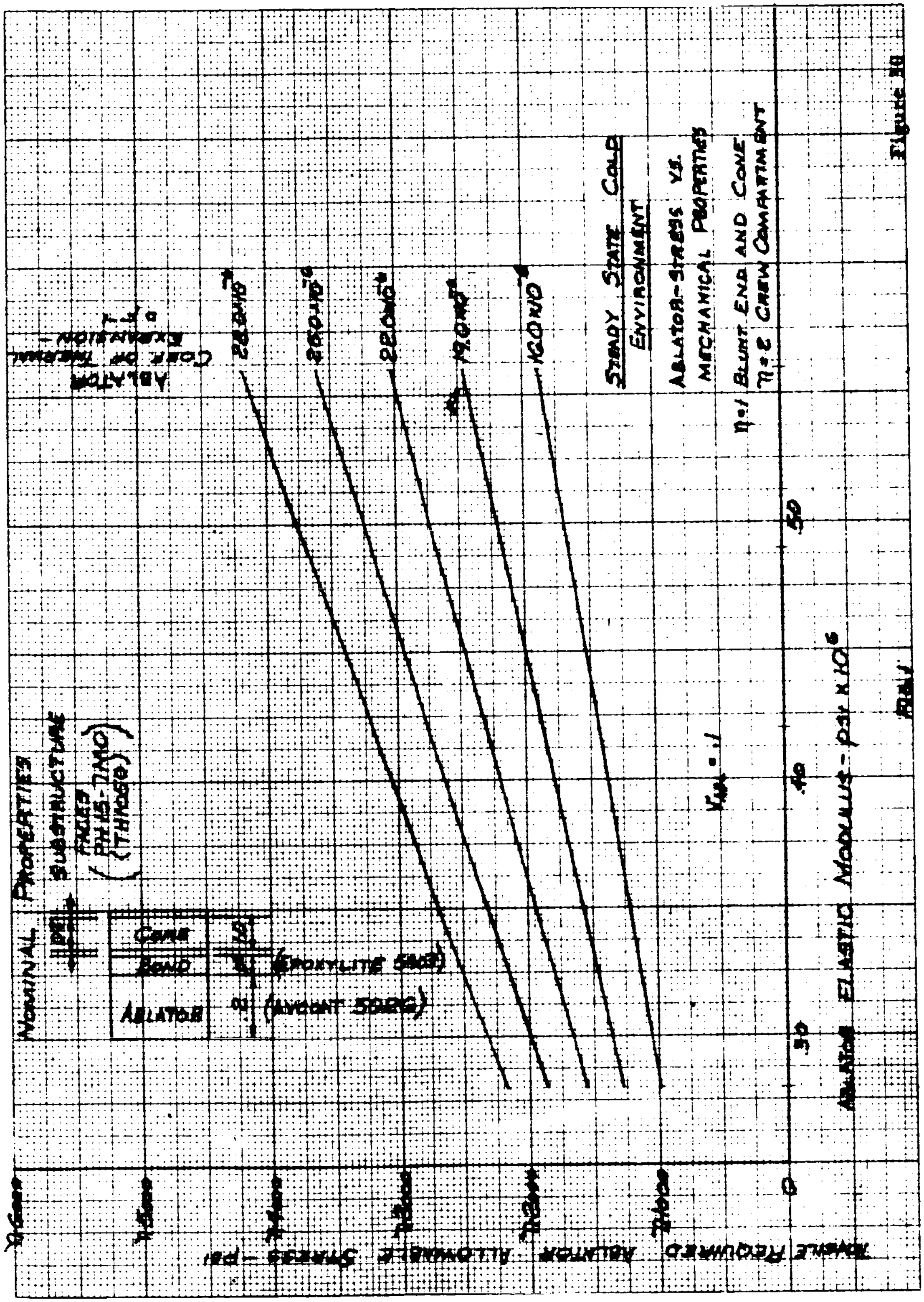
NOMINAL PROPERTIES
SUBSTRUCTURE
FACES (PH15-7MO) (TH1050)
CORE
BOND (EPOXYLITE 5403)
ABLATOR (AVCOAT 5026)
ABLATOR COEF. OF THERMAL EXPANSION - °F⁻¹
28.0×10⁻⁶
26.0×10⁻⁶
22.0×10⁻⁶
19.0×10⁻⁶
16.0×10⁻⁶
STEADY STATE COLD ENVIRONMENT
ABLATOR-STRESS VS. MECHANICAL PROPERTIES
η=1 BLUNT END AND CONE
η=2 CREW COMPARTMENT
TENSILE REQUIRED ABLATOR ALLOWABLE STRESS - PSI
0
30
40
50
ABLATOR ELASTIC MODULUS - psi × 10⁶

Figure 30

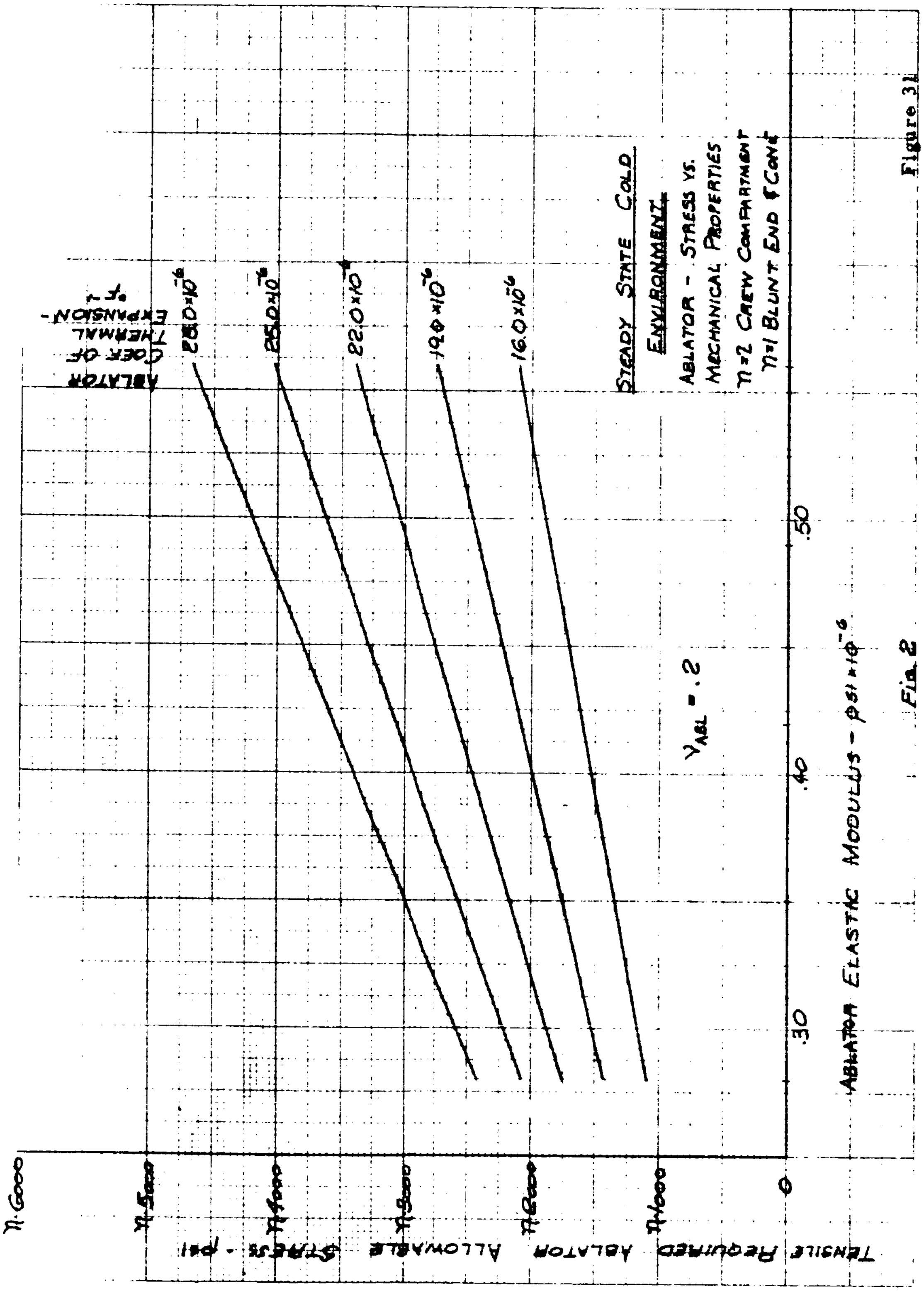
Steady State Cold Environment
Ablator - Stress vs. Mechanical Properties
n=2 Crew Compartment
n=1 Blunt End & Cone
Ablator Coef of Thermal Expansion - °F⁻¹
28.0×10⁻⁶
25.0×10⁻⁶
22.0×10⁻⁶
19.0×10⁻⁶
16.0×10⁻⁶
ν_ABL = .2
.30
.40
.50
Ablator Elastic Modulus - psi × 10⁻⁶
Tensile Required Ablator Allowable Stress - psi
0
n·1000
n·2000
n·3000
n·4000
n·5000
n·6000
Fig 2

Figure 31

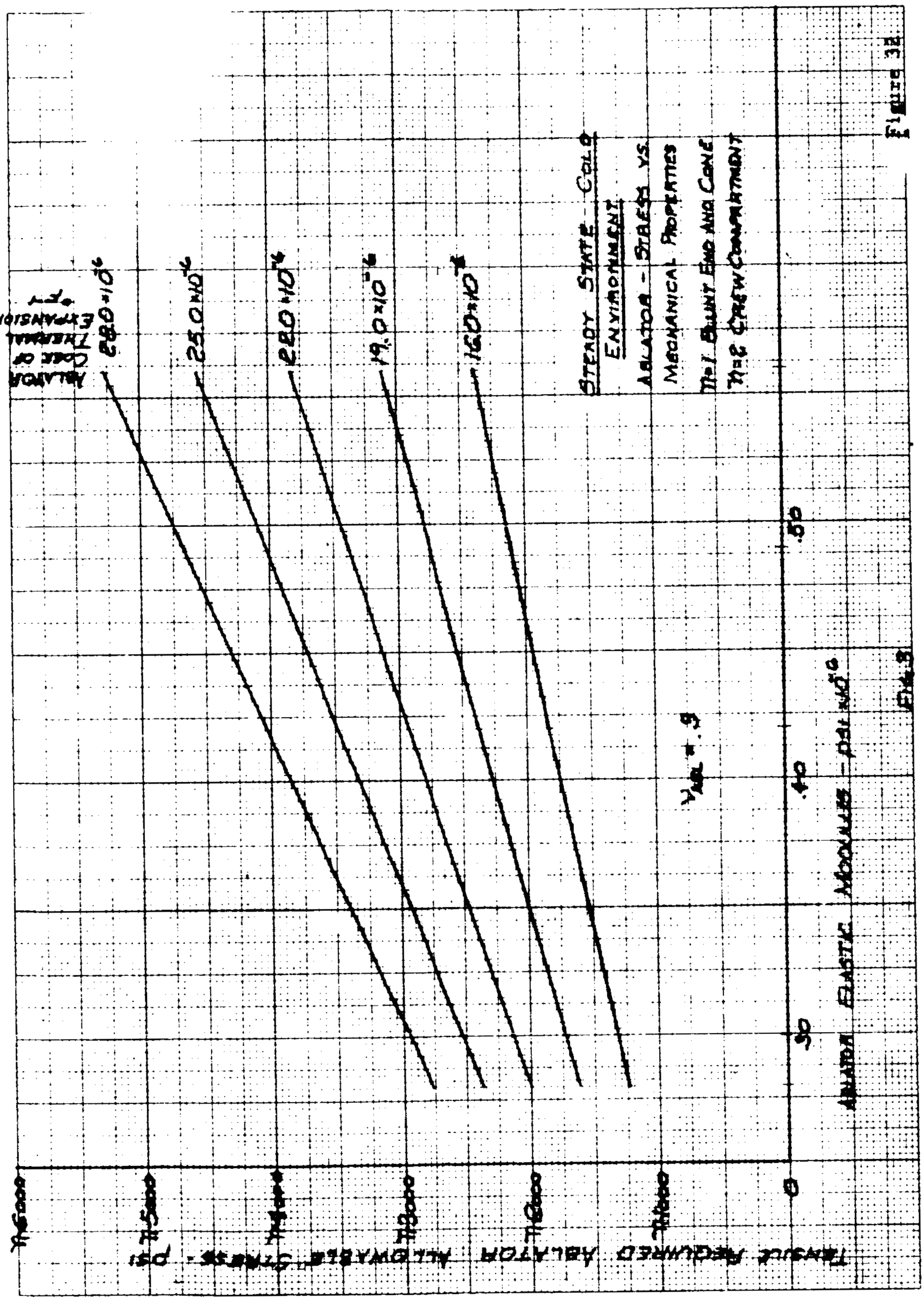
Figure 32
Steady State - Cold
Environment
Ablator - Stress vs.
Mechanical Properties
n=1 Blunt End and Cone
n=2 Crew Compartment
Ablator Coef of Thermal Expansion in/in °F
28.0×10⁻⁶
25.0×10⁻⁶
22.0×10⁻⁶
19.0×10⁻⁶
16.0×10⁻⁶
ν_{ABL} = .9
0
.30
.40
.50
Ablator Elastic Modulus - psi ×10⁶
0
1000
2000
3000
4000
5000
6000
Tensile Required Ablator Allowable Stress - psi

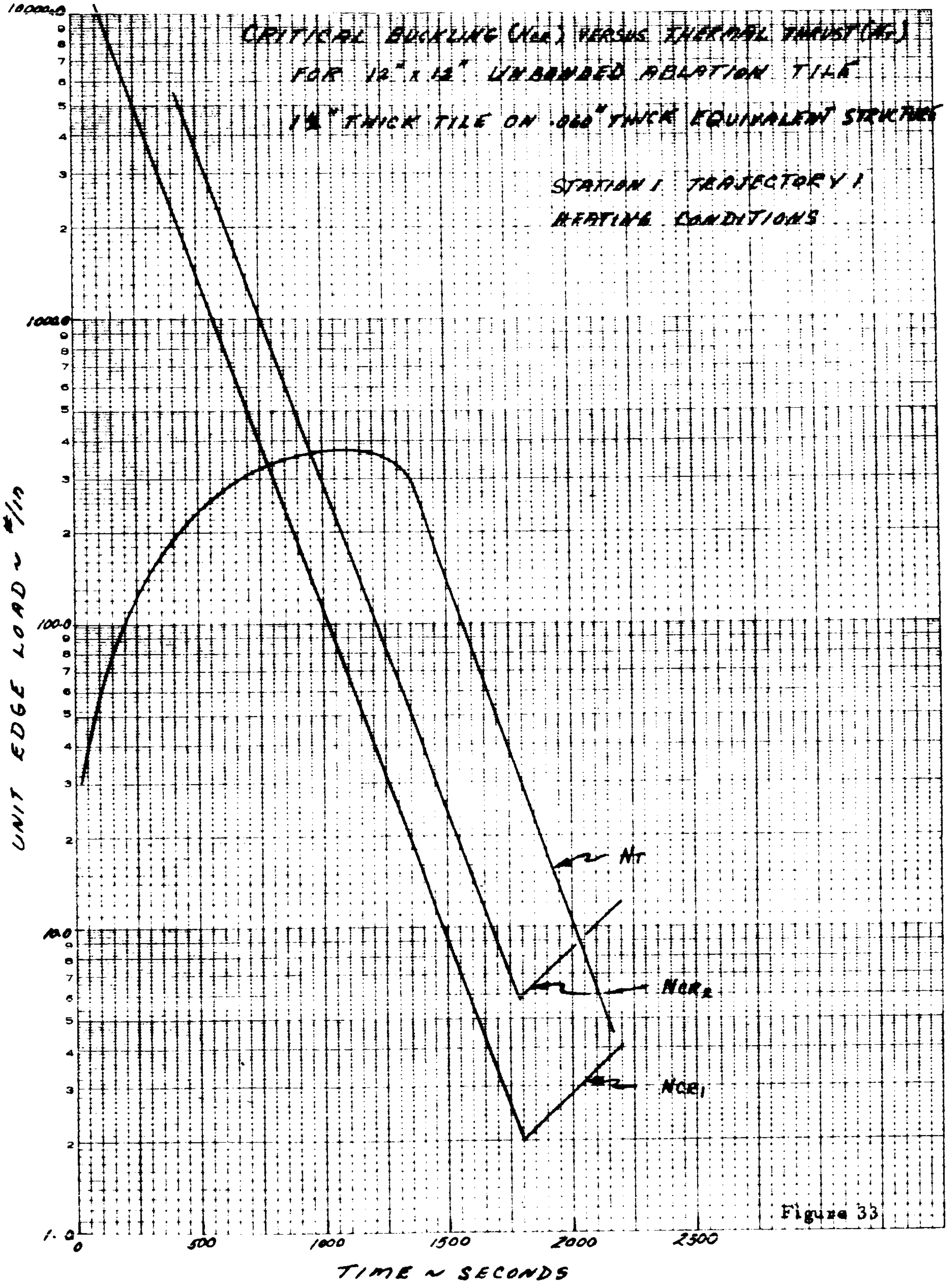
CRITICAL BUCKLING (N_{CR}) VERSUS THERMAL THRUST (N_T)
FOR 12" x 12" UNBONDED ABLATION TILE
1½" THICK TILE ON .060" THICK EQUIVALENT STRUCTURE
STATION 1 TRAJECTORY 1
HEATING CONDITIONS
N_T
N_{CR_2}
N_{CR_1}
UNIT EDGE LOAD ~ #/in
TIME ~ SECONDS
10000.0
1000.0
100.0
10.0
1.0
0
500
1000
1500
2000
2500

Figure 33

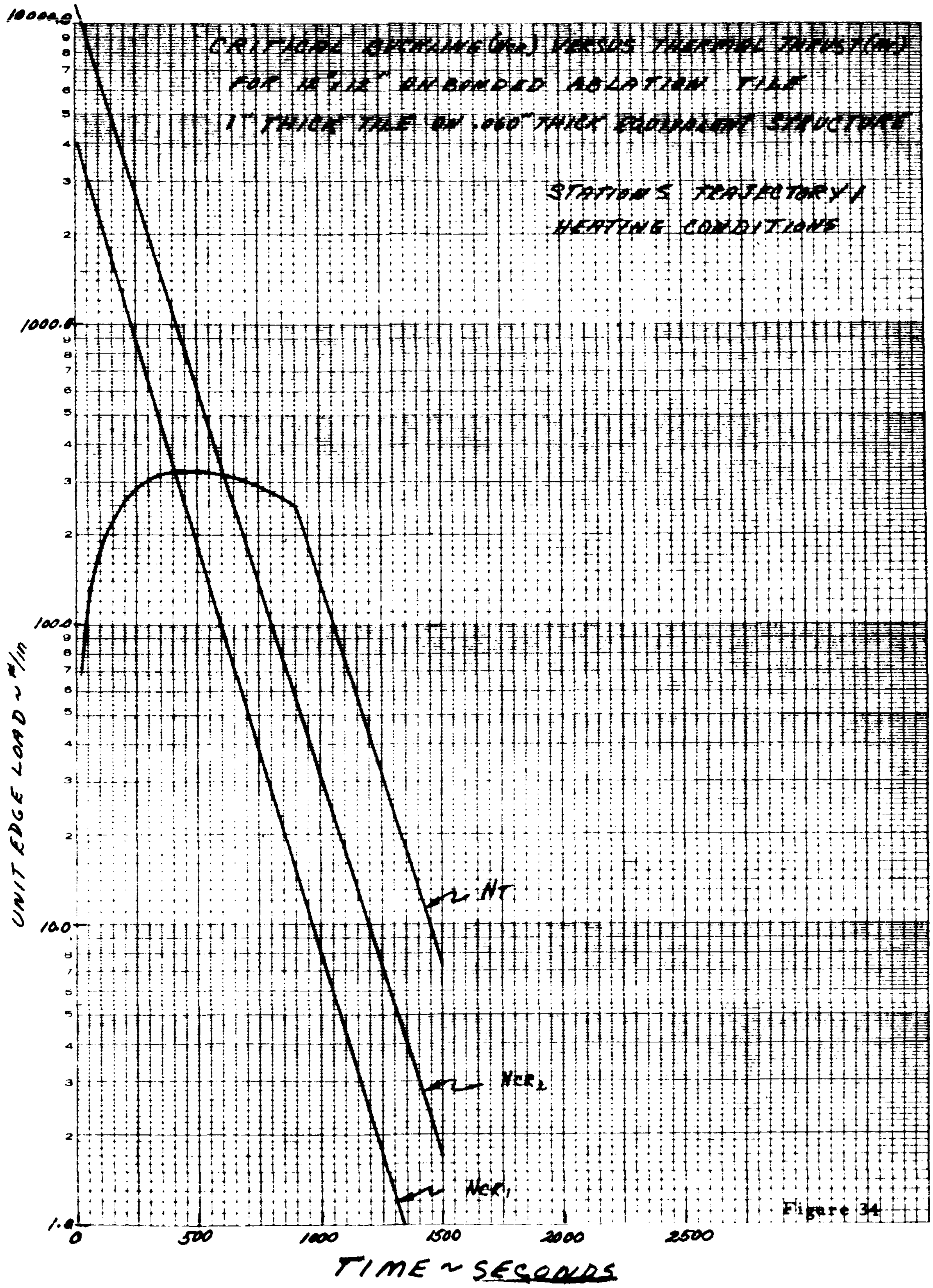
CRITICAL BUCKLING (NCR) VERSUS THERMAL THRUST (NT)
FOR 12"x12" UNBONDED ABLATION TILE
1" THICK TILE ON .060" THICK EQUIVALENT STRUCTURE
STATION 5 TRAJECTORY 1
HEATING CONDITIONS
10000.0
1000.0
100.0
10.0
1.0
UNIT EDGE LOAD ~ #/in
NT
NCR2
NCR1
0
500
1000
1500
2000
2500
TIME ~ SECONDS

Figure 34

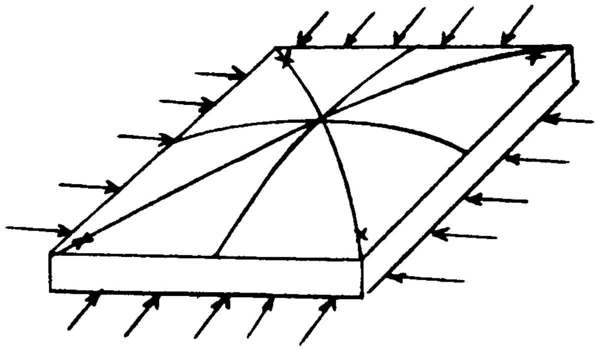

FASTENER LOCATION AND BUCKLING PATTERN FOR N_{CR_1}

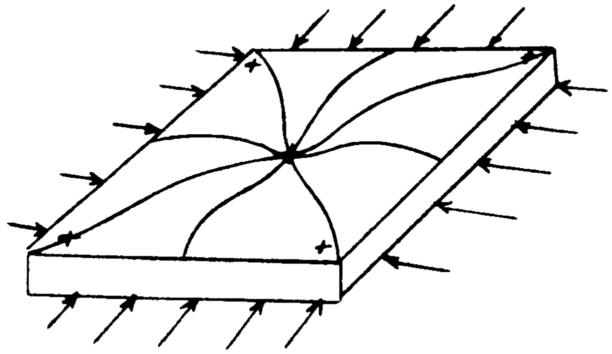

FASTENER LOCATION AND BUCKLING PATTERN FOR N_{CR_2}

Figure 35

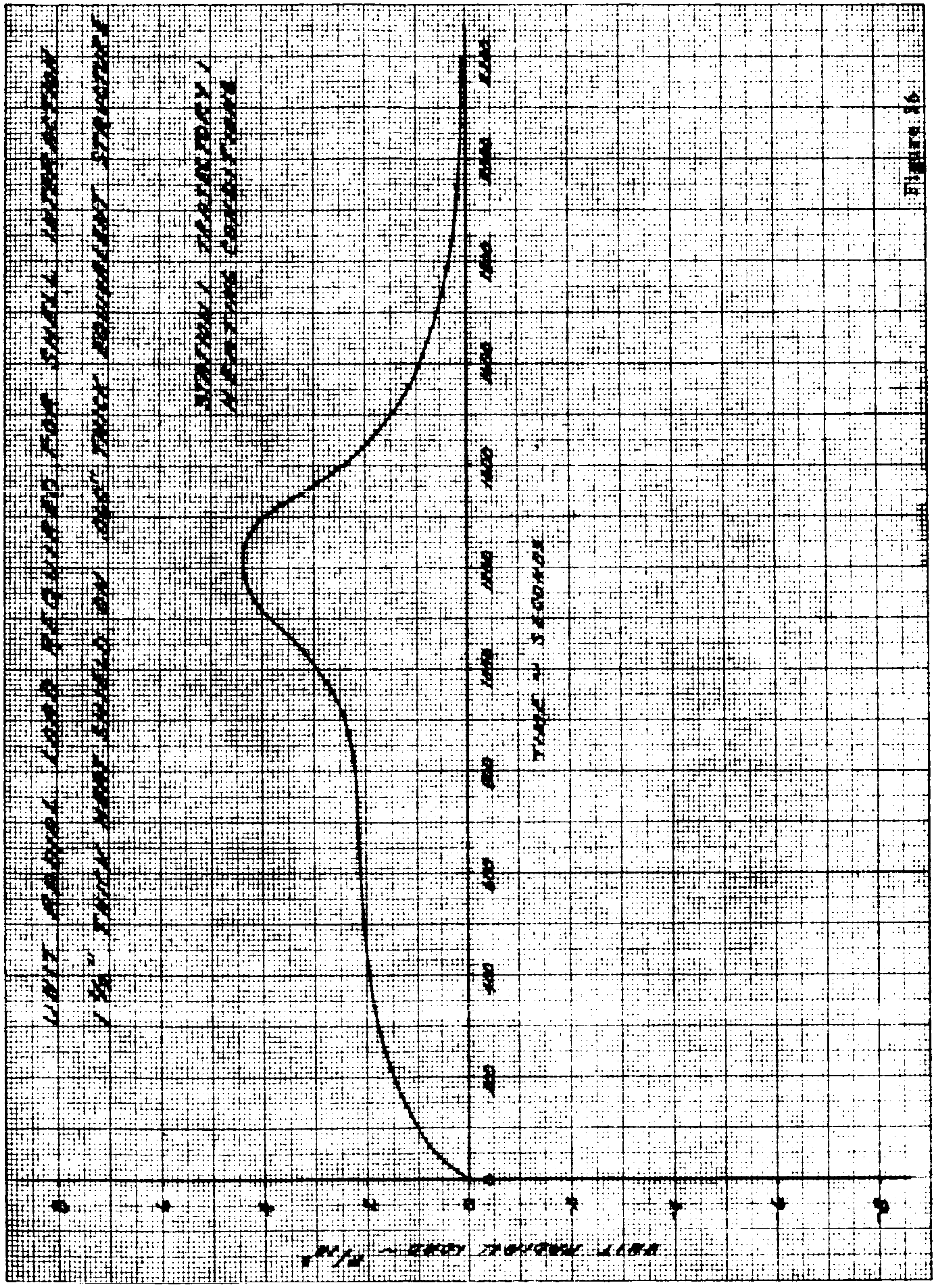

Figure 16

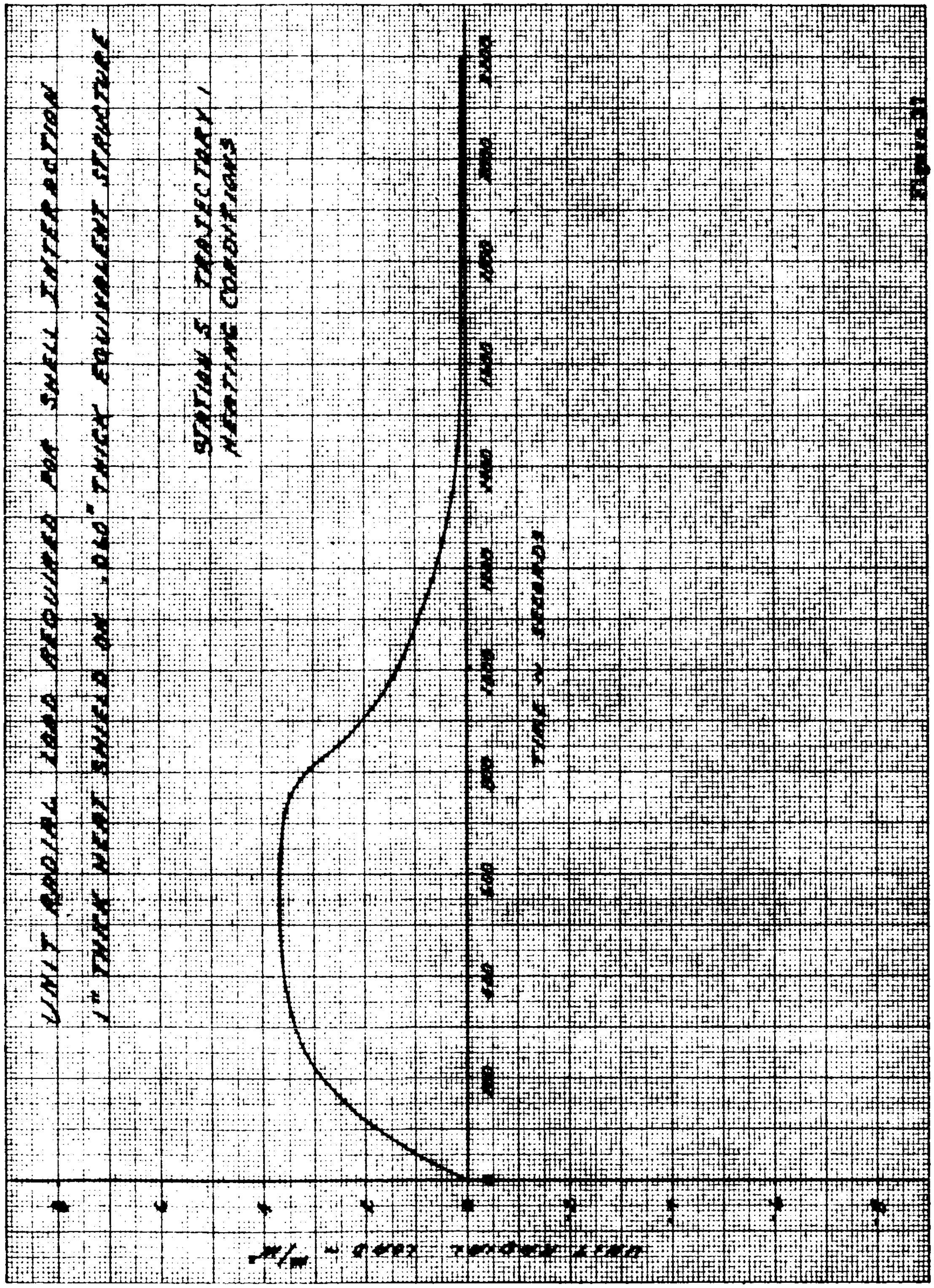
UNIT RADIAL LOAD REQUIRED FOR SHELL INTERACTION
1" THICK HEAT SHIELD ON .060" THICK EQUIVALENT STRUCTURE
STATION 5 TRAJECTORY I
HEATING CONDITIONS
TIME IN SECONDS

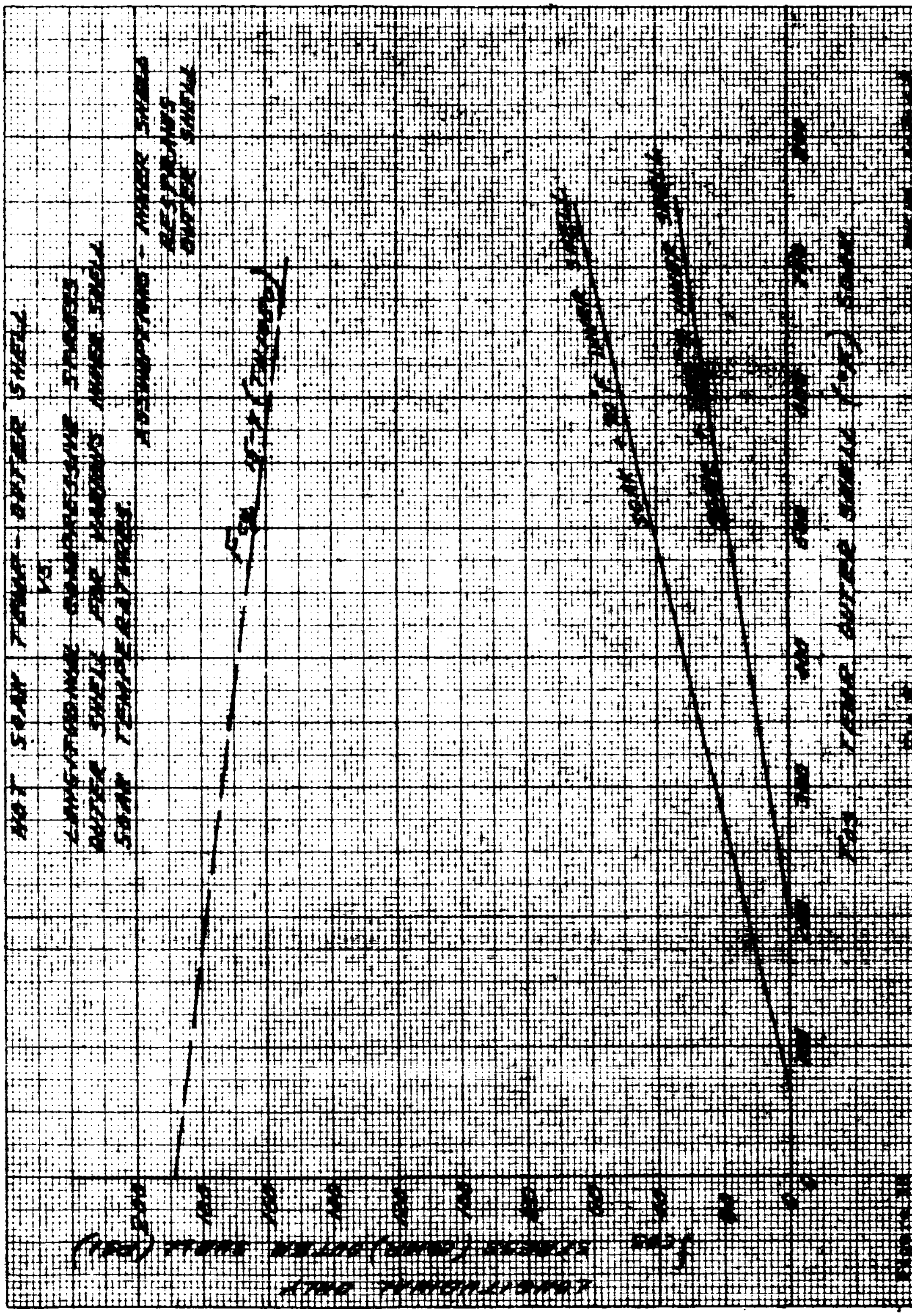
HOT SPAN TEMP - OUTER SHELL
VS
LONGITUDINAL COMPRESSIVE STRESS
OUTER SHELL FOR VARIOUS INNER SHELL
SPAN TEMPERATURES
ASSUMPTION - INNER SHELL
RESTRAINS
OUTER SHELL
TEMP OUTER SHELL (°F) SPAN

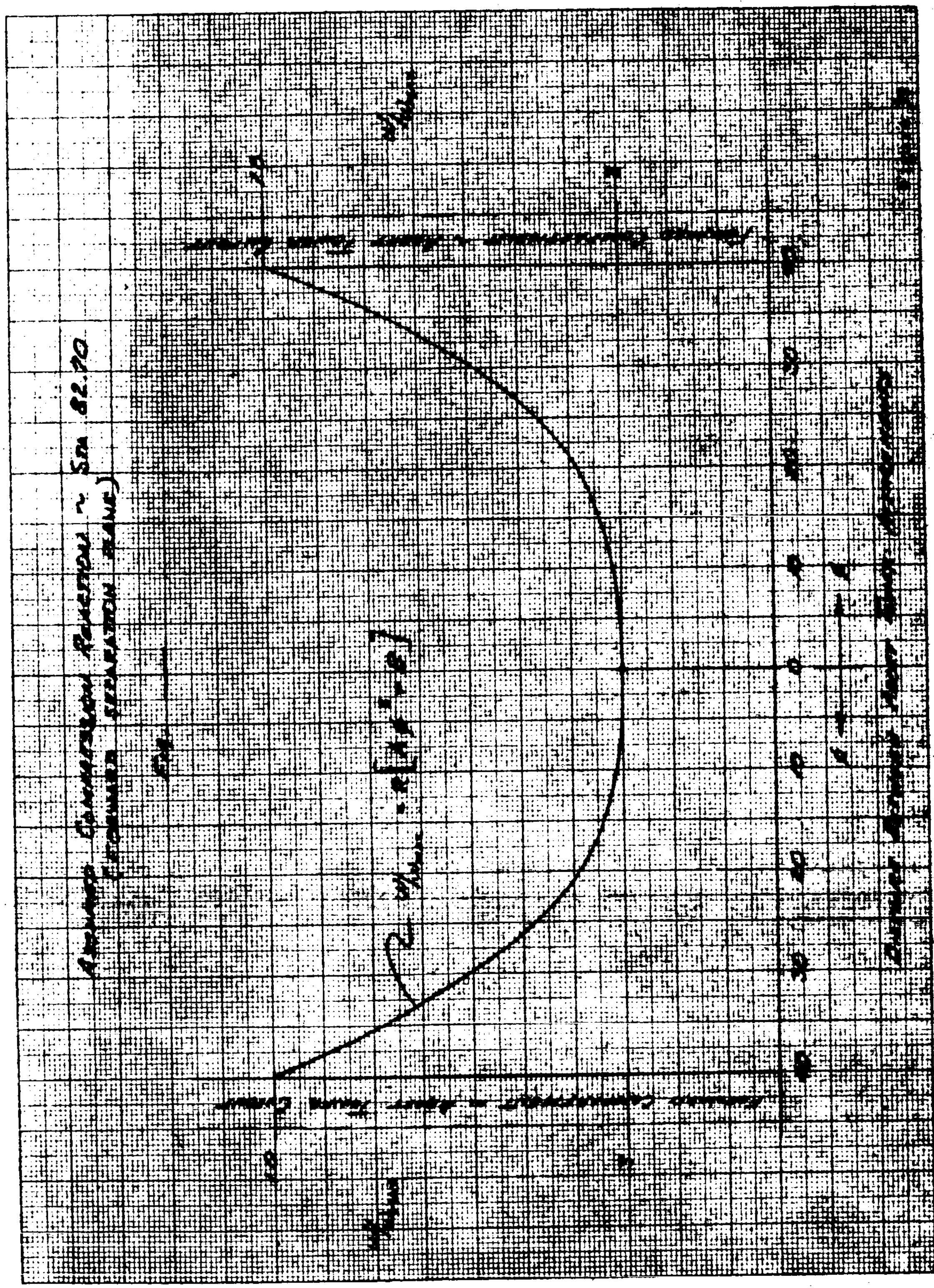

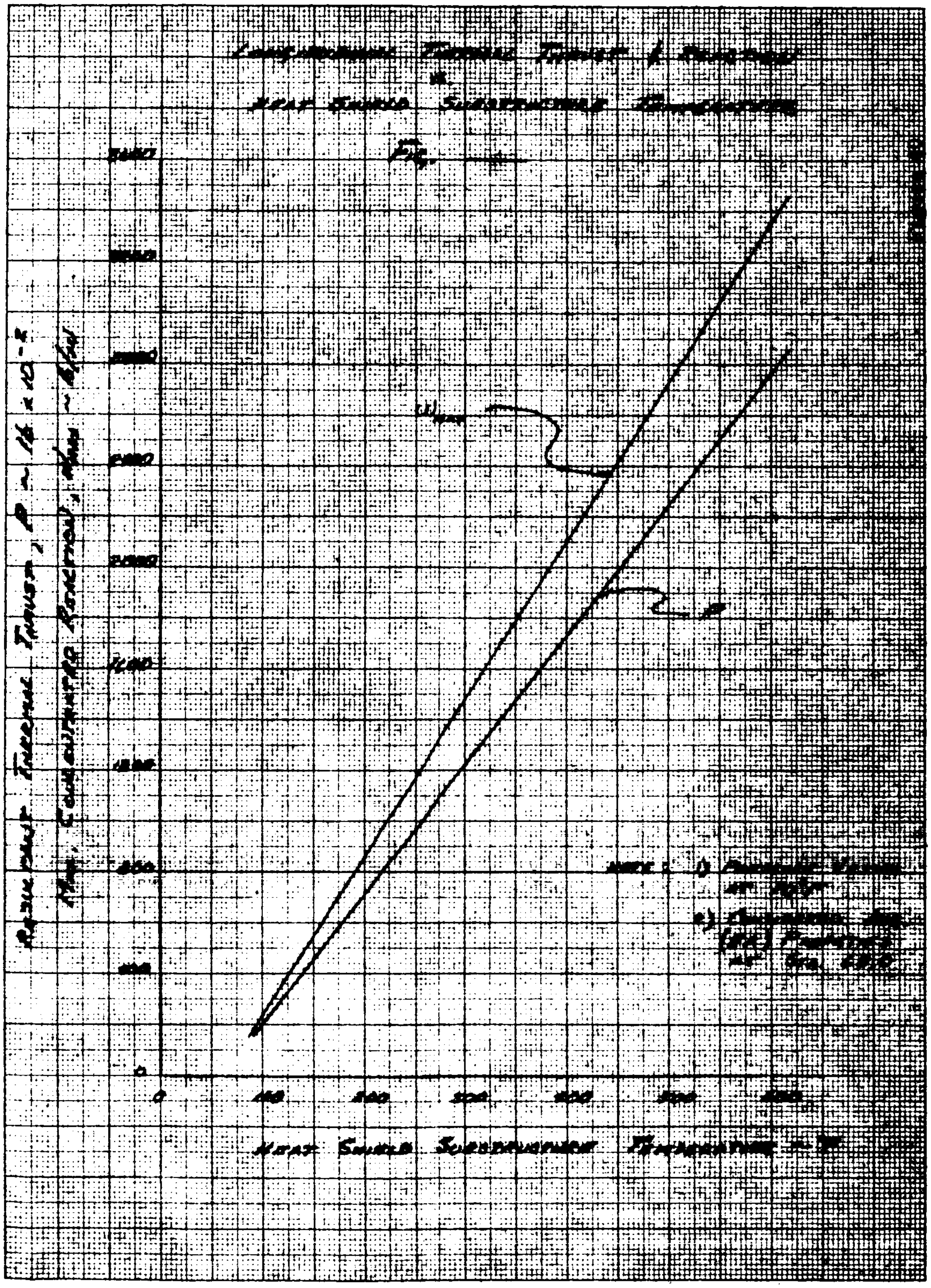

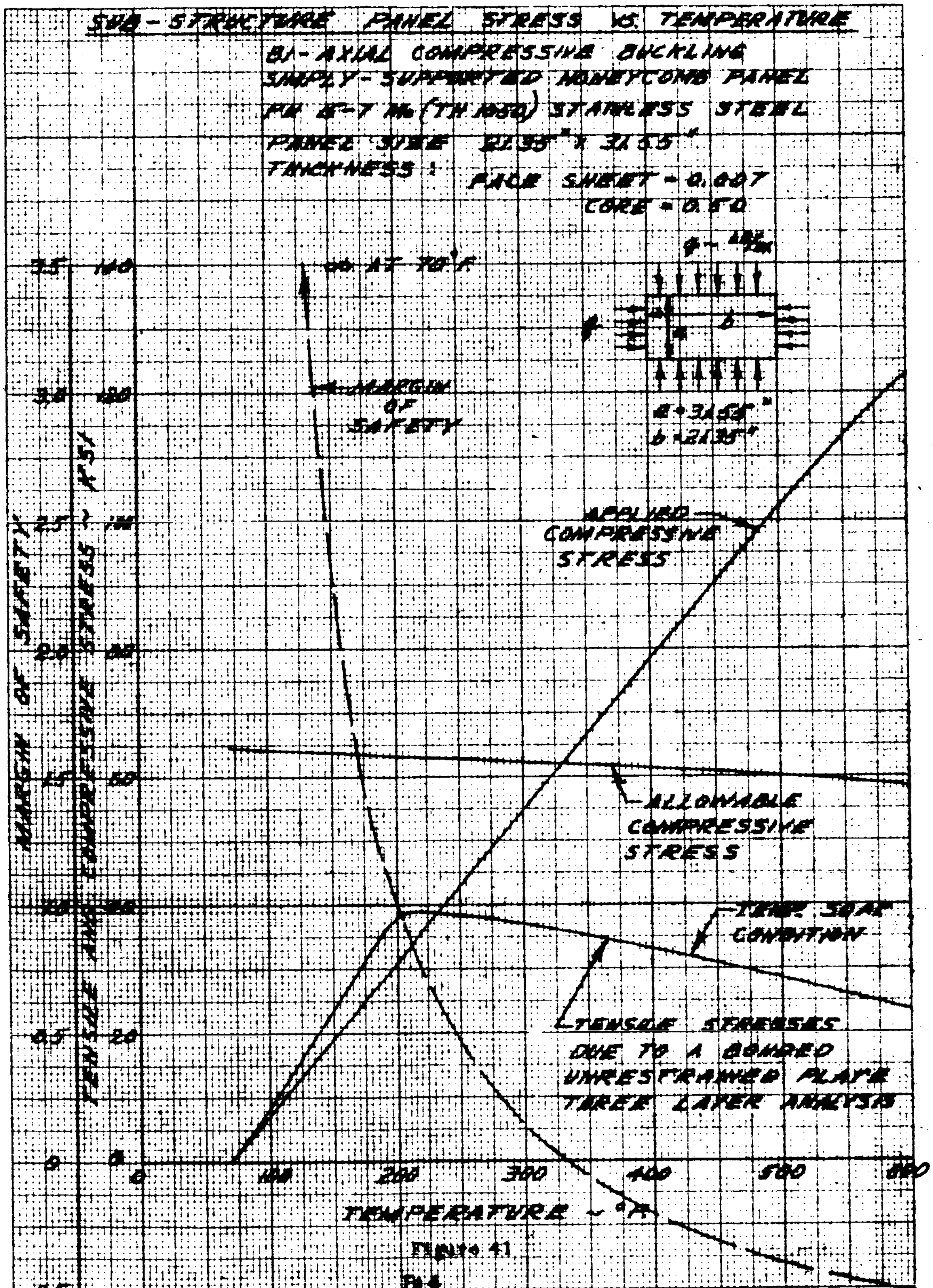

Figure 41

PS 1-14-62

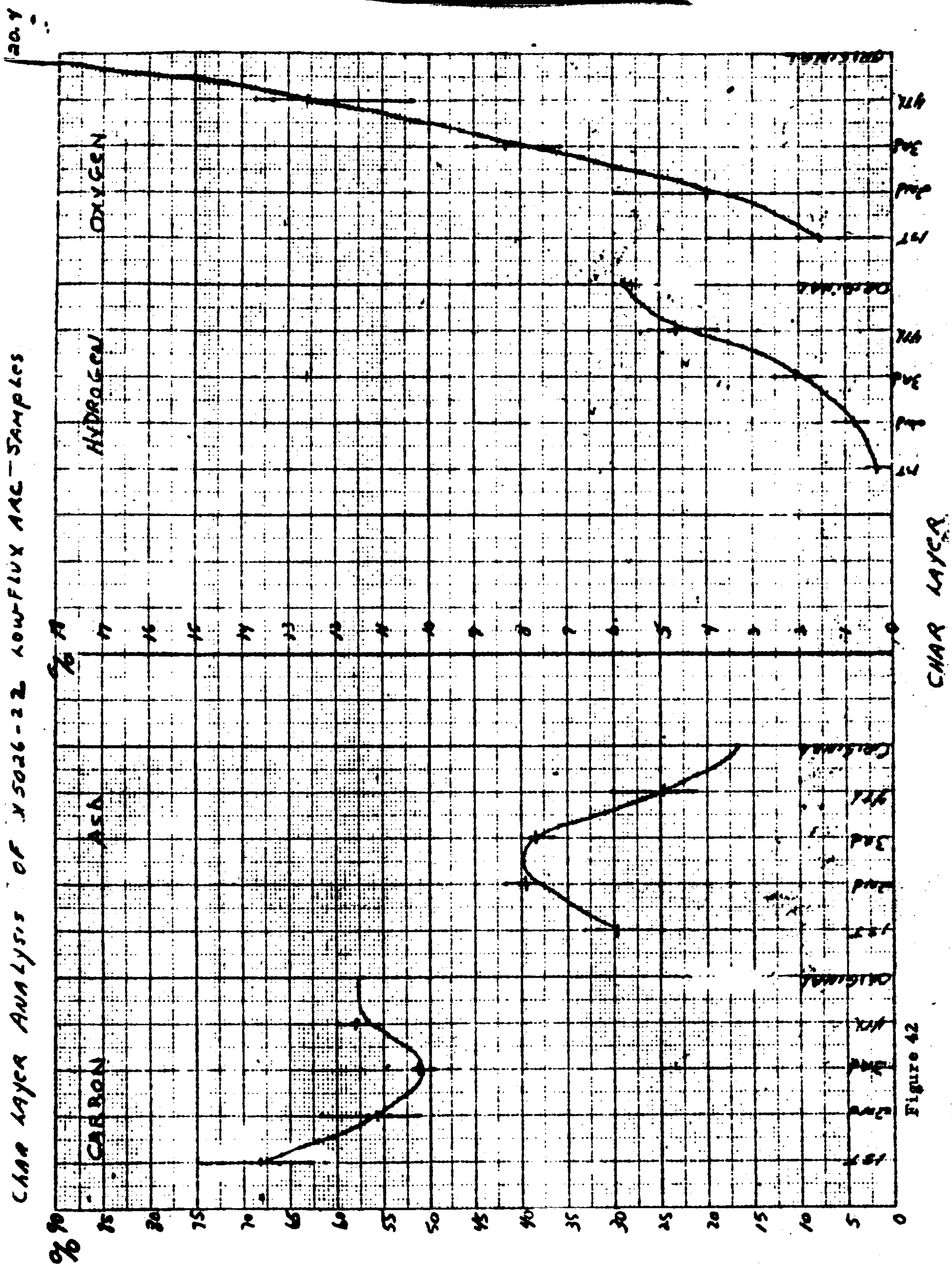
CHAR LAYER ANALYSIS OF X5026-22 LOW-FLUX ARC-SAMPLES
OXYGEN
HYDROGEN
ASH
CARBON
CHAR LAYER
%

Figure 42

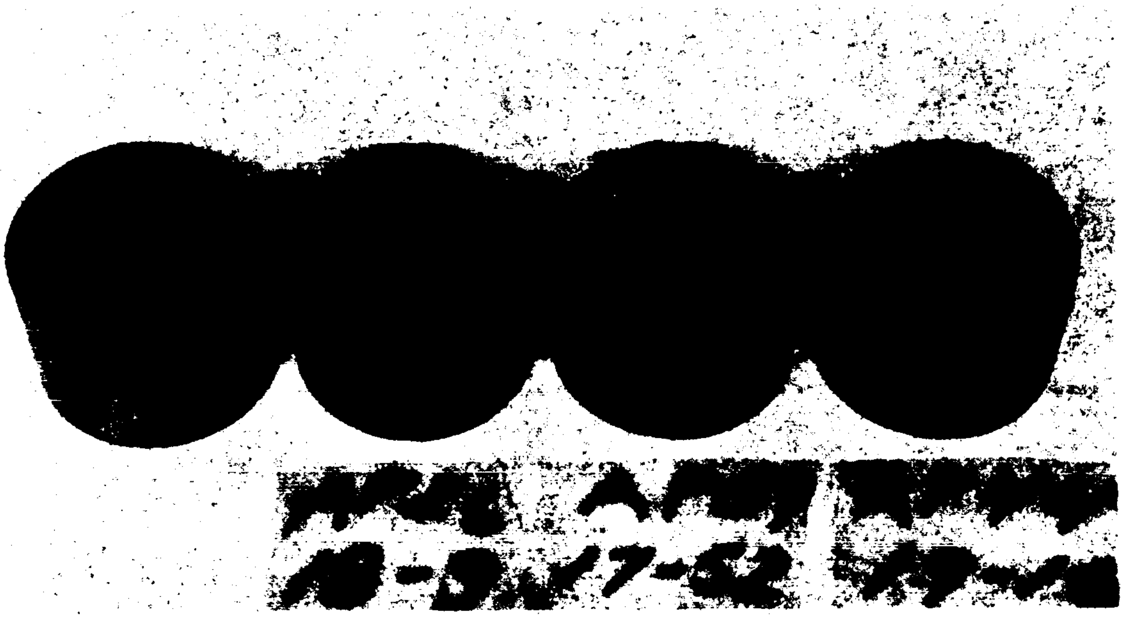

Figure 43 a) Untested sample (left)

b) Tested samples (right)

Facility: OVERS

Gas Enthalpy: 7000 Btu/lb

Heat Flux (cold wall): 60 Btu/ft^2 sec

Time: $2\frac{1}{2}$ minutes

Gas: air

Figure 44 Sectioned Samples

a) Untested sample (left)

b) Tested sample (right)

Facility: OVERS

Gas Enthalpy: 7000 Btu/lb

Heat Flux: 60 Btu/ft^2 sec

Time: $2\frac{1}{2}$ minutes

Gas: air

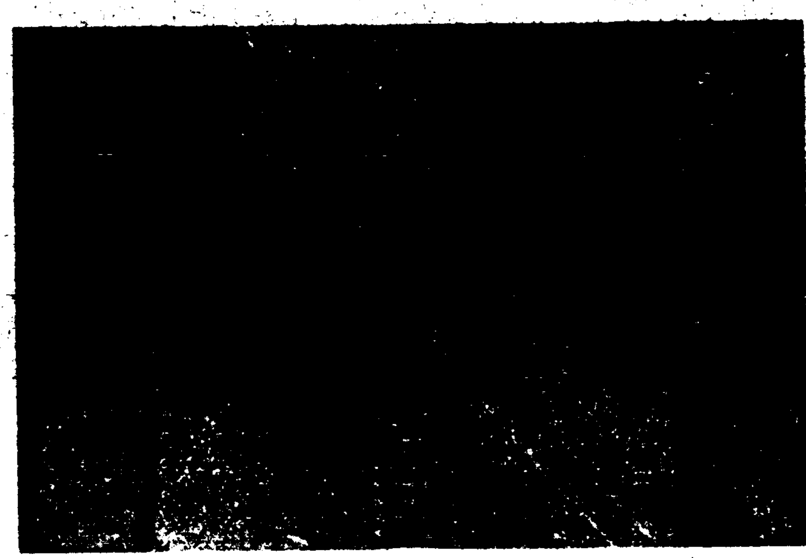

Figure 45 **Half Section View of Untested Sample**

Figure 46 Half Section View of Tested Sample
5026-29
Facility: OVERS
Gas Enthalpy: 7000 Btu/lb
Heat Flux: 60 Btu/ft^2-sec
Time: 2½ minutes
Gas: air

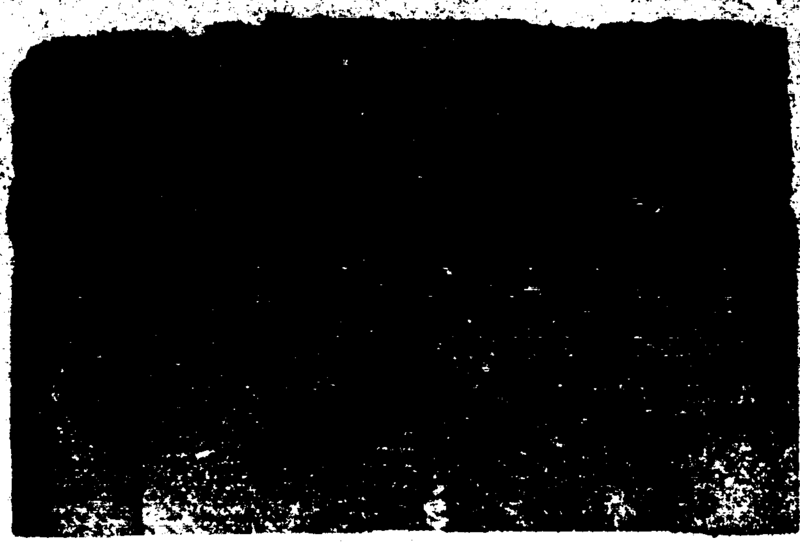

Figure 47 Half Section View of Tested
Sample 5026-23 (AP87)
Facility: OVERS
Gas Enthalpy: 7000 Btu/lb
Heat Flux: 60 Btu/ft^2-sec
Time: $2\frac{1}{2}$ minutes
Gas: air

Figure 48 Half Section View of Tested Sample
5026-22 (AP44)
Facility: OVERS
Gas Enthalpy: 7000 Btu/lb
Heat Flux: 60 Btu/ft^2-sec
Time: 2½ minutes
Gas: air

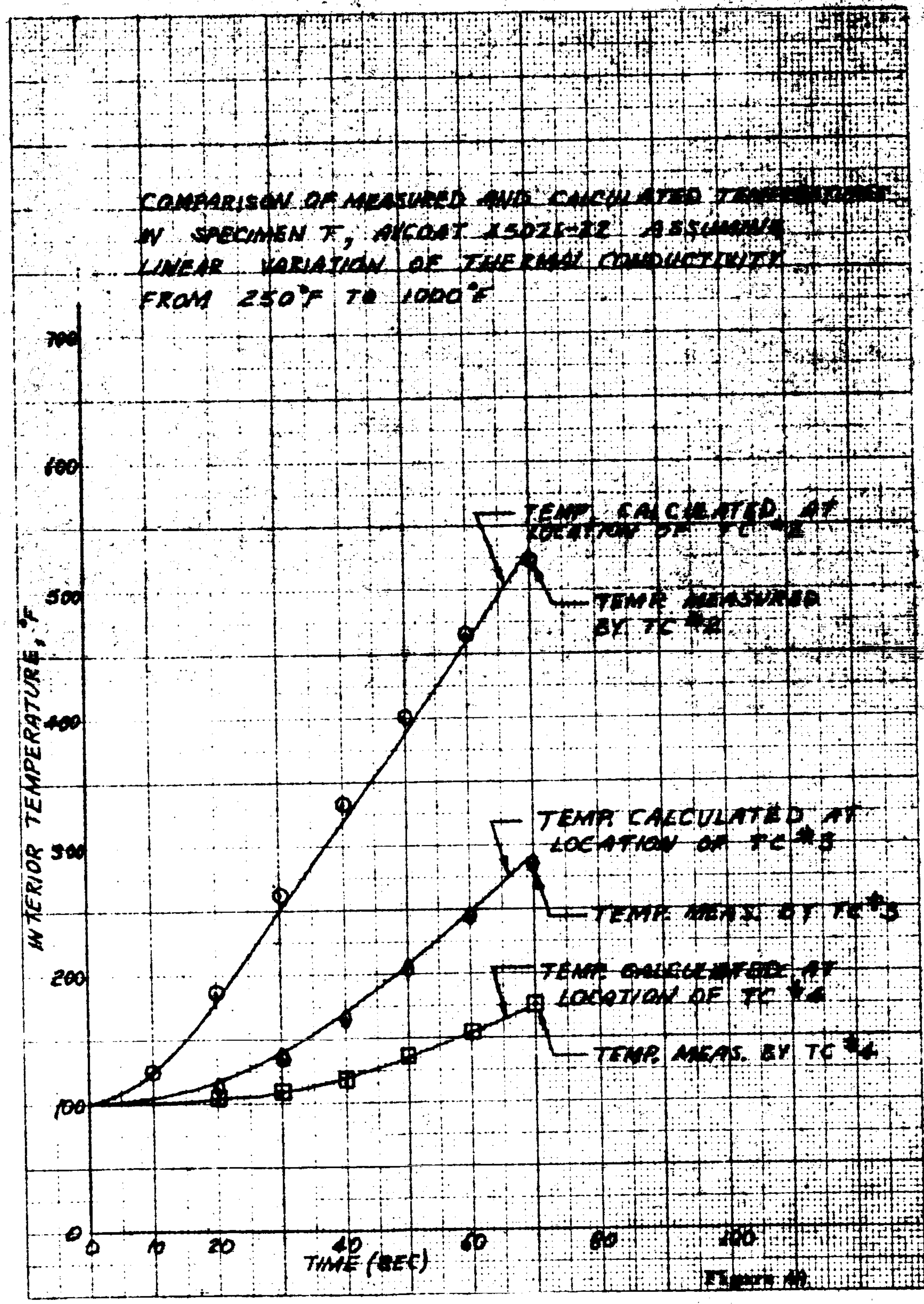

COMPARISON OF MEASURED AND CALCULATED
IN SPECIMEN F, AVCOAT X5026-22 ASSUMING
LINEAR VARIATION OF THERMAL CONDUCTIVITY
FROM 250°F TO 1000°F
TEMP. CALCULATED AT LOCATION OF TC
TEMP. MEASURED BY TC #2
TEMP. CALCULATED AT LOCATION OF TC #3
TEMP. MEAS. BY TC #3
TEMP. CALCULATED AT LOCATION OF TC #4
TEMP. MEAS. BY TC #4
INTERIOR TEMPERATURE, °F
TIME (SEC)
0
100
200
300
400
500
600
700
10
20
40
60
80
100

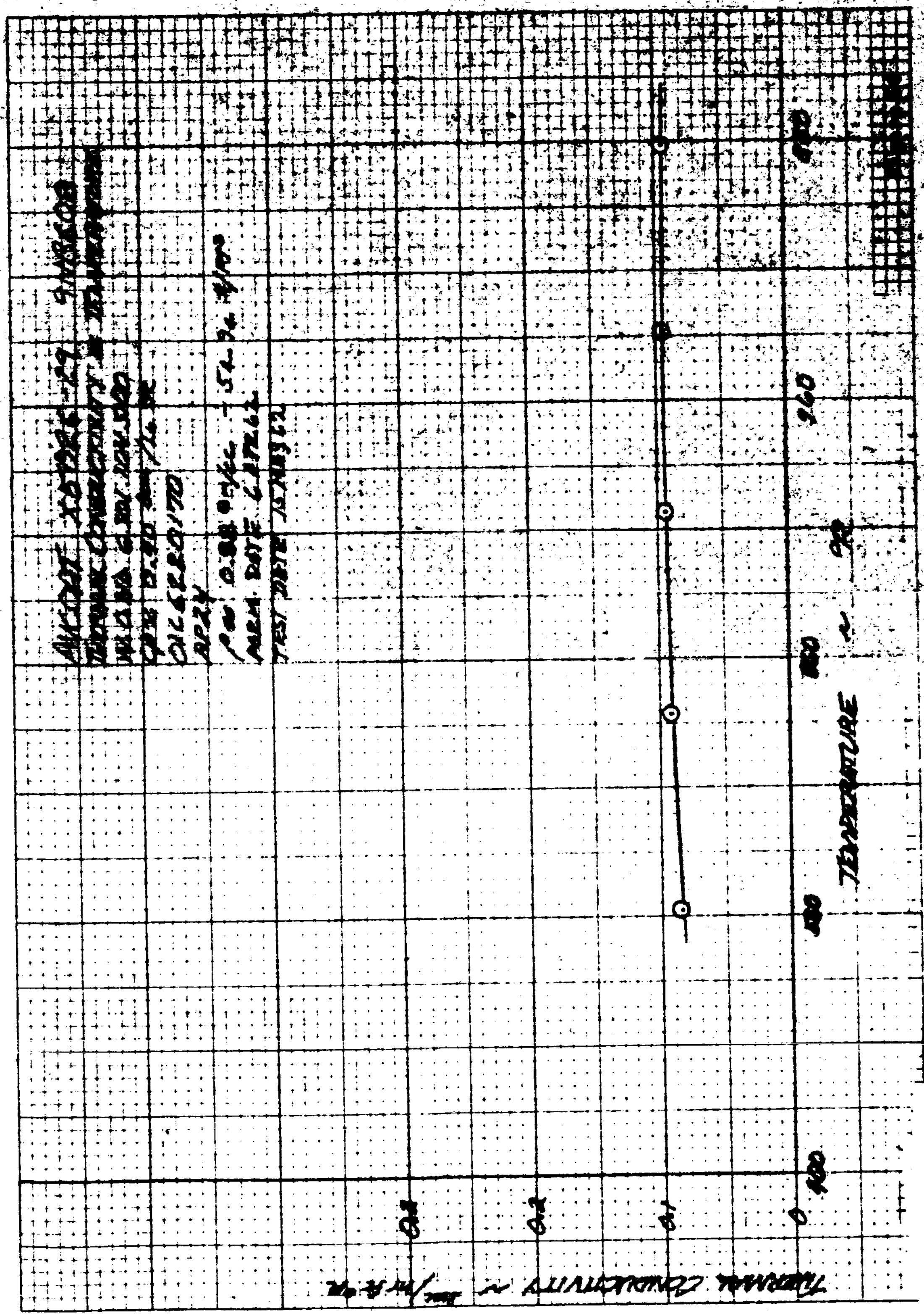
0.1
0.2
0
TEMPERATURE


AVCOAT X5026-22
THERMAL CONDUCTIVITY vs TEMPERATURE
THERMAL CONDUCTIVITY
0.3
0.2
0.1
0
TEMPERATURE

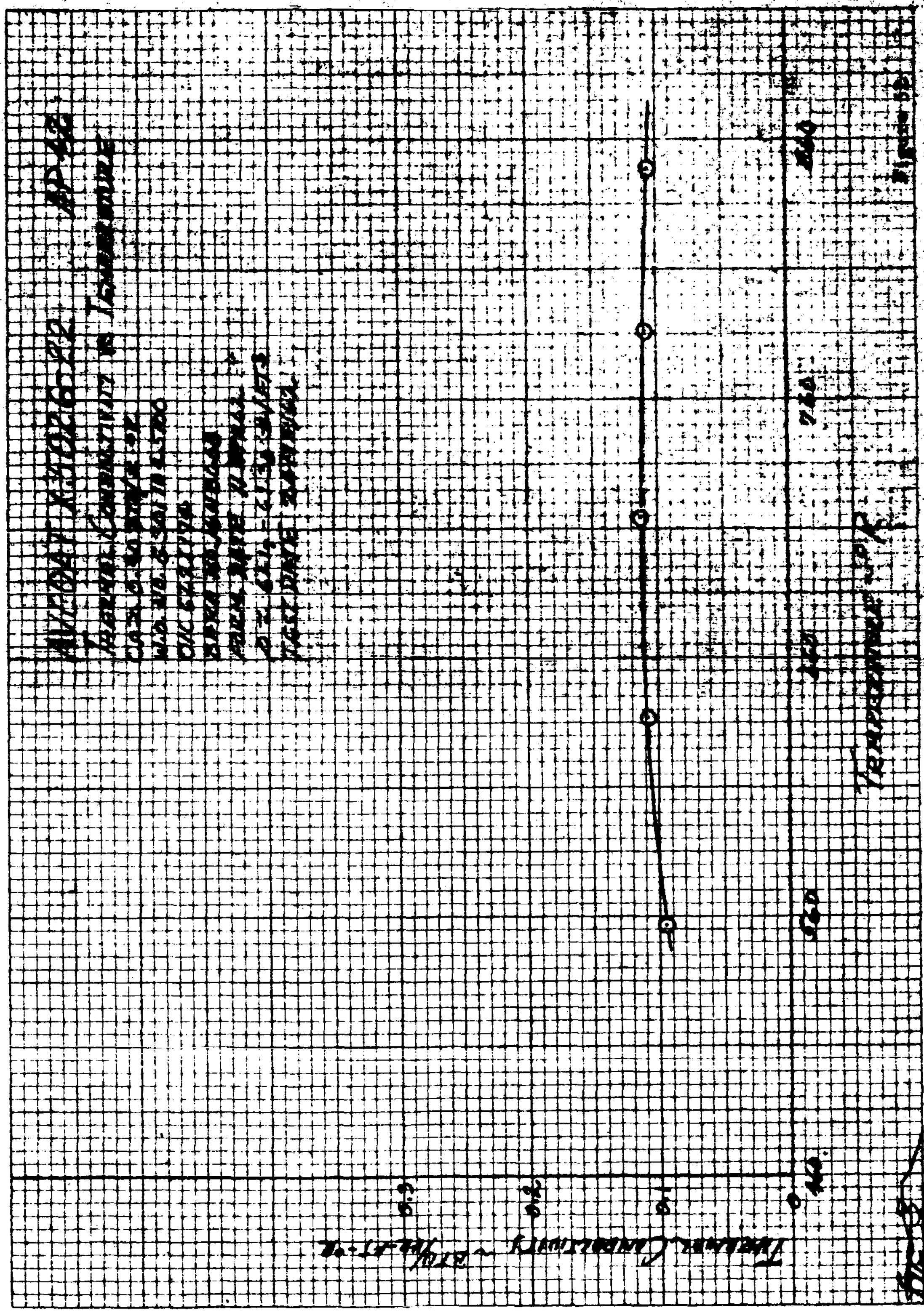
Thermal Conductivity vs Temperature
0.1
0.2
0.3
460
560
660
760
860
Temperature °R

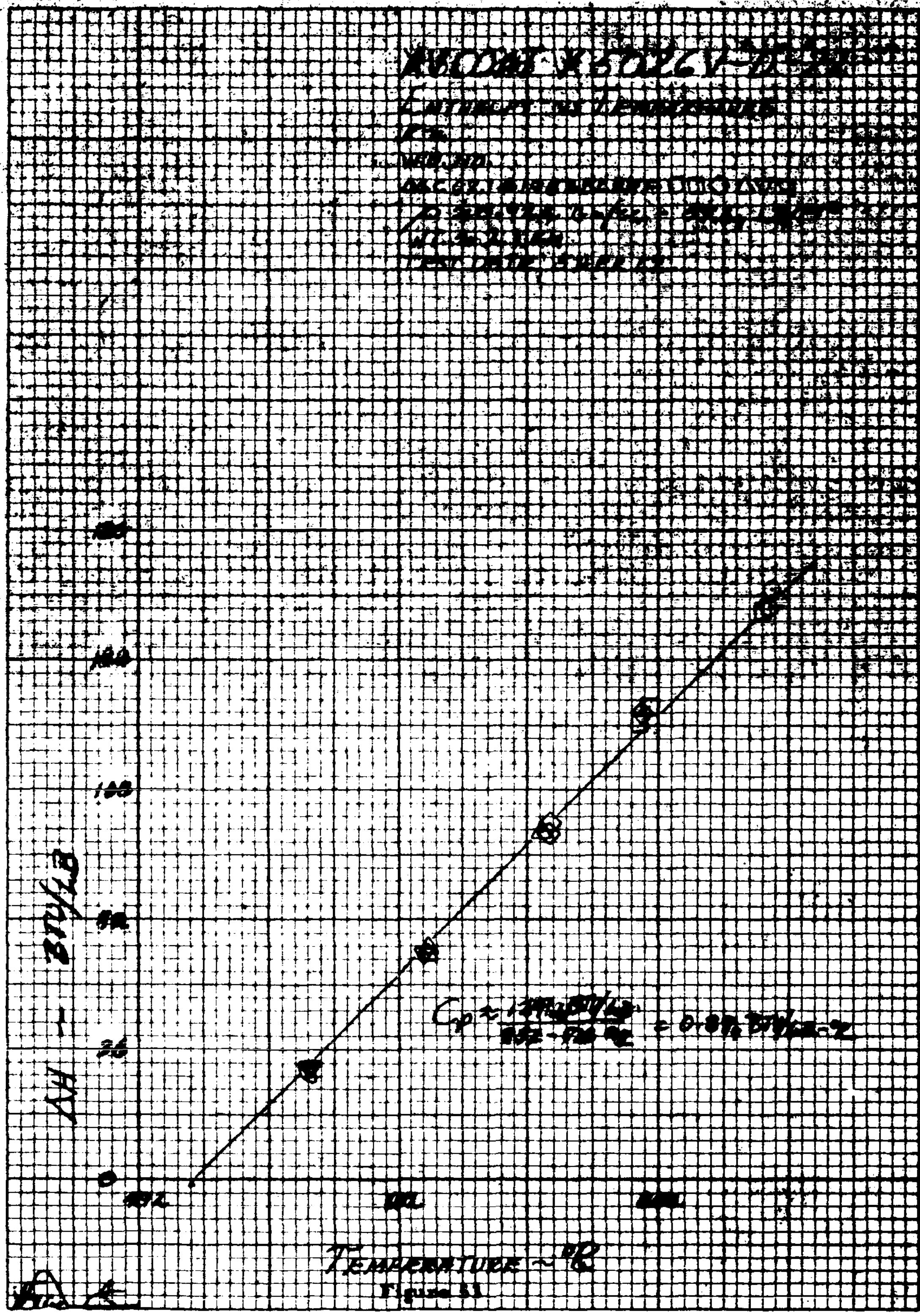

Figure 51

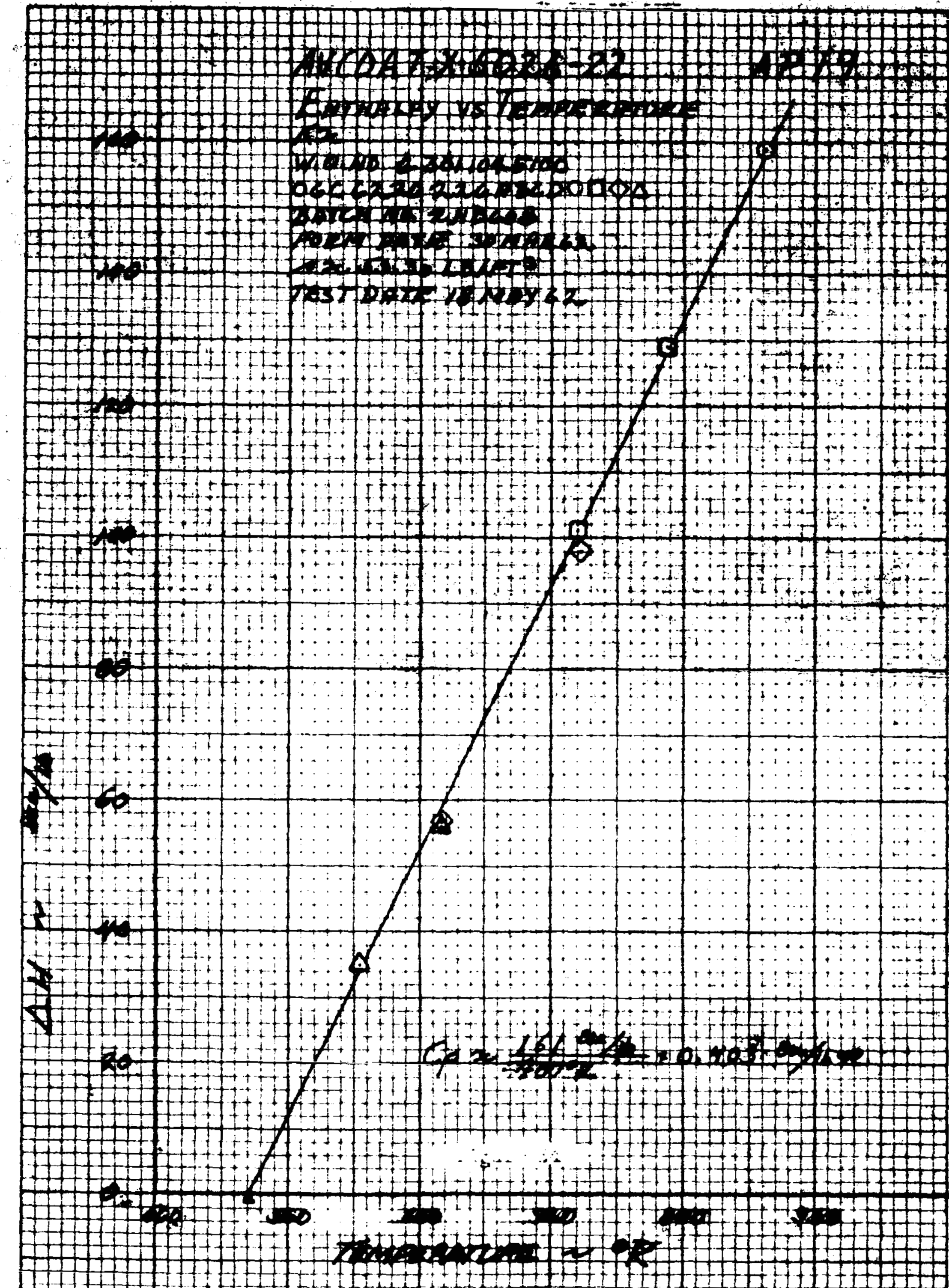

Figure 54

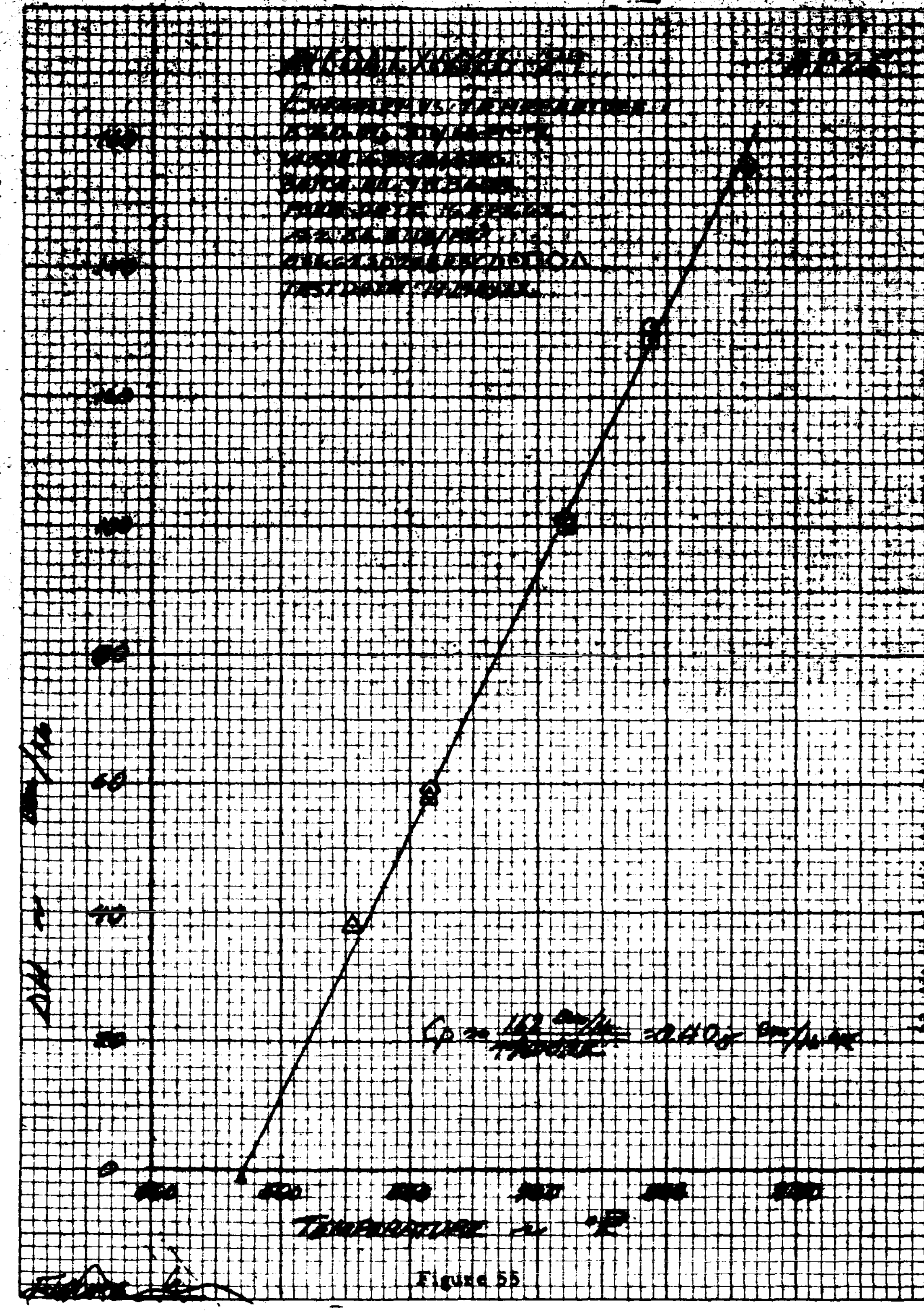

Figure 55

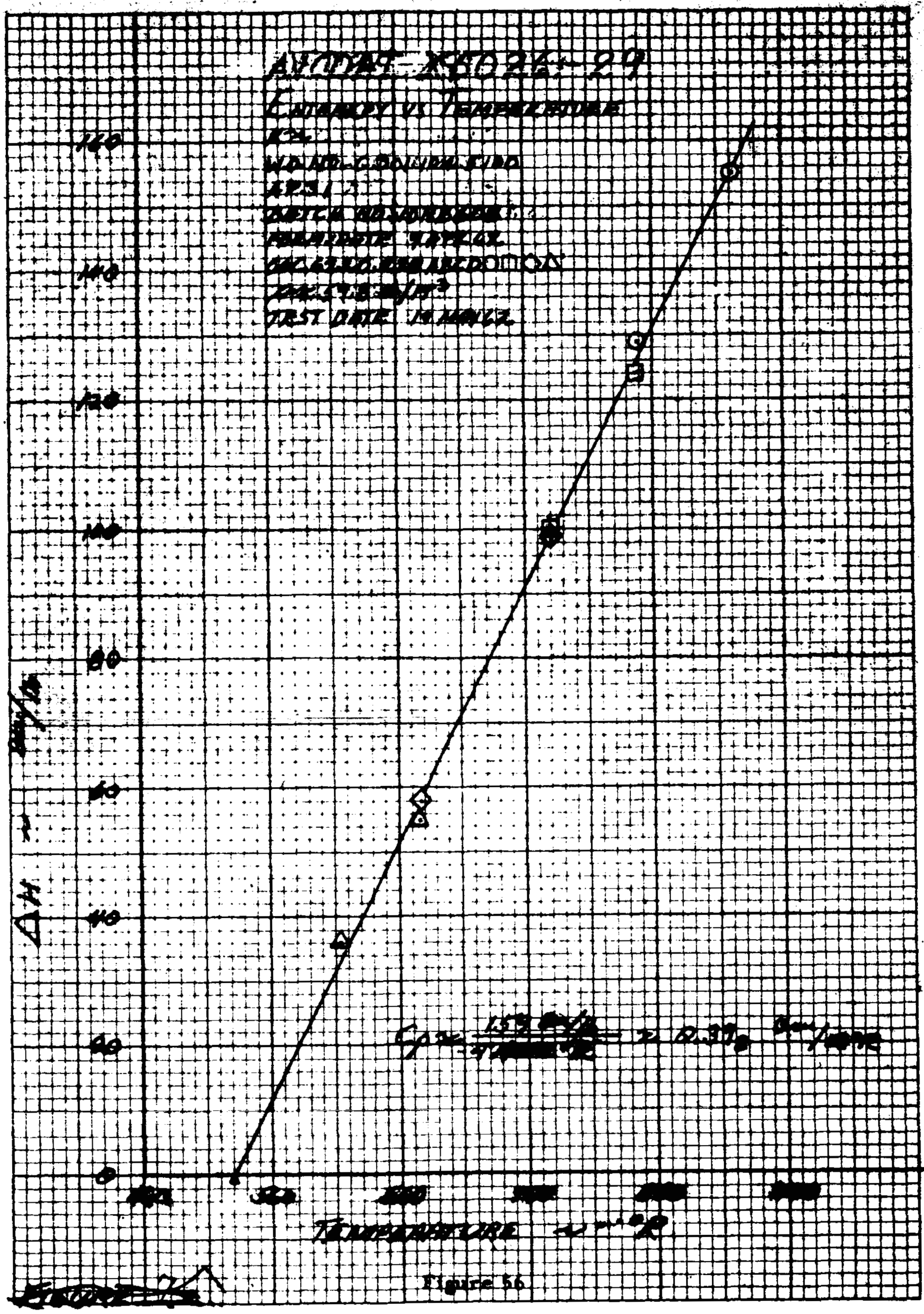

Figure 56

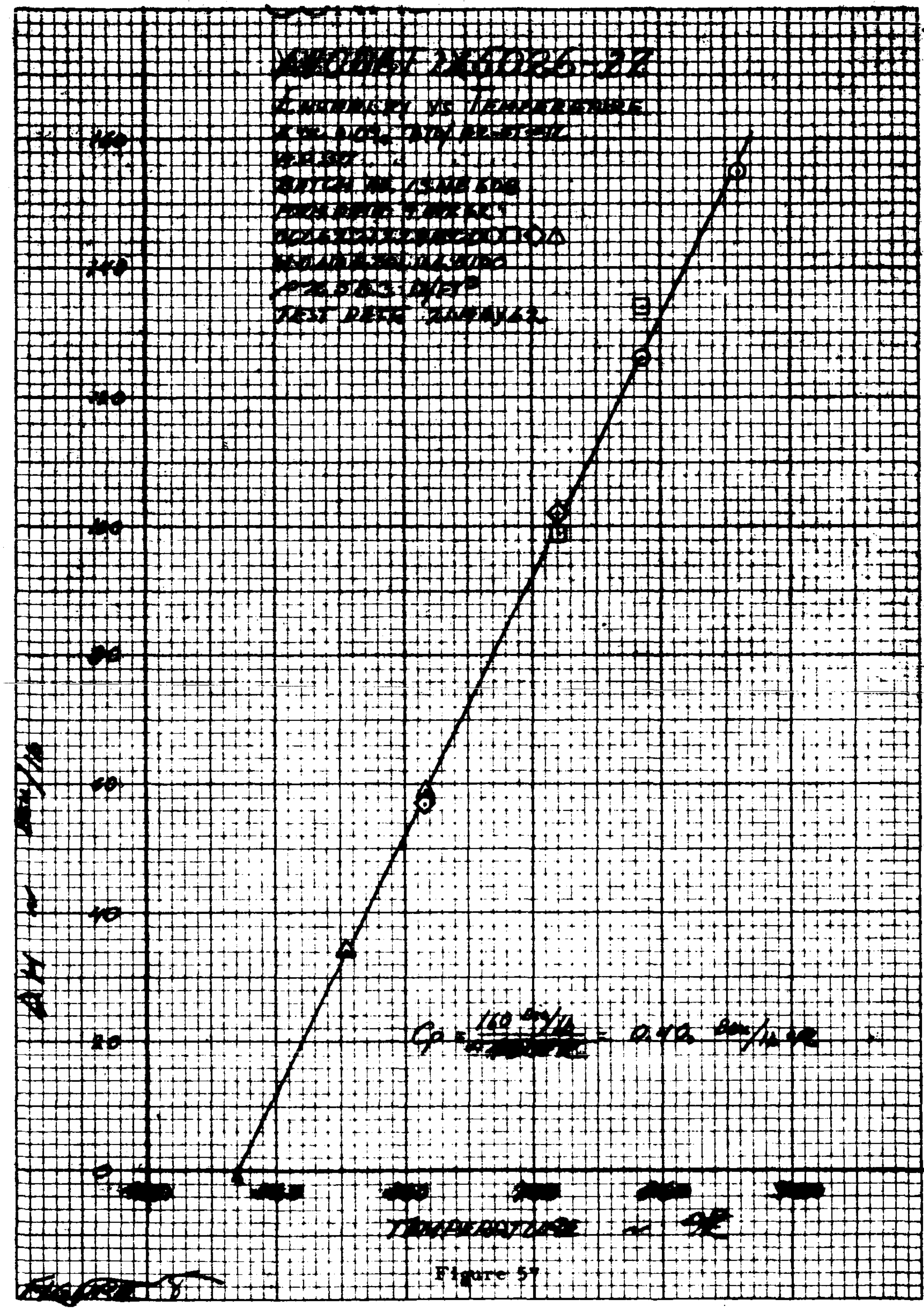

Figure 57

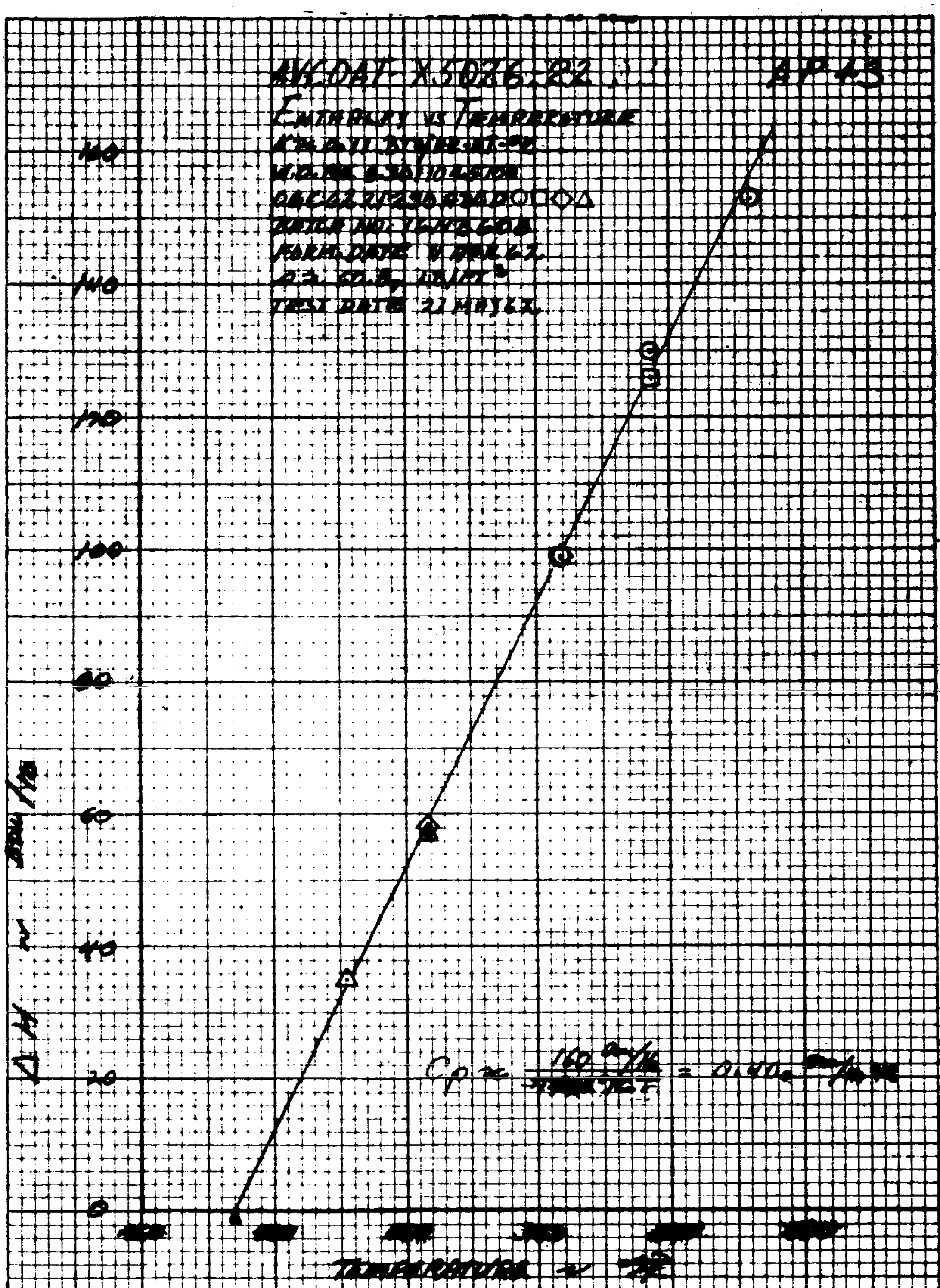
ENTHALPY VS TEMPERATURE
TEST DATE 21 MAY 62
160
140
120
100
80
60
40
20
0

Figure 58

(NOT USED)

DISTRIBUTION

Addressee	No. of Copies
NAA/S&ID Attn: J. M. Kerr (+ 1 reproducible)	25
M. C. Adams	1
R. Alberts	1
M. T. Anderson	1
E. Belason	1
R. Bentley	1
C. Berninger	1
W. Broding	1
C. Caputo	1
C. Cohen	1
J. Collins	1
W. deFee	1
R. E. Demming	1
F. Diederich	1
J. Edwards	1
J. Graham	1
D. Haas	1
L. Hammond	1
~~B. Henshall~~	~~1~~
H. Hoercher	1
A. J. Hanawalt	1
C. Huffine	1
R. H. Huggins	1
E. Kaminsky	1
W. Ihnat	1
R. John	1
A. E. Johnson, Jr.	1
R. Knower	1
J. Kyger	1
G. Larson	1
C. H. Leigh	1
E. G. Lowery, NAA Resident Representative	1
M. Malin	1
M. Mitrovich	1
T. Mix	1
D. Mosher	1
B. Nordquist	1
E. Offenhartz	1
R. Peterson	1
P. Quaiel	1
G. Quayle	1
A. Rothstein	1
S. Ruby	1

DISTRIBUTION (Concl'd)

Addressee	No. of Copies
I. Sacks	1
E. Schurmann	1
D. Stafford	1
V. Strang	1
H. Tereshkow	1
T. Vasilos	1
A. C. Walker	1
H. Weisblatt	1
W. Zeh	1
Central Files	1
Document Control	5
Research Library	2
Apollo Central File (+ 1 reproducible)	5